Fall 2009

Population pharmacokinetics of artesunate and its active metabolite dihydroartemisinin

Bee San Tan
University of Iowa

POPULATION PHARMACOKINETICS OF ARTESUNATE AND ITS ACTIVE METABOLITE DIHYDROARTEMISININ

by

Bee San Tan

An Abstract

Of a thesis submitted in partial fulfillment
of the requirements for the Doctor of
Philosophy degree in Pharmacy
in the Graduate College of
The University of Iowa

December 2009

Thesis Supervisor: Professor Lawrence L. Fleckenstein

ABSTRACT

Artemisinin compounds are the most potent anti-malarial drugs available in the market. Today, malaria treatment is largely relies on the artemisinin-based combination therapies. Artesunate (AS) is the most widely used artemisinin derivative.

In this thesis, we characterized the population pharmacokinetics of AS and its active metabolite dihydroartemisinin (DHA) following oral administration of AS in different populations. In Chapter II, we developed a population pharmacokinetic model of AS and DHA in healthy subjects. These subjects received either single- or multiple-dosing of oral AS, as a monotherapy regimen or in combination with pyronaridine, with or without food. In Chapter III, we developed a population pharmacokinetic model of AS and DHA in adult and pediatric patients with uncomplicated falciparum and vivax malaria who were administered oral pyronaridine/artesunate combination once daily for 3 days.

We modeled the AS and DHA data simultaneously using a parent-metabolite model that assumed complete conversion of AS to DHA. Following oral administration, AS is rapidly absorbed with maximum concentrations reached at about 0.5 hours post-dose. AS is rapidly converted to DHA. DHA then undergoes rapid metabolism, with an elimination half-life of about 0.8 hours in malarial patients. Inter-individual variability for almost all pharmacokinetic parameters and residual variability for both compounds were estimated by the models. Substantial variability was seen in the pharmacokinetic parameters between the subjects.

In healthy subjects, intake of food with the dose was found to delay the absorption of AS significantly, but not the extent of absorption. Weight was also included in this model as a determinant of DHA clearance. When modeling the data from patients, we included weight as part of the model *a priori* using an established allometric function. No other covariates examined in the analysis were statistically significant.

The performance of final models was evaluated using non-parametric bootstrap technique and visual predictive check. The models were found to adequately described the data at hand, and robust with sufficient predictive power. The results can be used as the base to develop a population pharmacokinetic-pharmacodynamic model and as prior information in guiding the selection of optimal sampling schedule for future pharmacokinetic studies of AS.

Abstract Approved: _____
Thesis Supervisor

_____
Title and Department

_____
Date

POPULATION PHARMACOKINETICS OF ARTESUNATE AND ITS ACTIVE METABOLITE DIHYDROARTEMISININ

by

Bee San Tan

A thesis submitted in partial fulfillment
of the requirements for the Doctor of
Philosophy degree in Pharmacy
in the Graduate College of
The University of Iowa

December 2009

Thesis Supervisor: Professor Lawrence L. Fleckenstein

Graduate College
The University of Iowa
Iowa City, Iowa

CERTIFICATE OF APPROVAL

_____

PH.D. THESIS

_____

This is to certify that the Ph.D. thesis of

Bee San Tan

has been approved by the Examining Committee
for the thesis requirement for the Doctor of Philosophy
degree in Pharmacy at the December 2009 graduation.

Thesis Committee: _____
Lawrence L. Fleckenstein, Thesis Supervisor

_____
Erika J. Ernst

_____
Lee E. Kirsch

_____
Dawei Liu

_____
Daryl J. Murry

To Dad, Mum, and Phil, for their love, patience, humor and wit.
To Yuxuan and Yuyang, in hope to inspire them.

There is no fun in doing nothing when you have nothing to do. Wasting time is merely an occupation then, and a most exhausting one.

Jerome K. Jerome
On Being Idle

ACKNOWLEDGMENTS

This work would never have been completed without the labor and support of many hands and minds, and thus my deepest gratitude goes to them:

My mentor Dr. Larry Fleckenstein for his insightful discussion, inspiring work attitude and his ever open door.

Drs. Erika Ernst, Lee Kirsch, Dawei Liu, and DJ Murry for being my committee members and for the comments and suggestions.

Dr. Peter Veng-Pedersen for changing my perspective on pharmacokinetics and letting me sit in his class every year.

My friends and colleagues Thitima Wattanavitjitkul for her support, motivation and the precious discussion, Dr. Himanshu Naik for his advice and encouragement, Denise Morris and Dr. Amal Al Omari for the pow-wows, Paul Imming and Mark Schmidt for the hard work in analyzing the samples, Grace Kim for checking the data, and Drs. Sherry Wei and George Lien for their kind assistance.

My many friends in Iowa City who have extended their helping hands and kind words. The list is long, but you know who you are.

Dr. Jitkang Lim for being a true friend of life.

My family, both the Tan's and Larese-Casanova's, for their love and for all the good and bad times we've been through.

My husband and my best friend Philip Larese-Casanova for everything you have given me. I love you.

ABSTRACT

Artemisinin compounds are the most potent anti-malarial drugs available in the market. Today, malaria treatment is largely relies on the artemisinin-based combination therapies. Artesunate (AS) is the most widely used artemisinin derivative.

In this thesis, we characterized the population pharmacokinetics of AS and its active metabolite dihydroartemisinin (DHA) following oral administration of AS in different populations. In Chapter II, we developed a population pharmacokinetic model of AS and DHA in healthy subjects. These subjects received either single- or multiple-dosing of oral AS, as a monotherapy regimen or in combination with pyronaridine, with or without food. In Chapter III, we developed a population pharmacokinetic model of AS and DHA in adult and pediatric patients with uncomplicated falciparum and vivax malaria who were administered oral pyronaridine/artesunate combination once daily for 3 days.

We modeled the AS and DHA data simultaneously using a parent-metabolite model that assumed complete conversion of AS to DHA. Following oral administration, AS is rapidly absorbed with maximum concentrations reached at about 0.5 hours post-dose. AS is rapidly converted to DHA. DHA then undergoes rapid metabolism, with an elimination half-life of about 0.8 hours in malarial patients. Inter-individual variability for almost all pharmacokinetic parameters and residual variability for both compounds were estimated by the models. Substantial variability was seen in the pharmacokinetic parameters between the subjects.

In healthy subjects, intake of food with the dose was found to delay the absorption of AS significantly, but not the extent of absorption. Weight was also included in this model as a determinant of DHA clearance. When modeling the data from patients, we included weight as part of the model *a priori* using an established allometric function. No other covariates examined in the analysis were statistically significant.

The performance of final models was evaluated using non-parametric bootstrap technique and visual predictive check. The models were found to adequately described the data at hand, and robust with sufficient predictive power. The results can be used as the base to develop a population pharmacokinetic-pharmacodynamic model and as prior information in guiding the selection of optimal sampling schedule for future pharmacokinetic studies of AS.

TABLE OF CONTENTS

LIST OF TABLES

LIST OF FIGURES

CHAPTER I

INTRODUCTION

Malaria

Malaria is one the most devastating global public health burdens contributing to substantial morbidities, mortalities and poverty in many countries in the world. World Health Organization (WHO) estimated that half of the world's population in 109 endemic countries was at risk of malaria infection. In 2006, malaria claimed nearly a million lives; primarily in children less than 5 years of age (1). Malaria infection also has immense negative socioeconomic impact, reducing the economic growth rates by up to 1.3% in endemic countries (2).

Human malaria is caused by five species of parasites that belong to genus *Plasmodium*: *P. falciparum*, *P. vivax*, *P. ovale*, *P. malariae*, and until recently *P. knowlesi* (3-6). Figure 1.1 shows the life cycle of malaria parasites (7). Transmission of the parasites begins when a female anopheline mosquito inoculates sporozoites into the bloodstream of the human host during a blood meal. These sporozoites then migrate rapidly to the liver and infect hepatocytes to begin the asexual reproduction stage. Subsequently, the sporozoites multiply into merozoites. Infected hepatocytes eventually burst and release merozoites into the bloodstream. Released merozoites then infect the red blood cells, where they develop into trophozoites and mature into schizonts, which rupture to release merozoites. Gametocytes, the sexual form, are also produced. The gametocytes, if ingested by a female anopheline mosquito, will infect the definitive host and begin the sexual development cycle to eventually produce sporozoites which make their way to the mosquito's salivary glands. The malaria life cycle is perpetuated when the mosquito bites a human host and inoculates the sporozoites into the human bloodstream. In *P. vivax* and *P. ovale* infections, some of the intra-hepatic sporozoites

enter an arrested stage of development called hypnozoite and remain dormant for a period of time before schizogony begins. This delayed primary infection is known as relapse.

Falciparum and vivax malaria are the most common malaria. Falciparum malaria is the most severe form of the disease due to the high prevalence and virulence of the parasite in addition to increased drug resistance. Individuals who are most susceptible to the disease are those with limited immunity against the disease. The most vulnerable groups include young children, particularly those less than five year olds in highly endemic areas, travelers and migrants from areas with no or little malaria transmission to malaria endemic regions, pregnant women especially those who are pregnant for the first time, and individuals who are co-infected with immunosuppressive diseases such as HIV infection.

Malaria can be categorized as uncomplicated or severe. Infected individuals are often present with acute febrile symptoms which include cyclical malarial fever, chills and sweats, headaches, nausea and vomiting as well as other manifestations such as abdominal discomfort, malaise and mild anemia. If promptly and appropriately treated, the mortality associated with uncomplicated falciparum malaria is about 0.1%. However, a more severe form of falciparum malarial infection may develop if patients are not treated in a timely manner. The manifestations of severe malaria include severe anemia, cerebral malaria, hypoglycemia, respiratory distress and other organ failures which will eventually lead to coma and death. The mortality in patients with severe malaria rises to about 15-20% despite treatment (8, 9).

Control of malaria consists of two aspects: control of the anopheline mosquito vector and management of malaria cases. Removal of mosquito breeding sites, use of insecticide-treated bed nets and indoor residual insecticide spraying are efficacious vector-control measures. However, the emergence of resistance to pyrethroid, an insecticide used in insecticide-treated bed nets, has been reported in a some African countries (10).

Malaria case management has traditionally relied on anti-malarial drugs while the world is waiting for an effective malaria vaccine. Chloroquine and sulfadoxine-pyrimethamine are inexpensive, readily available and therefore the most widely used anti-malarial drugs until recently. Their usefulness is now very limited due to parasite resistance in most malaria-affected areas. Resistance to mefloquine and atovaquone are also well-established. The rapid emergence of resistance to anti-malarial agents has prompted WHO to advocate the use of combination-based therapies, particularly artemisinin-based combination therapies (ACTs).

Artemisinin and Derivatives

General Properties and Mechanism of Action

Artemisinin is a naturally occurring sesquiterpene lactone containing an endoperoxide group extracted from the leaves of Chinese herb *Artemisia annua*. Artemisinin itself is not oil- nor water-soluble and so is only available in enteral formulations. Several oil- or water-soluble derivatives of artemisinin have been synthesized. Dihydroartemisinin (DHA) is synthesized from artemisinin through reduction process. From DHA, artesunate (AS), artemether and arteether are synthesized. Figure 1.2 shows the chemical structures of the compounds. These artemisinin derivatives have been formulated for oral, rectal and parenteral administration (11-13). From hereon, ‘artemisinins’ will be used when artemisinin and its derivatives are discussed collectively as a class.

The exact mechanism of which artemisinins exert their anti-malarial properties is not known. Several theories have been proposed. One theory suggests that free radicals are formed when artemisinins bind to hem, through an iron-mediated cleavage of the peroxide bridge. These free radicals are damaging to various parasite membranes, thereby killing the parasites. An alternative hypothesis suggests that artemisinins inhibit the sarcoplasmic endoplasmic reticulum calcium ATPase, or SERCA, of the malarial

parasite. It is also possible that artemisinins exert their anti-malarial properties via a combination of different mechanisms. These theories on how artemisinins act have been reviewed elsewhere (14-16).

Anti-Malarial Efficacy

Artemisinins are the most potent and effective anti-malarial drugs available, with broadest parasite stages activity and highest parasite reduction ratio (17). More importantly, artemisinins are effective against chloroquine- and mefloquine-resistant strains (18-21). Most anti-malarial drugs, including artemisinins, are primarily active against the mature ring stage of *P. falciparum*, when the parasites are most metabolically active. However, artemisinins also target the young ring stages of the parasites. Another potential benefit is that artemisinins are active against the gametocytes, which are transmitted from humans to mosquitoes. In fact, it has been shown that the use of artemisinins resulted in a significant reduction of gametocytaemia and subsequent transmission to mosquitoes when compared to previous first-line non-artemisinin anti-malarial drugs (22). However, these compounds are not active against the pre-erythrocytic stages or the dormant hypnozoite stages of *P. vivax* and *P. ovale* in the liver.

The reported geometric mean for 50% inhibitory concentration (IC_{50}) in *P. falciparum* isolates were 4.2, 4.3, and 16.1 nM for AS, DHA, and artemether respectively (23). The estimated *in vivo* parasite reduction ratio, defined as the ratio of baseline parasite count to parasite count 48 hours later, ranges from 10^3-10^5 for artemisinins (24). This means artemisinins are capable of killing >99.9% of the parasites per asexual cycle. Despite the fast parasite killing rates, blood concentration of artemisinins need to be at a parasiticidal level for at least 6 days (corresponding to 3 asexual life cycles for *P. falciparum*) in order to remove all parasites from the blood. Therefore, when given alone, 7-day regimens are required to maximize their cure rates. Unfortunately, compliance to 7-day treatment courses is poor, especially when the clinical symptoms of malaria

disappear within a couple days of treatment initiation. When used in combination with partner drugs of longer elimination half-lives, 3-day treatment courses are sufficient (25).

The efficacy and clinical use of artemisinins have been extensively reviewed elsewhere (14, 26-29).

Clinical Toxicology and Safety

In experimental animal studies, the safety profiles of artemisinins are generally good. However, when given in high and repeated doses to the animals, these compounds have produced selective pattern of damage to the brain stem, affecting in particular those involve with auditory system (30-34). The damage was especially obvious with artemether or arteether administration. Clinical features of brain stem neurotoxicity included tremor, gait impairment, loss of spinal and pain response, auditory impairment, loss of eye reflexes and death. It is suggested that neurotoxicity is greater when the central nervous system is constantly exposed to artemisinins than intermittent brief exposure (35). Thus it is not surprising that intramuscular formulation of artemether and arteether are more neurotoxic in experimental animals than AS given by any route.

Many clinical trials involving artemisinins have been conducted in different populations and in various parts of the world (36-43). All studies have indicated that artemisinins are generally well tolerated with minimal adverse drug reactions. A systematic review of 108 published and unpublished studies involved artemisinins conducted in healthy subjects and patients with uncomplicated or severe malaria showed similar results (44). No serious adverse drug event was reported in any of the studies. The most common adverse events were gastrointestinal-related. Other adverse reactions reported were neutropenia (1.3%), reticulocytopenia (0.6%), elevated liver enzymes (0.9%), transient bradycardia (1.1%) and prolonged QT interval (1.2%).

Price et al. conducted a similar systematic review on the adverse effects of artemisinins using data generated from a series of large prospective trials conducted in

Karen community living in the Thai-Burmese border region (45). In these studies, 836 patients received either AS or artemether as monotherapy regimen, while 2826 patients received the combination of mefloquine plus an artemisinin derivative. The combination regimens were associated with higher adverse events than the monotherapy, for example 31% versus 16% for acute nausea, 51% versus 34% for anorexia, 24% versus 11% for vomiting and 47% versus 15% for dizziness. When given alone, oral AS and artemether are well-tolerated.

The results from animal studies and clinical trials clearly show a discrepancy regarding the safety profile of artemisinins. Gordi and Lepist suggested two possible explanations for this discrepancy (46). The adverse effects seen in experimental animals may be caused by prolonged exposure to artemisinins administered in oil-based intramuscular formulations. When given orally, these compounds are absorbed and eliminated rapidly, and therefore less likely to produce neurotoxic effects. Additionally, the relatively high doses of artemisinins used in animal studies may have contributed to the higher incidence of toxicity seen in these animals.

The developmental toxicity of artemisinins has also been studied in different animal models, including rats, rabbits and monkeys (47-50). Artesunate exposure induced embryo loss, cardiovascular malformations, and skeletal defects in both rats and rabbits, in the absence of apparent maternal toxicity (48, 49). When AS was administered to cynomolgus monkeys at 12 and 30 mg/kg/day orally once daily from days 20 to 50 of gestation, AS caused 55% and 100% embryo lethality, respectively (47). However, no artesunate-related embryo deaths or malformations were observed when the treatment period at 12 mg/kg/day was shortened to 3 or 7 days. Li et al. studied the tissue distribution of radio-labeled AS after intravenous injection and toxicokinetics of AS following single or multiple intramuscular injections in pregnant and non-pregnant rats (50). Their data showed that the level of radio-labeled AS was 2- to 4-fold higher in uterus, placenta, and ovary than in blood. Furthermore, AS and DHA in the blood of

pregnant rats were 1.53- and 3.74-fold higher than the non-pregnant rats. These two observations may explain the severe embryotoxicity of AS in pregnant animals.

Clinical trials of artemisinins conducted in pregnant women appear to be encouraging so far (51-54). In a study involving 461 pregnant women with acute falciparum malaria who were treated with AS (n = 528) and artemether (n = 11), the rates of abortion, stillbirth and congenital abnormalities were similar to rates in local community (54). Deen et al. studied the safety of artesunate plus pyrimethamine-sulfadoxine combination in 287 pregnant women in Gambia and concluded that no difference was observed in the proportion of abortions, stillbirths, or infant deaths among those exposed or not exposed to the drugs (51). Combinations of artemether/lumefantrine and mefloquine plus artesunate were also well tolerated and safe in pregnant women (52, 53). However, these studies were conducted in pregnant women in their second or third trimester. The safety of artemisinin compounds during first trimester is unknown.

Auto-induction Phenomenon

Numerous studies have shown that artemisinin exhibits remarkable time-dependent pharmacokinetics after repeated oral and rectal administration both in healthy subjects (55-57) and in malaria patients (58, 59). Ashton and colleagues (55) studied the pharmacokinetics of artemisinin in 8 healthy male subjects after the administration of 250, 500 and 1000 mg of oral artemisinin in a cross-over design with a 7-day washout period. Artemisinin oral clearance was found to decrease with dose. In another study conducted in 10 healthy male subjects who received a 7-day oral daily regimen of 500 mg, artemisinin area under the concentration-time curve (AUC) decreased to 34% of values obtained after the first day of administration on day 4 and to only 24% on day 7 (56). Similarly, a 4.7-fold increase in artemisinin oral clearance was observed in the study by Zhang et al. (57).

Similar observations have also been reported in patients with uncomplicated malaria. Thirty malaria patients were treated with 500 mg of either oral or rectal artemisinin daily for 5 days (58). Artemisinin AUCs on the last day of treatment were reduced to only 30% and 40% of the values after the first dose, for oral and rectal route respectively. A significant increase in artemisinin oral clearance from day 1 to day 5 was also observed in 77 male and female malaria patients (59).

The time-dependency of artemisinin pharmacokinetics is thought to be caused by its strong capacity for auto-induction. Various studies have shown that artemisinin induces different cytochrome P450 (CYP) enzymes, including CYP2B6, the primary enzyme responsible for the metabolism of artemisinin, and CYP2C19 (60-63). Pharmacokinetic models for artemisinin that incorporates the auto-induction component have also been proposed (64, 65).

Similarly, time-dependent pharmacokinetics has been reported for artemether in both healthy subjects and patients with uncomplicated malaria (66, 67). However, the attempts to study this phenomenon in AS and DHA yielded mixed results (68-70). Plasma concentrations of DHA and to a lesser extent AS showed a time-dependent decline in a study done in 6 patients who received AS treatment for 5 days (68). However, the results from this report is not very convincing as pharmacokinetic analysis was not done due to the sparseness of blood sampling times. Hence, the comparison was done based solely on the concentration values but not pharmacokinetic parameters. In another study, 10 healthy subjects received oral AS once daily for 5 days (69). All pharmacokinetic parameters were similar on days 1 and 5 for both AS and DHA, indicating an absence of time-dependent pharmacokinetics. It is suggested that the decline in DHA concentration toward the end of treatment period may be due to the restoration of drug-metabolizing enzymes during the convalescent phase of malaria infection rather than the auto-induction of DHA metabolism (70).

Artemisinin-based Combination Therapies

In the past fifty years, anti-malarial drugs have been deployed on a large scale as monotherapies. The extensive deployment and the inappropriate use of the drugs have provided selective pressure on the parasites to evolve into mutants resistant to the drugs (9). Multidrug-resistant falciparum malaria is now widely prevalent in South East Asia, South America, and Africa. The wide-spread resistant resulted in WHO recommending that all countries experiencing resistance to conventional monotherapies should use combination therapies, preferably ACTs for falciparum malaria (71). The rationale behind combination therapies is that when two drugs with different modes of action, and therefore different resistance mechanisms, are used in combination, the probability of the development of resistant parasite to both compounds is far lower than the chance of selection of individual mutations.

Nosten and Brasseur (72) suggested that 'ideal' anti-malarial combination should possess the following properties:

1. The components of the combination should have different mode of action on the parasite.
2. There should not be any negative pharmacological interactions between the components.
3. The duration of the regimen should ideally not exceed 3 days.
4. It should include at least one fast-acting component which clears asexual form of the parasite rapidly.
5. One of the drugs should have reasonably long half-life.
6. The combination should be well tolerated with minimal toxicity.
7. It must have broad spectrum of action against all stages of the parasite.
8. It should be co-formulated.
9. It must be inexpensive.

Currently used ACTs include AS plus amodiaquine, AS plus sulfadoxine/pyrimethamine, AS plus mefloquine, artemether/lumefantrine, dihyroartemisinin/piperaquine. None of these is ideal, but artemether/lumefantrine is viewed as closest in meeting all the criteria. Pyronaridine/artesunate is another fixed-dose ACT currently under development as a once a day for three days treatment for uncomplicated falciparum and vivax malaria.

Pharmacokinetic Properties of Artesunate and Dihydroartemisinin

AS is the only artemisinin derivative available in oral, rectal and intravenous formulations for use in human. Pharmacokinetics of AS and its active metabolite DHA has been studied quite extensively in different populations. However, AS data were very limited in these studies due to the fact that AS is rapidly converted to DHA and that the assays used were not sensitive enough to detect AS in the samples collected. Consequently, many pharmacokinetic studies of AS either report only the pharmacokinetic parameters for DHA without the parameters related to AS, or report the combined anti-malarial activities of AS and DHA.

AS was rapidly absorbed into the systemic circulation following oral administration. Using limited information available for AS, Batty et al. reported the absolute bioavailability for oral AS of 15% and 23% for patients with uncomplicated falciparum malaria and vivax malaria, respectively (73, 74). The relative bioavailability of DHA following oral AS was high in these patients, with mean values of 82% and 85% for patients with uncomplicated falciparum malaria and vivax malaria, respectively. In another study, total anti-malarial activity (i.e. the combined activities of both AS and DHA) was used to assess the bioavailability (75). Mean absolute anti-malarial bioavailability after the administration of oral AS was 61%.

The absorption of rectal AS was slower than oral AS, with mean time to reach peak concentration (t_{max}) for AS of 1.43 h versus 0.66 h, and mean t_{max} for DHA of 1.8 h versus 0.93 h (76). In pediatric patients who received different doses of intravenous AS and rectal AS, the median relative bioavailability values of DHA were 58% in low-dose rectal group and 23% in high-dose rectal group (77). These values were lower than the values reported for oral AS (73, 74).

The tissue distribution pattern of AS and DHA has been studied in rats using radio-labeled techniques (78, 79). Using quantitative whole-body autoradiography method, the tissue distribution of intravenous [^{14}C] labeled AS was assessed in 40 organs and tissues in rats (78). At 0.5 h and 1 h post dose, most of the AS activity was concentrated in the intestine and its contents, followed by bile. At 4 h post dose, drug distribution in all tissues was higher than that at 2 h post dose, possibly due to intestinal re-absorption and/or enterohepatic circulation. Subsequently, AS radioactivity dropped rapidly but not uniformly in all tissues. After 96 hours of dose administration, high density of radioactivity was still found in the spleen, bone marrow, and intestine. The distribution of [^{14}C] labeled AS was estimated to be 6-fold higher in red blood cells than in plasma.

Similar result was observed in rats treated with intravenous [^{14}C] labeled DHA (79). The highest radioactivity was found in small intestine at 1 h post dose. DHA distribution to other tissues increased significantly at 6 h after injection, with highest level still found in the intestine. Measured radioactivity declined rapidly after that with residual activity found in spleen, kidney, adrenals, large intestine content, liver, and lungs at 96 h post dose. The ratio of drug concentration in red blood cells to plasma was about 3.54:1.

The protein binding of [^{14}C] labeled AS was studied in human and rat plasma using equilibrium dialysis method over a concentration range of 0.2 to 78125 ng/mL (80). The binding profile was shown to be concentration-dependent. In both species, the

percent of drug bound to plasma proteins ranged from 73% to 81%. At drug concentrations more than 125 ng/mL, the percent bound declined to 62-66%. The protein binding of [^{14}C] labeled DHA was also studied in human and rat plasma using similar method over a concentration range of 0.15 to 57800 ng/mL (79). The binding of [^{14}C] DHA was concentration-dependent in human plasma but not in rat plasma. At higher concentrations, the binding percentage in human plasma decreased from 82% to 66%.

Metabolism and pharmacokinetic studies have shown that AS is rapidly hydrolyzed to DHA, primarily by plasma or tissue choline esterases. Following intravenous administration of AS, the peak concentration (C_{max}) was reached at 9 minutes after the injection (73). For oral and rectal AS, the t_{max} of DHA was very close to the t_{max} of AS (0.66 h and 0.93 h for oral route, 1.43 h and 1.8 h for rectal route), indicating rapid conversion of AS to DHA (76). Due to the rapid conversion, AS is often considered as pro-drug of DHA. Following oral administration of AS, the ratio of AUC for DHA to AUC for AS can be as high as 10:1 (81). Figure 1.3 shows the typical concentration-time profiles for AS and DHA follwing oral administration of AS.

Studies in rats demonstrated that DHA undergoes rapid metabolism via conjugation and biliary elimination (79, 82, 83). The metabolic pathways for DHA was studied in humans by analyzing metabolites in urine collected from patients who had received intravenous AS and metabolites produced by human liver microsomes (84). Using V79 cells expressing different human UDP-glucuronosyltransferases (UGTs), such as UGT1A1, UGT1A6, UGT1A9 and UGT2B7, it was shown that DHA is metabolized by UGT1A9 and UGT2B7, but not UGT1A1 and UGT1A6. The major metabolite identified was α-DHA-β-glucuronide. AS and DHA undergo extensive first-pass metabolism with very high extraction ratio (85, 86). For drugs with high extraction ratio, clearance approaches blood flow and is therefore perfusion rate limited.

Pharmacometrics

Mathematical and statistical modeling has been widely used in various scientific disciplines for a long time. However, the use of such modeling in analyzing the interactions between drugs and patients in a quantitative manner is relatively new. This discipline is termed 'pharmacometrics'. A formal definition of pharmacometrics was given by Williams and Ette (87). They defined pharmacometrics as 'the science of developing and applying mathematical and statistical methods to (a) characterize, understand, and predict a drug's pharmacokinetic and pharmacodynamics behavior; (b) quantify uncertainty of information about that behavior; and (c) rationalize data-driven decision making in the drug development process and pharmacotherapy. In practice, pharmacometrics often involves pharmacokinetic, pharmacodynamic, pharmacodynamic-biomarker-outcome link and/or disease progression models.

In the white paper published in 2004 on critical path assessment of medical products development (88), the U.S. Food and Drug Administration (FDA) recognized the need for "new tools to get fundamentally better answers about how the safety and effectiveness of new products can be demonstrated in faster time frames, with more certainty, and at lower costs." Low efficiency in drug development has been the largest challenge facing the pharmaceutical and biotechnology industries. Kola and Landis analyzed the success rates from first-in-human to registration from year 1991 to 2000 for ten pharmaceutical companies in the United States and Europe and found out that the average success rate for all therapeutic areas is only approximately 11% (89). Model-based drug development was cited by the FDA, along with advances in clinical pharmacology, as essential elements for innovative drug development in its Critical Path Initiative (88).

Recognizing the role of pharmacometrics in drug development and regulatory domains, FDA has taken various initiatives to integrate this discipline as part of the drug application review process (90, 91). As the results, pharmacometric applications were

incorporated in 42 of a total of 244 New Drug Applications (NDAs) submitted to cardio-renal, neuropharmacology, and oncology drug products between 2000 and 2004, and a pharmacometric component was involved in approvals for 26 NDAs and labeling in 37 NDAs (92). Similarly, a pharmacometric component was involved in approvals for 20 NDAs and labeling in 17 NDAs out of a total of 31 NDAs with pharmacometric analysis from February 2005 through June 2006 (93).

Among all the different types of pharmacometric modeling, population pharmacokinetic modeling is perhaps the most commonly applied. Consequently, guidance documents on population pharmacokinetic analyses were published by both the FDA and European Medicines Agency (EMEA) (94, 95).

Population Pharmacokinetics

Population pharmacokinetics is the study of the sources and correlates of variability in drug concentrations between individuals (96). Population pharmacokinetic analysis comprises the characterization of variation in pharmacokinetic behavior within the population and the identification of demographical, pathophysiological, and therapeutic characteristics, such as body weight, renal function, disease state, smoking status, concurrent medications etc, that may account for the variability (94-97). This knowledge is essential in mapping the response surface of the drug of interest, explaining differences seen in subgroups, developing and evaluating dosing strategies, and designing future studies (98-100). Currently, population pharmacokinetic analyses are mainly applied in characterizing the pharmacokinetics of the drug in the target population and in special populations, such as pediatric and elderly populations, and in recommending the dosing strategies in these populations (95). In drug development, this type of analyses is often carried out in patients, but much less in Phase I studies (101). It is suggested that this approach should be implemented in all phases of drug development (98).

Population pharmacokinetic approach offers several advantages over the traditional pharmacokinetic studies. Traditional pharmacokinetic studies are often done in a small homogenous group of individuals with intensive sampling, and involve fitting the model to data obtained from each individual separately. The population approach, on the other hand, allows both sparse and intensive data to be used. The sparse sampling approach has enabled pharmacokinetic studies to be carried out ethically in special populations such as neonates (102-105), pediatrics (106-108), pregnant women (109-111), critically ill patients (112-115) and elderly (116, 117). The population approach also allows the pooling of heterogeneous data into one dataset, for example data from different study centers or different trials, trials with intense and sparse sampling, data from children and adults, or experimental plus observational data. Data from trials with unbalanced design, where the number of samples per subject may differ, can also be incorporated.

Various methods have been proposed and used in population pharmacokinetic modeling, including naïve pooled data, standard two-stage approach, Bayesian estimation and nonlinear mixed-effects modeling. Briefly, naïve pooled data approach estimates population mean parameters by treating all data as if the data arose from a single individual, while standard two-stage approach estimates each individual's pharmacokinetic parameters and then uses the individual parameters to estimate the population parameters. In Bayesian analysis, the prior distribution of the parameters in a population of subjects and the actual data from an individual are used to estimate the individual's parameters. Nonlinear mixed-effects modeling is a one-stage analysis that allows for the all fixed and random parameters to be estimated simultaneously. A detailed discussion on the advantages and disadvantages of each approach can be found elsewhere (118). Currently, the most commonly used method is the nonlinear mixed-effects modeling, and the majority of population pharmacokinetic analyses employing this approach are carried out using NONMEM package developed by Beal and Sheiner (119).

However, it is unfortunate that NONMEM has become synonymous with population pharmacokinetics.

Nonlinear Mixed-Effects Modeling

As the name implies, nonlinear mixed-effects modeling allows for the simultaneous estimation of parameters relating the fixed effects and random effects to the observed data. Fixed-effect parameters are the estimated parameters relating the observed or measured variables to model prediction. These parameters can be model parameters, such as clearance and volume of distribution, or impact of covariates on the pharmacokinetic parameters. The random-effect parameters measure the unexplained random variability, including the inter-individual variability and the residual variability. Inter-individual variability accounts for the difference between the estimated parameter for an individual and the expected value for the parameter (i.e. the population estimate). In pharmacokinetic modeling, inter-individual variability is sometimes viewed incorrectly as a nuisance. Residual variability accounts for the difference between measured and model-predicted concentrations for an individual. It can be due to the intra-individual variability, inter-occasion variability, measurement error, or model misspecification error (97, 120, 121).

In population pharmacokinetic modeling, nonlinear mixed-effects population pharmacokinetic models consist of three components: structural, covariate, and variance models. The pharmacokinetic model that best describes the concentration-time profile of a drug forms the structural model, also known as the base model. The covariate model describes the impact of subject specific covariates on the pharmacokinetic parameters. Lastly, the variance component takes into account the inter-individual variability and the residual variability.

Mathematically, a general nonlinear mixed-effects model used to describe the observed response in an individual can be written as:

$$y_{ij} = f(\mathbf{x_{ij}}, \boldsymbol{\beta_i}) + \varepsilon_{ij}$$

$$\varepsilon_{ij} \sim N(0, \sigma^2)$$

where y_{ij} is the jth observed response for individual i, $f(\mathbf{x_{ij}}, \boldsymbol{\beta_i})$ is the nonlinear function used to predict the response, $\mathbf{x_{ij}}$ denotes the vector of independent variables (e.g. dose and time), $\boldsymbol{\beta_i}$ denotes the vector of model parameters, and ε_{ij} represents the residual variability which is assumed to be independent and normally distributed with zero mean and variance σ^2. Σ is used in NONMEM to denote the covariance matrix for ε, and its dimension is related to the number of residual variance terms.

Correspondingly, $\boldsymbol{\beta_i}$, which varies quantitatively among individuals due to inter-individual variability, can be mathematically written as:

$$\boldsymbol{\beta_i} = g(\boldsymbol{\theta}, \mathbf{z_i}) + \eta_i$$

$$\eta_i \sim N(0, \omega^2)$$

where g is a known function describing the expected value of $\boldsymbol{\beta_i}$, in terms of individual specific covariates $\mathbf{z_i}$, and the vector of population parameters $\boldsymbol{\theta}$. η_i represents the deviation of the individual parameter vectors from the population predictions, and is assumed to be independent and normally distributed with zero mean and variance ω^2. Ω is used in NONMEM to denote the covariance matrix for η, and its dimension is determined by the number of inter-individual variance parameters.

Using a simple one-compartmental pharmacokinetic model with first order elimination following single intravenous bolus dose administration as an example, the mixed-effects model describing the drug concentration-time profile can then be written as:

$$C_{ij} = D_i/V_i \cdot \exp^{-(CLi/Vi)\cdot tij} + \varepsilon_{ij}$$

where C_{ij} denotes the jth blood concentration of the drug for individual i, while D, V, CL and t are the dose administered, volume of distribution, clearance and elapsed time since dose administration respectively. ε_{ij} represents the residual variability, as defined previously.

Furthermore, if the volume of distribution is a linear function of body weight, then the value V for individual i can be described by:

$$V_i = \theta_1 + \theta_2 \bullet (\text{weight})_i + \eta_{V,i}$$

where θ_1 and θ_2 are the intercept and slope describing the linear relationship between V and weight for individual i and $\eta_{V,i}$ accounts for the deviation in V for individual i from the population estimate for V.

Model Evaluation

After a population pharmacokinetic model has been developed, the model needs to be evaluated for its performance. Different terms have been used for this process, such as “model evaluation”, “model validation”, “model qualification”, “model performance” and “model assessment”. Model evaluation was defined by Yano et al. as an assessment of the predictive ability of a model for domain-specific quantities of interest, or an assessment whether the model deficiencies have a noticeable effect in substantive inferences (122). The amount and type of model evaluation procedures should therefore be chosen based on the objectives of the modeling and the intended use of the model (94, 95, 123). A population pharmacokinetic model is developed either for descriptive or predictive purposes. Descriptive population pharmacokinetic models are developed to describe the variability of the pharmacokinetics of a drug based on the data at hand and to evaluate potential covariate effects and are often used for interpolation purposes within the range of observed values. On the other hand, predictive models allow for interpolation and extrapolation purposes.

There are two general approaches for population model evaluation: external evaluation and internal evaluation. External evaluation is the most stringent method for testing a developed model. In external evaluation, the model is compared to an independent data set. However, it is often time consuming and sometimes difficult to obtain a test data set. Internal validation can be further categorized into basic internal

evaluation and advanced internal evaluation (124). Basic internal evaluation often involves assessment of goodness-of-fit plots, uncertainty of the parameter estimates and/or model sensitivity to outliers. Advanced internal evaluation may include more complex techniques such as data splitting, resampling techniques (e.g. bootstrap, cross-validation) or simulation-based techniques. Brendel and colleagues performed a systematic review of all population pharmacokinetic and/or pharmacodynamic analyses published between 2002 and 2004 with objectives to survey the current methods used in model evaluation and to assess if the evaluation methods performed were adequate (124). They found out that 45% of the pharmacokinetic models employed only the basic internal methods in model evaluation. 28% of the pharmacokinetic models were evaluated using advanced internal evaluation with or without basic internal evaluation while external validation was performed for only 7% of the pharmacokinetic models.

We used a combination of basic and advanced internal evaluation techniques to evaluate the descriptive and predictive performance of the models developed. The assessment of goodness-of-fit plots, uncertainty of the parameter estimates, bootstrap resampling technique, visual predictive check, which is a simulation-based diagnostic, and condition number were used to evaluate the models developed. Informative graphics play an important role in model evaluation (125). The commonly used goodness-of-fit plots in population include plot of observations versus population predictions, plot of observations versus individual predictions, plot of weighted residuals or conditional weighted residuals versus population predictions, and plot of weighted residuals or conditional weighted residuals versus time among others. These plots are useful in identifying model misspecifications. However, the usefulness of these plots can be limited under certain circumstances and therefore should be used along with other approaches (126). The measures used to evaluate the precision of parameter estimates include the percent relative standard error (%RSE) and bootstrap confidence interval. %RSE is expressed as the standard error of a parameter estimate relative to the parameter

estimate itself. Bootstrap confidence intervals are calculated from bootstrap runs and will be discussed further in the following section.

Bootstrap resampling technique was first introduced by Efron (127). It is a method of resampling with replacement that has the advantage of using the entire data set for model development, which in contrast to data splitting that uses only a subset of the entire data set. The basic idea behind this procedure is that if the sample we have is a good approximation of the population, then the bootstrap method will provide a good approximation of the sampling distribution of the statistic of interest. Bootstrap analysis procedure involves repeatedly generating random samples of size equal to the size of original data set by sampling with replacement from the original data set. Each random sample will be treated as a new data set and the population model will be fitted to the new data set to estimate parameters of interest for that data set. The fitting and parameter estimation are repeated for each new data set generated. The bootstrap estimates and 95% confidence intervals of the parameters can be calculated and compared to the parameter estimates obtained form the final population model. The parameter estimates from the final model are considered reliable if the values are similar to the bootstrap estimates and fall within the bootstrap 95% confidence intervals. FDA recommends that at least 200 bootstrap replicates to be generated when this method is used (94). Bootstrap estimates can be computed as follows (128):

$$T^* = \frac{1}{N} \sum_{1}^{N} T_j$$

where T* denotes the bootstrap estimate, and T_j represents the parameter estimate for each of N bootstrap replications.

The 95% bootstrap confidence intervals (CI) are calculated as:

$$CI = T^* \pm 1.96\ SE$$

where SE is the standard error and is given by:

$$SE = [\sum_{1}^{N}(T_j - T^*)^2 / (N-1)]^{1/2}$$

A relatively new model evaluation tool is called visual predictive check, which originates from the posterior predictive check (122, 129, 130). In visual predictive check, observations based on the results of the final population model were simulated. These simulated predictions were then compared with the original observations to evaluate whether an identified model is able to reproduce the central tendency and variability in the present and future data sets (131). If the model derived from the observed data is adequate, it should generate similar data as the observed data when used in the simulation setting. From the simulated predictions, the median and non-parametric 90% confidence interval (5th and 95th percentiles) of the simulations are calculated. These prediction lines are plotted with the original observations on the same graph to compare the distribution of the simulations and the distribution of the observed concentrations. The percentage of observations outside the 90% confidence interval of the simulated data is also calculated. If approximately 10% or less of the observed data falls outside the 90% confidence interval of the simulations, then the final model and the parameter estimates are said to describe the data adequately (132).

Another useful model diagnostic is the condition number. A condition number is defined as the ratio of the largest eigenvalue to the smallest eigenvalue, and is a measure of the stability of computational problems. A large condition number is indicative of ill conditioning. In this case, small changes in the data may lead to large changes in the parameter estimates. Ill conditioning can be due to either insufficient data to support estimating all parameters in a model or a poor model (133). Generally, a condition number exceeding 1000 is considered “large” (134).

Thesis Overview and Research Objectives

The general aim of this thesis was to develop population pharmacokinetic models of AS and DHA in different populations, including the estimation of pharmacokinetic

parameters, variability associated with these parameters, and identification of covariates that might explain the variability seen. The specific aims were to:

1. Develop a population pharmacokinetic model of AS and DHA in healthy subjects who received either single- or multiple-dosing of AS, as a monotherapy regimen or in combination with pyronaridine.
2. Develop a population pharmacokinetic model of AS and DHA in adult and pediatric patients with uncomplicated falciparum and vivax malaria who were administered oral pyronaridine/artesunate combination once daily for 3 days.

This thesis is organized such that Chapter II and Chapter III correspond to each of the above specific aims. Each chapter is independent and contains individual literature review, problem formulation, and discussion of the original results. Chapter IV summarizes the works in this thesis and provides recommendation for future works. Computer codes used in the modeling and summaries of the result output can be found in the appendices.

Figure 1.1 Schematic representation of malaria life cycle.

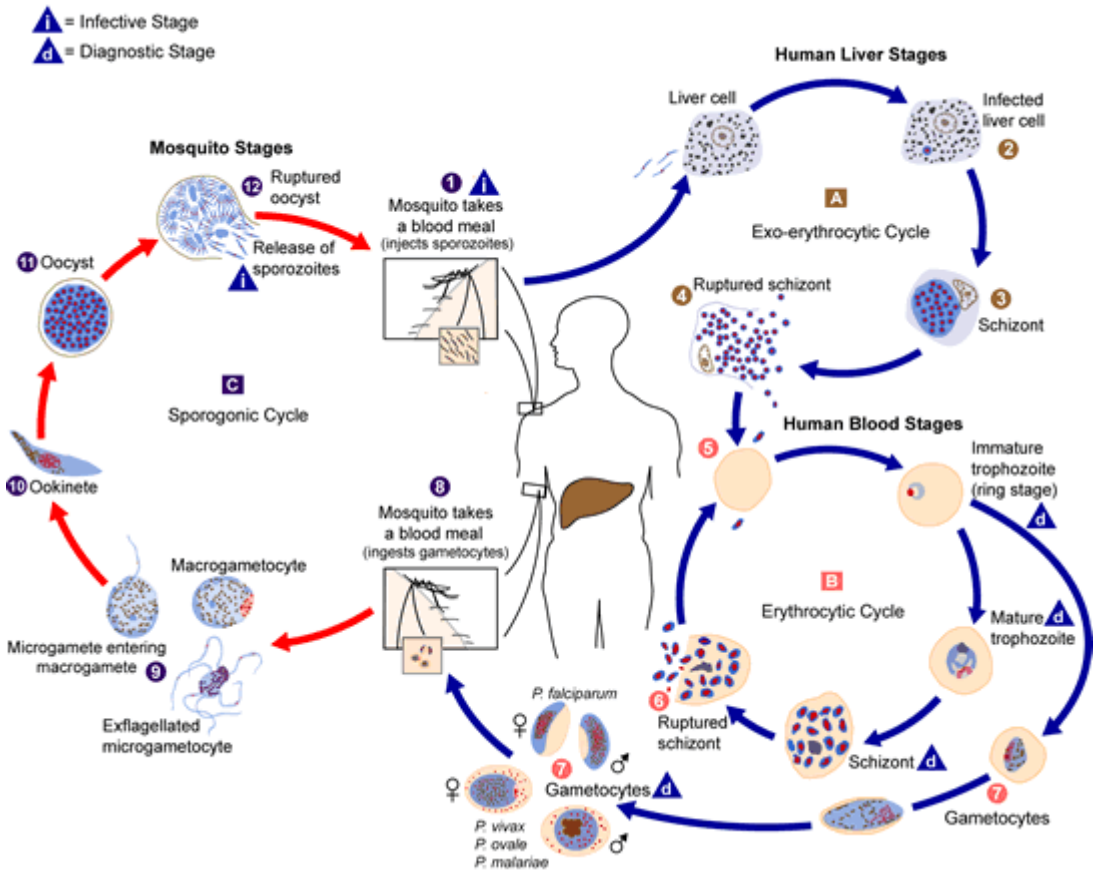

Figure 1.2 Chemical structures of artemisinin derivatives.

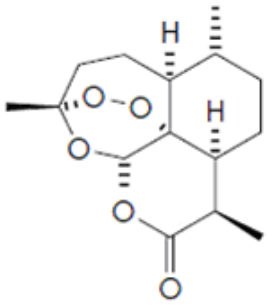

Artemisinin

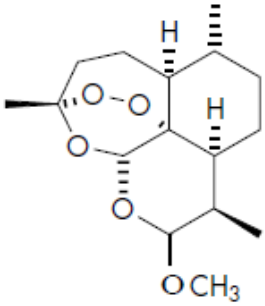

Artemether

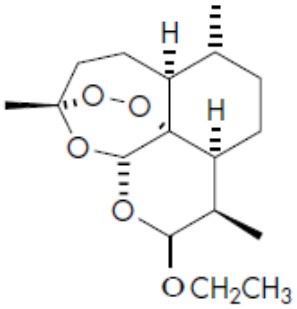

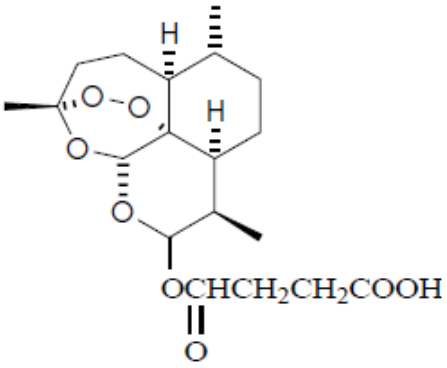

Artesunate

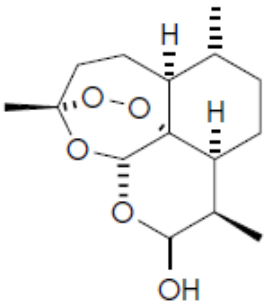

Dihydroartemisinin

Figure 1.3 Typical concentration-time profiles for AS (solid line) and DHA (broken line) follwing oral administration of AS.

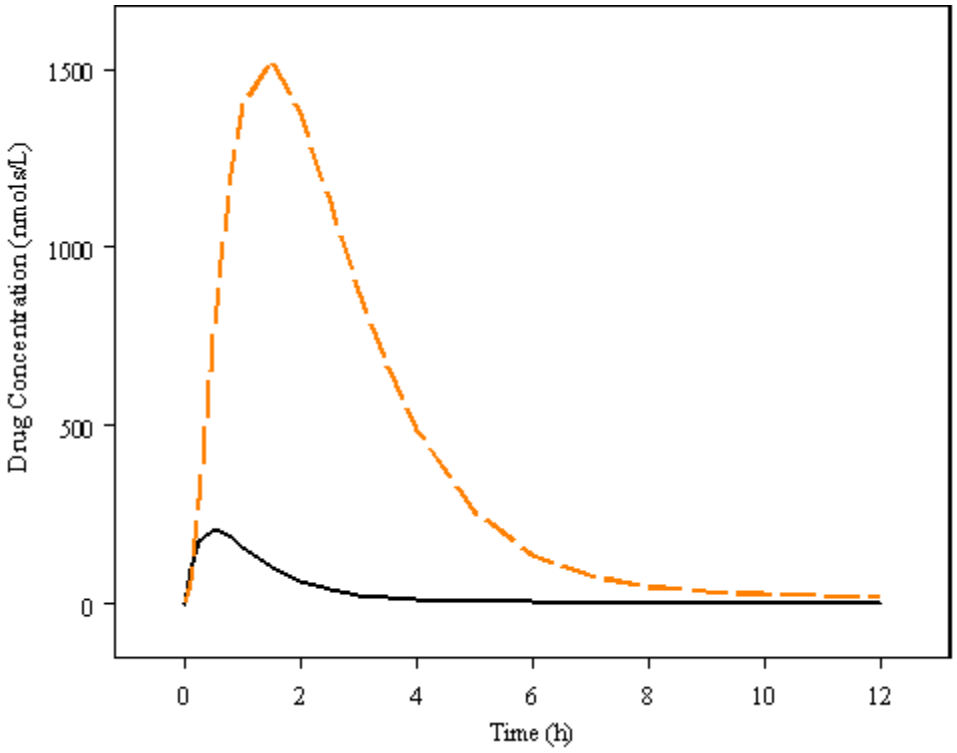

CHAPTER II

POPULATION PHARMACOKINETICS OF ARTESUNATE AND DIHYDROARTEMISININ IN HEALTHY SUBJECTS

Introduction

Malaria is one of the deadliest infectious diseases in the world, causing nearly a million deaths among more than 3 billion people who were at risk in 2006 (1). Unfortunately, given the high burden of the disease, the number of available anti-malarial drugs is relatively small. On top of that, the emergence of resistance to the most affordable anti-malarial drugs has seriously undermined the global effort to control malaria. As the result of chloroquine and sulfadoxine-pyrimethamine resistance, millions of lives that could otherwise be saved were sacrificed over the past 30 years (135). Artemisinin-based combination therapies (ACTs) are now being widely used as the first-line treatments for *P. falciparum* malaria throughout the world.

Artemisinin and its derivatives, dihydroartemisinin (DHA), artesunate (AS), artemether and arteether are fast acting anti-malarial drugs producing the most rapid reduction in parasitemia (136). These agents also have gametocytocidal activity, which contributes to the reduction in the disease transmission (22, 137). Among the available derivatives, AS has the most appealing physicochemical and pharmacological properties. It is more water soluble, thermally and chemically more stable, and rapidly converted *in vivo* to its active metabolite DHA which is responsible for most of the anti-malarial activity (138, 139).

Pyronaridine (PYR) is a Mannich-base derivative anti-malarial that has been shown to be efficacious against erythrocytic stages of *P. falciparum* using *in vitro* models (140-142). Clinical studies have also indicated that PYR is safe and efficacious against *P. falciparum* even in area with chloroquine-resistant strains (143-145). Pyronaridine

tetraphosphate plus artesunate (PA) is under development as a 3:1 fixed ratio combination for the treatment against *P. falciparum* and *P. vivax* malaria.

Population pharmacokinetics of AS and/or DHA following the administration of AS have been previously described in malaria patients. Karunajeewa and colleagues investigated the disposition of AS and DHA in 47 children from Papua New Guinea with uncomplicated malaria after the administration of AS suppositories (146). The population pharmacokinetics of DHA were also assessed in 164 patients with moderately severe falciparum malaria following intra-rectal dosing of AS and in 24 pregnant women with acute uncomplicated falciparum malaria after the administration of oral AS (147, 148). However, parent AS data were not modeled in these two studies, mainly because there were too few data points available for AS.

To date, no population pharmacokinetics analysis of AS and DHA has been published in healthy subjects receiving oral AS dosing. Such analysis will provide a means of comparing the pharmacokinetics of AS and DHA in malaria patients and healthy subjects and therefore expand our understanding in the effect of the disease state on the pharmacokinetics of AS and DHA. The aims of this analysis are to develop a population pharmacokinetic model of AS and DHA in healthy subjects following oral administration of PA combination or AS alone and to identify covariates that are important determinants of the variability seen in pharmacokinetic parameters of AS and DHA.

Materials and Methods

Subjects and Study Designs

Data used in performing this analysis were pooled from a four-part Phase I clinical trial (Protocol number SP-C-001-03). All studies were conducted at the Clinical Trial Center of Seoul National University, Seoul, South Korea, in accordance with the Guidelines of Good Clinical Practice and Declaration of Helsinki. Ethical approval was

obtained from Institutional Review Board of Seoul National University. Written informed consent was obtained from each subject prior to the studies. All subjects were healthy Korean men and women evaluated by a physician at screening (Day -21 to -2) based on physical examination, vital signs, electrocardiogram, medical history and laboratory evaluations. All study drugs and placebos were provided by Shin Poong Pharmaceuticals (Seoul, Korea) and were identical in appearance to maintain blinding.

The first part was designed as a single oral ascending dose, randomized, double-blind, placebo-controlled, staggered and parallel group study to evaluate the pharmacokinetics, safety and tolerability of PA following single oral administration of PA at following doses: 6+2 mg/kg, 9+3 mg/kg, 12+4 mg/kg or 15+5 mg/kg. Nine subjects were recruited for each dose level, and randomized to receiving either PA treatment or placebo in 7:2 ratio. It was also carefully noted that at least two of each gender should receive active in each cohort.

The second part was conducted to evaluate the potential of drug interaction between PYR and AS when used as a combination in 3:1 ratio. It was a 2-cohort parallel, 2-period randomized, blinded, crossover study of a single oral dose of PA 12+4 mg/kg versus each of the individual drug at the same dose plus placebo of the other drug. 20 subjects were enrolled into this study, and randomly assigned into either cohort 1 or cohort 2 in equal numbers. In cohort 1, 5 subjects received PYR alone in period 1 followed by PA combination in period 2, while another 5 received the treatments in reverse order. In cohort 2, 5 subjects received AS alone in period 1 followed by PA combination in period 2, while another 5 received the treatments in reverse order. There was a 21-day washout period between the two periods.

The third study was a 2-period, randomized and crossover study to investigate the effect of food on the pharmacokinetics of PA. 20 subjects were enrolled into the study and randomly allocated to each of the fasted or the fed arm in equal numbers. After an overnight fast of at least 10 hours, the subjects in the fasted arm received PA 12+4 mg/kg

with 240 mL of water and remained fasted for at least 4 hours post-dose while the subjects in the fed arm subjects were given the test meal 30 minutes prior to the treatment. The meal provided was a high-fat (approximately 50% of the total calorific content of the meal) and high calorie (approximately 800-1000 calories) meal. The meal contained approximately 150, 250, and 500-600 calories from protein, carbohydrate and fat, respectively. Meal composition was based on the FDA guidelines for food effect studies (149). Water was permitted as desired except for 1 hour before and after drug administration and a standard meal was scheduled at the same time in each period of the study for each subject. After a washout period of 21 days, the subjects returned for the crossover treatment.

The purpose of the last part of trial was to evaluate the pharmacokinetics, safety and tolerability of PA following multiple oral dosing of PA at following doses: 6+2 mg/kg, 9+3 mg/kg, 12+4 mg/kg or 15+5 mg/kg once daily for three consecutive days. The study design was otherwise similar to the design of the first study. Eight subjects were recruited for each dose level, and randomized to receiving either PA treatment or placebo in 6:2 ratio. The schematic representations of the study designs are shown in Figures 2.1-2.4.

Sample Collection and Storage

For the first three studies, venous blood samples for the determination of AS and DHA pharmacokinetics were collected prior to dosing and at 0.33, 0.67, 1.33, 1.67, 2, 2.5, 3, 4, 5, 8 and 12 hours post-dose. For the multiple-dosing study, the samples were taken prior to the dosing of each dose and at 0.33, 0.67, 1, 1.33, 1.67, 2, 2.5, 3, 4, 5, 8 and 12 hours after the third dose. Blood samples were collected into pre-chilled sampling tubes containing potassium oxalate/sodium fluoride (BD Vacutainer systems, Franklin Lakes, NJ) and placed on wet ice before centrifugation within 5 minutes of collection. Immediately after centrifugation, plasma was removed and transferred into two

approximately equal volume aliquots in screw cap Nalgene cryovials and then frozen immediately at or below -80°C until analysis.

Analytical Method

Plasma concentration of AS and DHA were determined using a validated liquid chromatography-mass spectrometric method described by Naik et al. (150). All samples were assayed in the same laboratory. The plasma samples spiked with internal standard artemisinin was cleaned up using solid phase extraction method. The extraction cartridges were activated with 1 mL of methanol followed by 1 mL of 1 M acetic acid. The plasma samples were then loaded to the cartridges. The cartridges were washed with 2 mL of 1 M acetic acid followed by 1 mL of 20% methanol in 1 M acetic acid. The analytes were eluted from the cartridges using 2 mL of 40% ethyl acetate in butyl chloride. The non aqueous step was applied immediately after the washing step. The eluent was evaporated by stream of nitrogen. The residue was reconstituted with 200 μL of mobile phase and 25 μL was injected on to column.

Analysis was performed with a Shimadzu Model 2010 liquid chromatograph-mass spectrometer (Shimadzu, Columbia, MD) in single ion monitoring positive mode using atmospheric pressure chemical ionization as an interface. Both α and β tautomers of DHA were separated, however only the α tautomer of DHA was taken into account for quantitation. Under the chromatographic condition, the ratio of α and β was about 4:1. The lower limit of quantification (LOQ) for AS and DHA using 0.5 mL of plasma was 1 ng/mL (equivalent to 2.6 nmols/L for AS and 3.5 nmols/L for DHA). The coefficient of variation for intra-day and inter-day precision ranged from 7% to 14% and 9% to 14% for AS, and 11% to 14.9% and 11% to 15% for DHA, respectively.

Population Pharmacokinetics Analysis

Base Model Development

Nonlinear mixed-effects model building was conducted using NONMEM software version VI, level 2.0 (ICON Development Solutions, Ellicott City, MD) (119), as implemented on a Windows XP operating system (Microsoft Corporation, WA, Seattle) with G95 Fortran compiler (Free Software Foundation, Boston, MA). All models were fitted using the first-order conditional estimation method. NONMEM output was processed using PDx-Pop 3.10 (ICON Development Solutions, Ellicott City, MD) and Xpose version 4.0 (Uppsala University, Uppsala, Sweden) (151). Graphical plots were produced using S-PLUS version 8.0 (Insightful Inc, Seattle, WA) and R 2.8.1 (Free Software Foundation, Boston, MA).

Measurements below the LOQ of the assay were excluded from the dataset. Since the molecular weights of AS and DHA are quite different (384.4 for AS and 284.9 for DHA), the concentrations were converted to the equivalent values in nmols/L. AS dose was also converted to the equivalent values in nmols. The concentrations were then natural log-transformed before the analysis.

Model selection was guided by the plausibility of the estimates, minimum objective function value (MOFV), equal to minus twice the log-likelihood function, Akaike Information Criterion (AIC), equal to MOFV plus two times the number of parameters, condition number, defined as the ratio of the largest eigenvalue to the smallest eigenvalue, visual inspection of diagnostic plots and the precision of parameter estimates.

In the initial stage of model building, one- and two-compartment pharmacokinetic models with first order absorption and first order elimination were fitted to the AS data to determine the best structural model for AS. Once the best pharmacokinetic model for AS was determined, DHA data was modeled as a metabolite compartment connected to the

central compartment of AS. It was assumed that conversion to DHA was the only significant route of elimination for AS and that the conversion was irreversible (84). One- and two-compartment models with first-order disposition were tested for DHA to develop the best metabolite structural model. For the two-compartment model, it was assumed that DHA was eliminated only from the central compartment. After the best structural model was determined, all parameters were estimated simultaneously using ADVAN 6 in NONMEM.

Inter-individual variability (IIV) of the pharmacokinetic parameters was modeled assuming a log-normal distribution, as follows:

$$P_i = P_{pop} \bullet \exp(\eta_i)$$

where P_i is the estimated parameter value for individual i, P_{pop} represents the typical population estimate for the parameter and η_i is the deviation of P_i from P_{pop}. The η random effects were assumed to be independent and symmetrically distributed with zero mean and variance ω^2. A diagonal covariance matrix was modeled, as the data did not support the implementation of a full variance-covariance matrix. The magnitude of inter-individual variability was expressed as coefficient of variation (%CV).

Residual variability (RV) was modeled using an additive model as shown below:

$$\ln C_{ij} = \ln C_{pred,ij} + \varepsilon_{ij}$$

where C_{ij} and $C_{pred,ij}$ represent the jth observed and model predicted AS or DHA concentrations, respectively, for individual i and ε_{ij} denotes the additive residual random error for individual i and observation j. The ε random effects were assumed to be independent and symmetrically distributed with zero mean and variance σ^2.

Covariate Model Development

After the optimum model for AS and DHA was determined, covariate analysis was carried out to assess additional variables as possible determinants of the variability seen in the pharmacokinetic estimates. Covariates examined include total body weight,

age, gender, type of dosing (single- or multiple-dosing), co-administration of PYR and food intake (fasted or fed). Body weight and age were treated as continuous covariates while gender, dosing type, co-administration of PYR and food intake were treated as categorical covariates. The coding for the categorical variables is as follows:

1. Gender was coded as 0 for female and 1 for male.
2. Dosing type was coded as 0 if subjects received single oral AS dose or 1 if subjects received multiple oral AS dose.
3. Co-administrationof PYR was coded as 0 if AS was administered as monotherapy or 1 if AS was administered in combnation with PYR.
4. Food intake was coded as 0 for fasted subjects or 1 for fed subjects.

Potential covariates were initially identified using generalized additive modeling (GAM) as implemented in the Xpose software. The potential covariates were then tested using stepwise forward addition followed by stepwise backward elimination procedure (152). The influences of the covariates were tested by adding a covariate to the model at a time in the forward addition step, and then by removing a covariate from the model at a time in the backward elimination step. The changes in MOFV between the 'full' and the 'reduced' models were then calculated. The difference in MOFV between two nested models was approximated by a χ^2 distribution. An MOFV change of 3.84 (corresponding to a significance level of 5% at one degree of freedom) was used as the cutoff to include a covariate in stepwise addition. When no more covariates could be included, the stepwise backward elimination was carried out. For a covariate to remain in the model, a change in MOFV of at least 10.83 (corresponding to a significance level of 0.1% at one degree of freedom) was needed.

The relationship between continuous covariates and pharmacokinetic parameters were evaluated using both linear and power functions, with the covariates centered or scaled at their median values:

$P = \theta_1+\theta_2 \bullet (WT-61.5)$ for linear function

$P = \theta_1 \bullet (WT/61.5)^{\theta 2}$ for power function

where θ_1 represents the parameter estimate P of an individual with a body weight of 61.5 kg and θ_2 is a factor describing the correlation between body weight and the parameter. The influences of binary covariates on the parameter were modeled using a proportional relationship, as follow:

$P = \theta_3 \bullet (1+\theta_4 \bullet FOOD)$

where θ_3 represents the parameter value in subjects receiving the test drug without food, and θ_4 is the fractional change in the parameter in subjects receiving the test drug with food. FOOD variable was coded as 0 for the fasted subjects and 1 for the subjects who received test drug with food.

Model Evaluation

The non-parametric bootstrap procedure was employed to evaluate the precision of the parameter estimates and the robustness of the final model. 500 bootstrap datasets were generated by repeated random sampling with replacement from the NONMEM input data file, and the final NONMEM model was fitted to the bootstrap datasets. Bootstrap parameter estimates, standard errors and 95% confidence intervals were obtained and compared with the parameter estimates from the original dataset.

Visual predictive check was also performed to evaluate the predictive ability of the model. 500 virtual observations at each sampling time point were simulated using the final model and its parameter estimates. The observed data were then plotted with the 5th, 50th and 95th percentiles of the simulated data that was above the LOQ. The percent of observations outside the 90% prediction interval was also calculated. The condition number of the final model was also calculated as a measure of the stability of the model.

Results

Data

Data from 118 concentration-time profiles arising from 91 healthy Korean subjects were pooled from four clinical studies. The subjects received single- or multiple-dosing of 2-5 mg/kg AS orally either in combination with PYR or as a monotherapy regimen with or without food. A total of 9 and 18 subjects contributed two pharmacokinetic profiles each in separate occasions for the drug-interaction and food effect study, respectively. Since the elimination half-lives for AS and DHA are very short and the elimination of the drugs are deemed to have completed after the 21-day washout period, the pharmacokinetic profiles arising from the same subject in different occasions were treated as independent profiles. 916 and 1352 concentration measurements for AS and DHA respectively were used in the modeling. The plots of observations versus time after dose for AS and DHA are shown in Figure 2.5 and Figure 2.6. Table 2.1 and Table 2.2 summarize the study and the data characteristics as well as demographics of the patients included in this analysis.

Model Development

A one-compartment model with first order absorption and first order elimination best described the AS data. When a two-compartment model was fitted to the AS data, minimum MOFV and AIC were reduced moderately (11.897 and 3.897 unit, respectively). However, the visual inspection of goodness-of-fit plots showed no improvement in the fit. The precision of the estimates obtained were also slightly worse. Consequently, the simpler one-compartment model was used to fit the AS data.

The DHA data were then sequentially modeled using a one-compartment model with linear elimination and also a two-compartment model. The two-compartment model fitted the DHA data better, leading to165.186 and 157.186 unit reduction in MOFV and

AIC respectively. Goodness-of-fit plots also showed obvious improvement in the overall fit.

The final model used to simultaneously model the AS and DHA data consisted of a dosing compartment, a central compartment for AS, a central compartment and a peripheral compartment for DHA, as shown in Figure 2.7. The model was parameterized in terms of absorption rate constant for AS (Ka), apparent clearance for AS (CL/F, where F is the unknown oral bioavailability), apparent volume of distribution of the central compartment for AS (V2/F), apparent clearance for DHA from the central compartment (CLM/F), apparent central volume of distribution for DHA (V3/F), inter-compartmental clearance for DHA (Q/F), and apparent peripheral volume of distribution for DHA (V4/F). Inter-individual variability was estimated for all parameters but Q/F and V3/F, since the available data would not support the inclusion of the two terms. Fixing the variance of the random effects for Q/F and V4/F to zero had little influence on the MOFV, and was essential for the model to minimize successfully and to calculate the covariance matrix of the estimates. The population estimates of apparent clearance (CL/F) and volume of distribution (V2/F) for AS were 1190 L/h with 36.2% inter-individual variability and 1210 L with 57.4% inter-individual variability, respectively. For DHA, the population estimates of apparent clearance (CLM/F) and central volume of distribution (V3/F) were 93.7 L/h with 28% inter-individual variability and 97.1 L with 30% inter-individual variability, respectively. The population estimates of apparent inter-compartmental clearance (Q/F) and peripheral volume of distribution (V4/F) for DHA were 5.74 L/h and 18.5 L, respectively.

A summary of the covariates evaluated is shown in Table 2.2. Food intake (FOOD) and total body weight (WT) were found to be significant covariates on Ka and CLM/F, respectively, in the following relationships:

$Ka = 3.85 \bullet (1-0.84 \bullet FOOD)$, where FOOD=0 if fasted and FOOD=1 if fed;

$CLM/F = 93.7+1.9 \bullet (WT-61.5)$

The typical value of Ka for subjects taken the test drug without food is 3.85 h^{-1}. When the drug was taken with high fat and high caloric meal, Ka of AS was reduced by 84%. The inclusion of food intake as a covariate in the final model reduced the inter-individual variability of Ka from 135% to 112%, indicating that this covariate accounted for 31% of the variability on Ka. The apparent clearance of DHA, CLM/F was correlated with total body weight, in which a unit change in the weight would result in 1.9 unit change in CLM/F in the same direction. With the incorporation of weight in the final model, the inter-individual variability of CLM/F was reduced from 31.4% to 28%, thus accounting for 20% of the variability.

Goodness-of-fit plots for AS and DHA indicated a reasonable fit of the model to the data (Figures 2.8-2.11). Final estimates of the parameters are shown in Table 2.3. The parameters were well estimated in general, with percent relative standard error ranged from 2.3% to 36%. Parameter related to absorption showed the most variability, with inter-individual variability for Ka was estimated to be 112% even after the incorporation of food intake as a covariate. Residual variability was higher for AS observations than DHA observations. Individual plots for every five subjects are presented in Figure 2.12 and Figure 2.13 for AS and DHA, respectively.

Model Evaluation

78% of the 500 non-parametric bootstrap runs converged successfully. The parameter estimates and 95% confidence interval for the parameters were calculated from the converged runs and are presented in Table 2.3. The parameter distributions were generally symmetrical. All the estimates obtained from the final model were comparable to the bootstrap estimates and were contained within the 95% bootstrap confidence intervals.

Figure 2.14 and Figure 2.15 shows the results of the visual predictive check for AS and DHA. Overall, the final model adequately described the observed concentrations.

About 11.6% and 9.8% of the AS and DHA observations were not contained within the 90% prediction interval. The condition number of the final model was 24, indicating that the model was stable.

Discussion

In the current analysis, we developed a parent-metabolite model to describe the population pharmacokinetics of AS and DHA in healthy subjects. To our best knowledge, this is the first population pharmacokinetic analysis of AS and DHA conducted using data derived from a large number of healthy subjects following oral administration of AS. The model developed was stable and was able to predict AS and DHA data arising from single- and multiple-dosing of oral AS equally well.

AS was rapidly absorbed into the systemic circulation, with an absorption half-life of 10.8 minutes estimated in this analysis. The conversion of AS to DHA was very rapid and the concentration of DHA was measurable as early as 20 minutes post-dose for all subjects. The sensitivity of the assay used in this study enabled the measurement of AS concentrations up to 8 hours post-dose and the measurement of DHA concentrations up to 12 hours post-dose, in 65% and 95% out of the total 1416 available samples, respectively. Therefore, we were able to characterize the distribution of lipophilic DHA to the peripheral tissue. The pharmacokinetic parameter estimates obtained using nonlinear mixed-effects modeling approach employed in this analysis are within similar range with those obtained using non-compartmental analysis for the same data set (153). Using non-campartmental analysis, the mean CL/F of AS and V/F of AS for the four studies ranged from 966.4-1728.6 L/h and 782.3-1558.6 L, respectively. The mean CL/F of DHA and V/F of DHA ranged from 89.4-139.5 L/h and 169.6-249.9L, respectively.

The pharmacokinetics of AS and DHA following orally administered AS in healthy subjects have been previously reported in different settings (76, 81, 154, 155). However, AS pharmacokinetics was not described in the reports by Benakis et al. (154)

and Na-Bangchang et al. (155). Navaratnam et al. (76) compared the pharmacokinetics of AS and DHA after administration of oral and rectal AS in 12 healthy male Malaysian volunteers using non-compartmental approach. Following a single oral dose of 200 mg AS, the mean area under the plasma concentration-time curve (AUC) to time infinity for AS was reported to be 119 ng.h/mL, corresponding to a CL/F of 1680 L/h. We reported a lower CL/F for AS (1190 L/h) in the current analysis using data from a much larger sample size. The bioanalytical method used to measure AS plasma concentrations was also more sensitive (LOQ = 1 ng/mL) in our analysis. Teja- Isavadharm and colleagues (81) studied the single-dose pharmacokinetics of AS following the administration of 100 mg of oral AS in 6 healthy subjects and 6 patients with uncomplicated falciparum malaria. In their study, the range of apparent clearance and apparent volume of distribution in healthy subjects were 4.69-29 L/h/kg and 4.2-49.6 L/kg for AS, 1.66-3.26 L/h/kg and 1.99-4.45 L/kg for DHA, respectively. The weight normalized apparent clearance and apparent volume of distribution obtained in this analysis were 19.3 L/h/kg and 19.7 L/kg for AS, 1.52 L/h/kg and 1.88 L/kg for DHA, respectively. The estimates obtained in this present analysis are within the similar magnitude compared to their findings.

Population pharmacokinetics of AS and/or DHA in malaria patients have been described in four other papers (146, 147, 156, 157). Karunajeewa et al. (146) proposed a three-compartment model (a rectal absorption compartment, a central compartment for AS and a central compartment for DHA) to describe the population pharmacokinetics of AS and DHA simultaneously in pediatric patients following administration of AS suppositories. Simpson et al. (147) modeled only the DHA data pooled from five Phase II and III studies conducted in adult and pediatric malaria patients. Both the weight-normalized CL/F and V/F for AS obtained in our analysis are much larger than the ones reported by Karunajeewa et al. (5.9 L/h/kg and 2.1 L/kg, respectively) (146). The larger CL/F and V/F for AS seen in our study might be attributed to the fact that the AS

bioavailability is reduced when oral AS is given compared to rectal AS (76). On the other hand, the weight-normalized CL/F and V/F for DHA obtained in our study are smaller than those reported by the two studies. Karunajeewa et al. reported values of 2.2 L/h/kg and 2.1 L/kg for the CL/F and V/F of DHA (146). The typical CL/F values of DHA reported by Simpson et al. were 3.17 L/h/kg for a male and 2.03 L/h/kg for a female. For an adult weighted 70 kg, the typical value for V/F of DHA was 6.34 L/kg (147). This finding is also consistent with the observations that the AUC for DHA following oral administration of AS was higher than that following rectal AS (76, 158), suggesting that the bioavailability of DHA was increased when oral AS was given.

McGready et al. (156) characterized the population pharmacokinetics of DHA in pregnant women with acute uncomplicated falciparum malaria following a three-day dosing of oral AS (4 mg/kg/day) and atovaquone plus proguanil. However, the pharmacokinetics of AS was not evaluated because AS was detectable only in about 6.5% of the total available samples. The pharmacokinetic parameter estimates for DHA were therefore derived using AS dose in DHA equivalents. The oral clearance for DHA was reported to be 88.5 L/h, which is similar in our analysis. However, the estimate for DHA apparent volume of distribution in healthy Korean subjects obtained in this analysis is about 60 % lower compared to the pregnant Karen patients in their study (4.63 L/kg). The larger volume of distribution seen in their study might be attributed to the physiological changes during pregnancy and the effect of the disease state.

Stepniewska et al. conducted a population pharmacokinetic study of AS in African children with acute malaria from six months to five years old (157). The subjects received either the fixed dose combination of AS and amodiaquine or the separate tablets of both drugs. The DHA data was modelled using nonlinear mixed-effects approach. The weight normalized CL/F of DHA reported in their study was 0.636 L/h/kg , which was almost 60% lower than the value analysis in healthy adults. The discrepancy could be related to the developmental changes of metabolizing enzymes that take place in the

young children. It has been demonstrated that the glucuronidation of DHA was catalyzed by UDP-glucuronosyltransferases (UGTs), in particular UGT1A9 and UGT2B7 (84). The capacity of these metabolizing enzymes in young children could be much less than the full capacity in adults and therefore resulted in lower CL/F of DHA. In a review on developmental patterns of UGT system, de Wildt et al. suggested that the use of per-kg model for clearance is adequate to address developmental changes in young children and may lead the underestimation of clearance by up to 200% in children under 3.4 kg of body weight (159). The reported weight-normalized V/F of DHA by Stepniewska et al. was 2.285 L/kg, which was quite similar to the value obtained in this analysis (157).

In the present analysis, food intake was found to significantly delay the absorption of AS. When AS dose was administered after the intake of high-fat and high-caloric meal, the population absorption half-life of AS increased from 10.8 minutes to 67.5 minutes. However, the extent of absorption was not altered significantly. Body weight affected CLM/F significantly and therefore was included as a covariate in the final model. The average CLM/F for a healthy subject with 61.5 kg of body weight was estimated to be 93.8 L/h. A unit deviation in body weight would result in 1.9 unit deviation in the CLM/F from the population estimate. None of the other covariates tested was significant determinants of the variability seen. Co-administration of PYR did not affect any of the pharmacokinetic parameters of AS and DHA.

Remarkable time-dependent pharmacokinetics of artemisinin has been observed in both healthy subjects and in malaria patients after single or repeated oral and rectal administration of artemisinin dose (55, 56, 58, 160). Auto-induction of CYP2B6 and CYP2C19 was proposed to be the main mechanism causing the decline of plasma artemisinin concentrations (62, 161, 162). A semi-physiological pharmacokinetic model taking into account the autoinduction phenomenon has been developed for artemisinin in healthy subjects (64). Conflicting observations have been reported concerning the autoinduction phenomenon after the administration of AS dose. In their unconvincing

report, Khanh et al. (68) observed a decline in DHA concentrations in 6 malaria patients following repeated AS dosing. However, the decline in either AS or DHA concentration was not observed in two other studies (57, 69). In this analysis, we tested the type of dosing in the covariate analysis to investigate any differences in the pharmacokinetics of AS and DHA following the administration of single- and multiple-dose of AS. None of the AS and DHA pharmacokinetic parameters was affected by the type of AS dosing received at a significance level of 0.05. Visual predictive check plots in Figure 2.14 and Figure 2.15 shows similar distributions for AS and DHA observations following single- or multiple-dose of AS, indicating no sign of decline in AS and DHA concentrations after repeated AS dosing. The model described the AS and DHA observations equally well regardless the type of dosing received by the healthy subjects.

In conclusion, a descriptive, robust and predictive parent-metabolite model has been developed using population approach to characterize the pharmacokinetics of AS and DHA simultaneously in healthy subjects following oral administration of AS. In addition, presence of food and weight were found to impact the absorption and disposition of AS and DHA. The pharmacokinetic parameter estimates obtained in this analysis will also serve as a comparison for future works involving the characterization of population pharmacokinetics of AS and DHA following oral AS in malaria patients.

Table 2.1 A summary of the study and data characteristics.

Characteristic	Single dose study	Drug interaction study	Food effect study	Multiple dose study	All studies combined
Number of subjects	28	19	20	24	91
Mean AS dose received (mg/kg) (± S.D.)	3.4 ± 1.1	3.9 ± 0.16	3.9 ± 0.08	3.4 ± 1.1	3.7 ± 0.8
No. of concentration-time profiles	28	28	38	24	118
Total number of observations					
AS	206	207	324	179	916
DHA	316	314	449	273	1352
Number of observations <LOQ [N (%)]					
AS	130 (38.7)	129 (38.4)	132 (28.9)	109 (37.8)	500 (35.3)
DHA	20 (6)	22 (6.5)	7 (1.5)	15 (5.2)	64 (4.5)
Sampling schedule	Predose, 0.33, 0.67, 1, 1.33, 1.67, 2, 2.5, 3, 4, 5, 8 and 12 h postdose	Predose, 0.33, 0.67, 1, 1.33, 1.67, 2, 2.5, 3, 4, 5, 8 and 12 h postdose	Predose, 0.33, 0.67, 1, 1.33, 1.67, 2, 2.5, 3, 4, 5, 8 and 12 h postdose	Immediately prior to each dose and 0.33, 0.67, 1, 1.33, 1.67, 2, 2.5, 3, 4, 5, 8 and 12 h after the third dose	NA

Table 2.2 A summary of the subject demographics and covariates included in the analysis.

Characteristic	Single dose study	Drug interaction study	Food effect study	Multiple dose study	All studies combined
Age (years)	24 (19-40)	23 (20-32)	21.5 (19-27)	23 (19-29)	23 (19-40)
Weight (kg)	62.5 (50.4-70)	60.9 (50.1-67.1)	59.9 (50.8-68.5)	62.2 (51.2-68.8)	61.5 (50.1-70)
Gender [N (%)]					
Female	9 (32.1)	10 (52.6)	10 (50)	9 (37.5)	38 (41.8)
Male	19 (67.9)	9 (47.4)	10 (50)	15 (67.9)	53 (58.2)
Type of dosing	Single	Single	Single	Multiple (once daily for 3 days)	Single and multiple
Food intake (number of profiles)					
Fasted	28	28	19	24	99
Fed	0	0	19	0	19

Continuous variables are given as median (range).

Table 2.3 A summary of the results obtained from the final model and the bootstrap analysis.

Parameter	Estimate	%RSE	Bootstrap estimate (95% CI)
CL/F (L/h)	1190	4.20	1176 (1060 – 1280)
V2/F (L)	1210	5.77	1199 (1020 – 1370)
Ka (h^{-1})	3.85	3.61	4.16 (2.66 – 6.67)
CLM/F (L/h)	93.7	3.30	92.6 (86.5 – 99.1)
V3/F (L)	97.1	4.85	96.5 (86.7 – 107)
Q/F (L/h)	5.74	12.8	5.69 (3.72 – 7.53)
V4/F (L)	18.5	10.6	18.7 (14.1 – 23.2)
$\theta_{FOOD-Ka}$	-0.84	2.32	-0.836 (-0.915 – -0.733)
$\theta_{WT-CLM/F}$	1.90	16.3	1.78 (0.993 – 2.58)
IIV (variances and %CV)			
IIV-CL/F	0.131 (36.2)	17.8	0.130 (0.0824 – 0.176)
IIV-V2/F	0.330 (57.4)	20.9	0.347 (0.201 – 0.497)
IIV-Ka	1.26 (112)	15.4	1.32 (0.751 – 2.00)
IIV-CLM/F	0.0786 (28.0)	22.5	0.0740 (0.0411 – 0.118)
IIV-V3/F	0.0901 (30.0)	36.0	0.0776 (0.0001 – 0.151)
RV (% CV)			
AS (nmols/L)	37.5	9.73	37.5 (31.0 – 45.2)
DHA (nmols/L)	28.2	11.2	27.7 (21.6 – 34.8)

RSE: relative standard error; CL/F: apparent clearance for AS; F: unknown bioavailability; V2/F: apparent volume of distribution of the central compartment for AS; Ka: absorption rate constant for AS, CLM/F: apparent clearance for DHA from the central compartment; V3/F: apparent central volume of distribution for DHA; Q/F: inter-compartmental clearance for DHA; V4/F: apparent peripheral volume of distribution for DHA; $\theta_{FOOD-Ka}$: parameter for the covariate food intake on Ka; $\theta_{WT-CLM/F}$: parameter for the covariate weight on CLM/F; CV: coefficient of variation; IIV: inter-individual variability; RV: residual variability; AS: artesunate; DHA: dihydroartemisinin.

Figure 2.1 Schematic representation of the single dose study design.

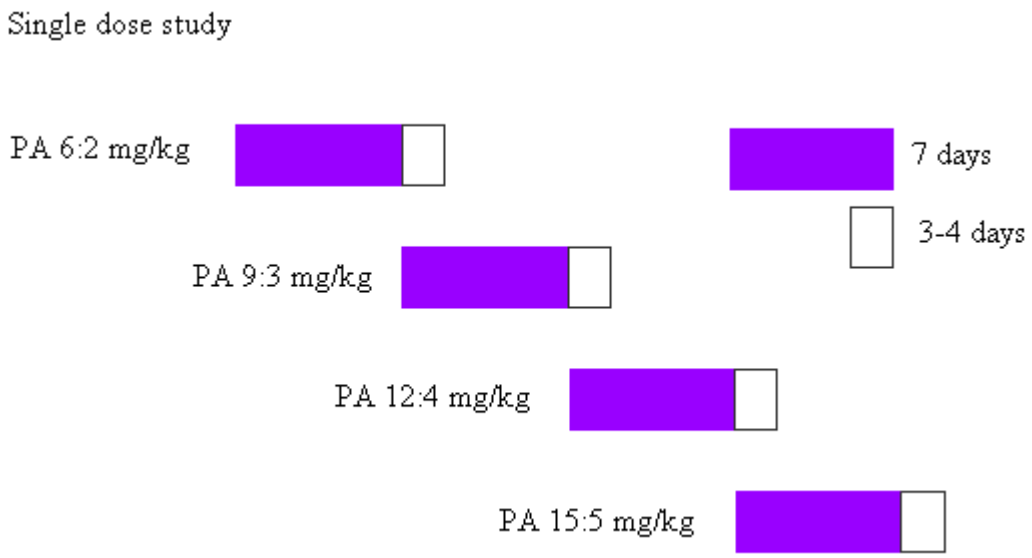

Figure 2.2 Schematic representation of the drug-interaction study design.

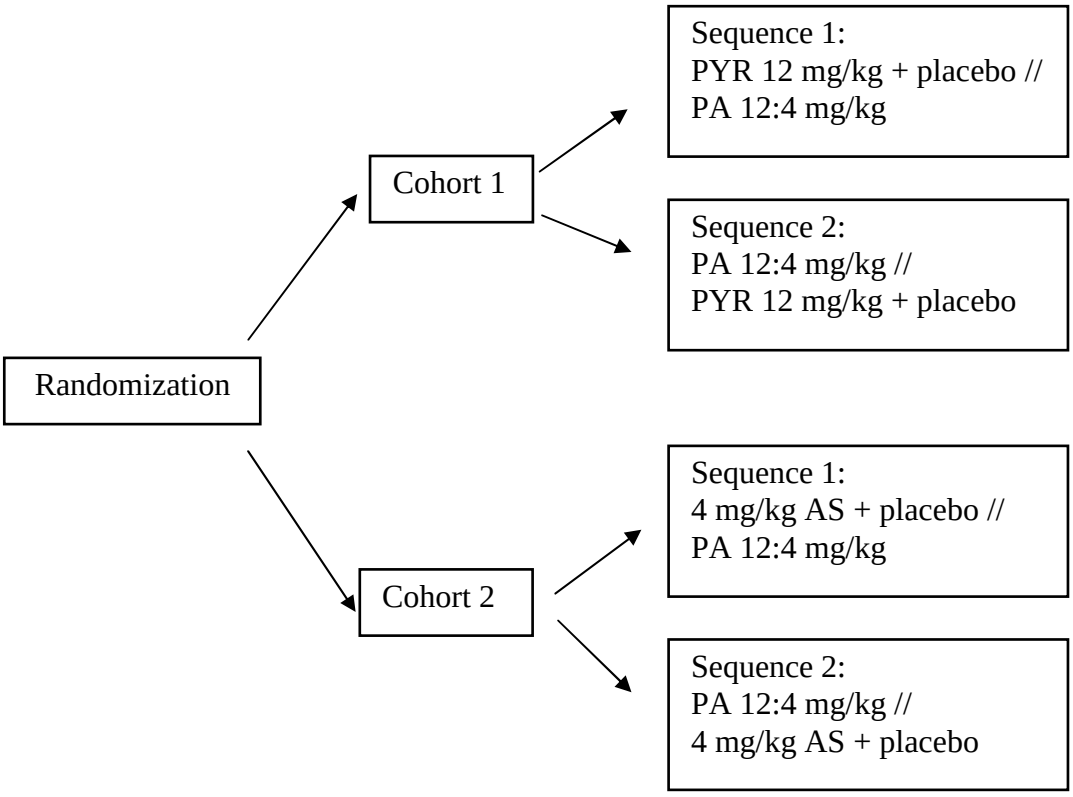

// Washout period of 21 days

Figure 2.3 Schematic representation of the food effect study design.

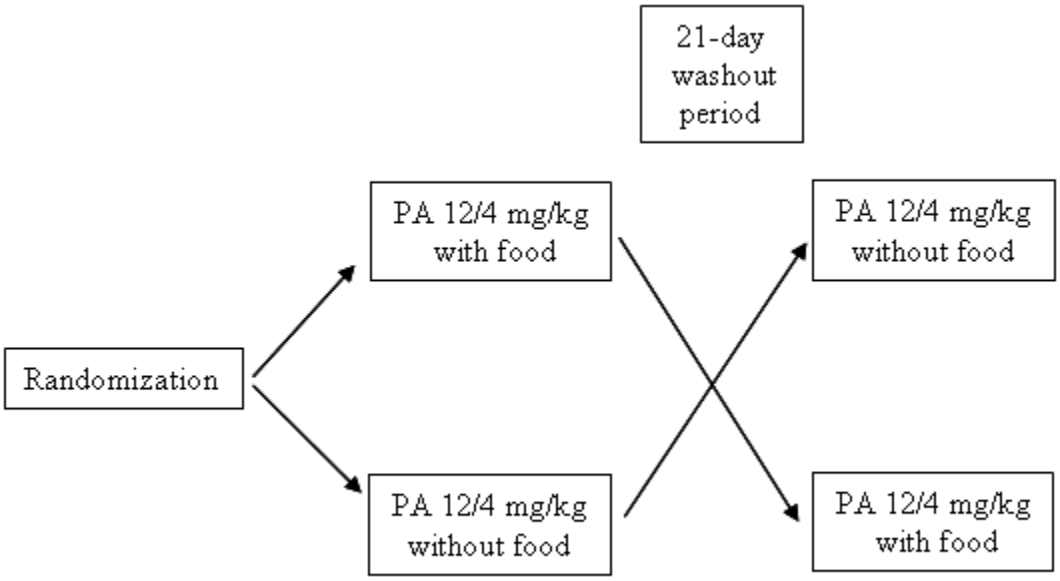

Figure 2.4 Schematic representation of the multiple dose study design.

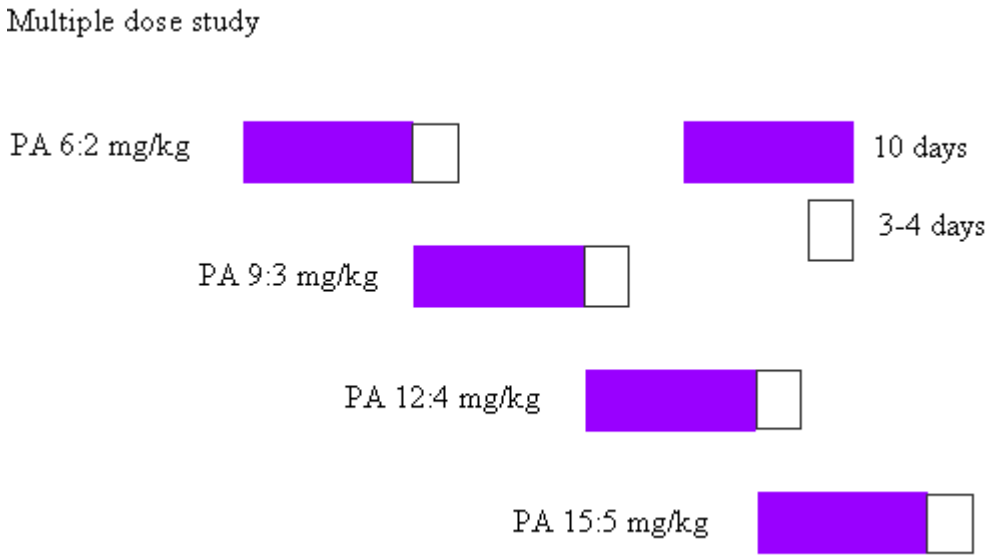

Figure 2.5 Semi-logarithmic plot of observed artesunate (AS) concentrations versus time after dose. The solid line is smoothing line.

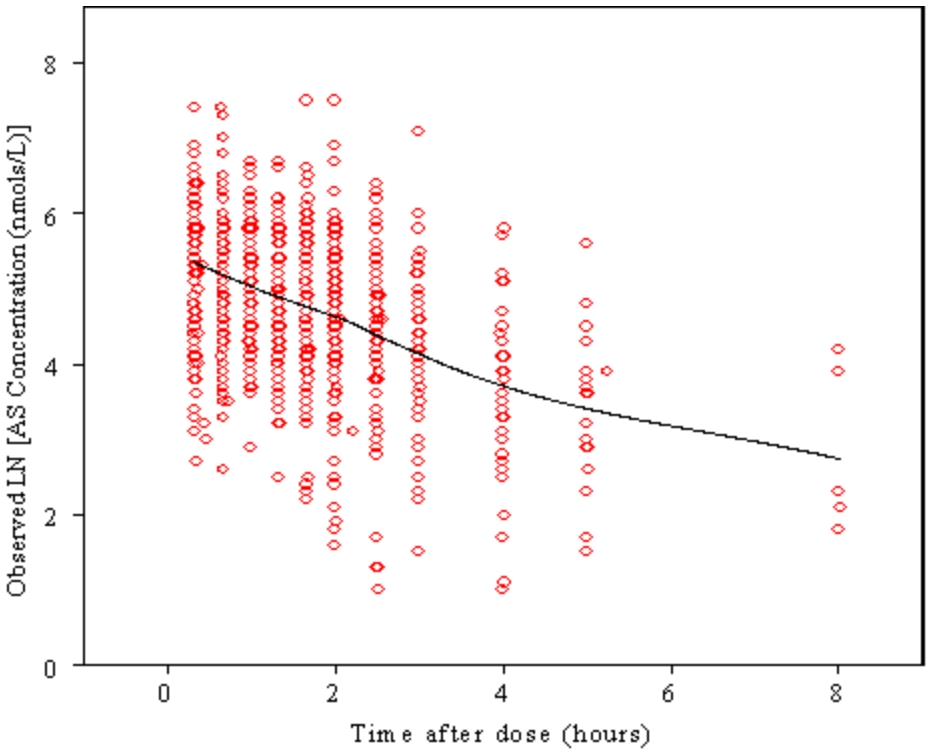

Figure 2.6 Semi-logarithmic plot of observed dihydroartemisinin (DHA) concentrations versus time after dose. The solid line is smoothing line.

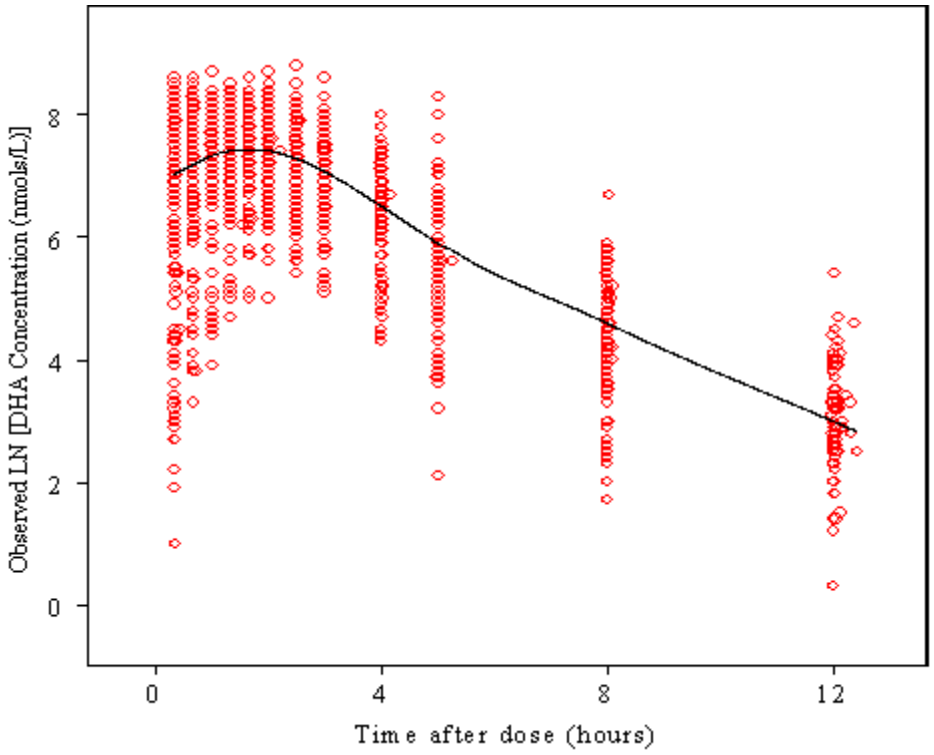

Figure 2.7 Schematic representation of the final structural model.

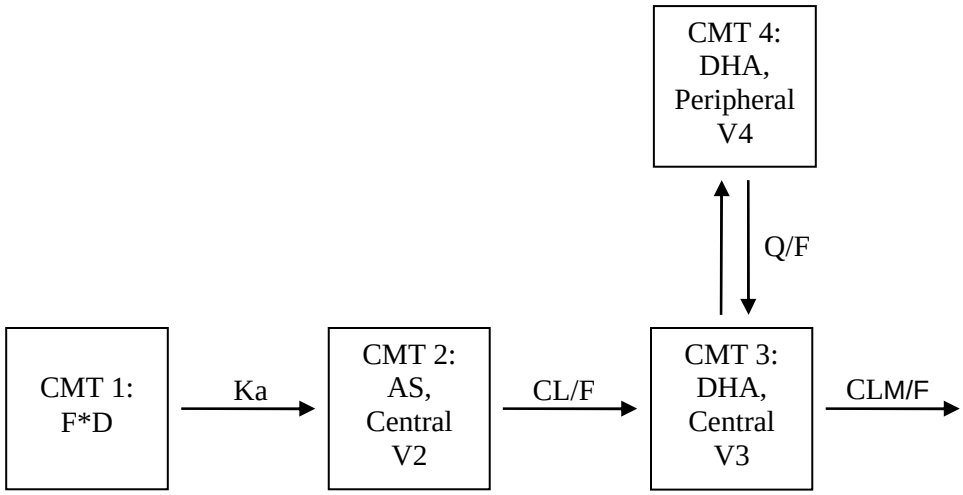

CMT, compartment; AS: artesunate; DHA, dihydroartemisinin; F, oral bioavailability; D, AS dose; Ka, absorption rate constant; CL, AS clearance; V2: central volume of distribution for AS; CLM, DHA clearance; V3; central volume of distribution for DHA; Q, inter-compartmental clearance; V4, peripheral volume of distribution for DHA.

Figure 2.8 Population and individual predicted concentration versus observed concentration plots of artesunate (AS) for the final model. The solid lines are lines of identity. The broken lines are smoothing lines.

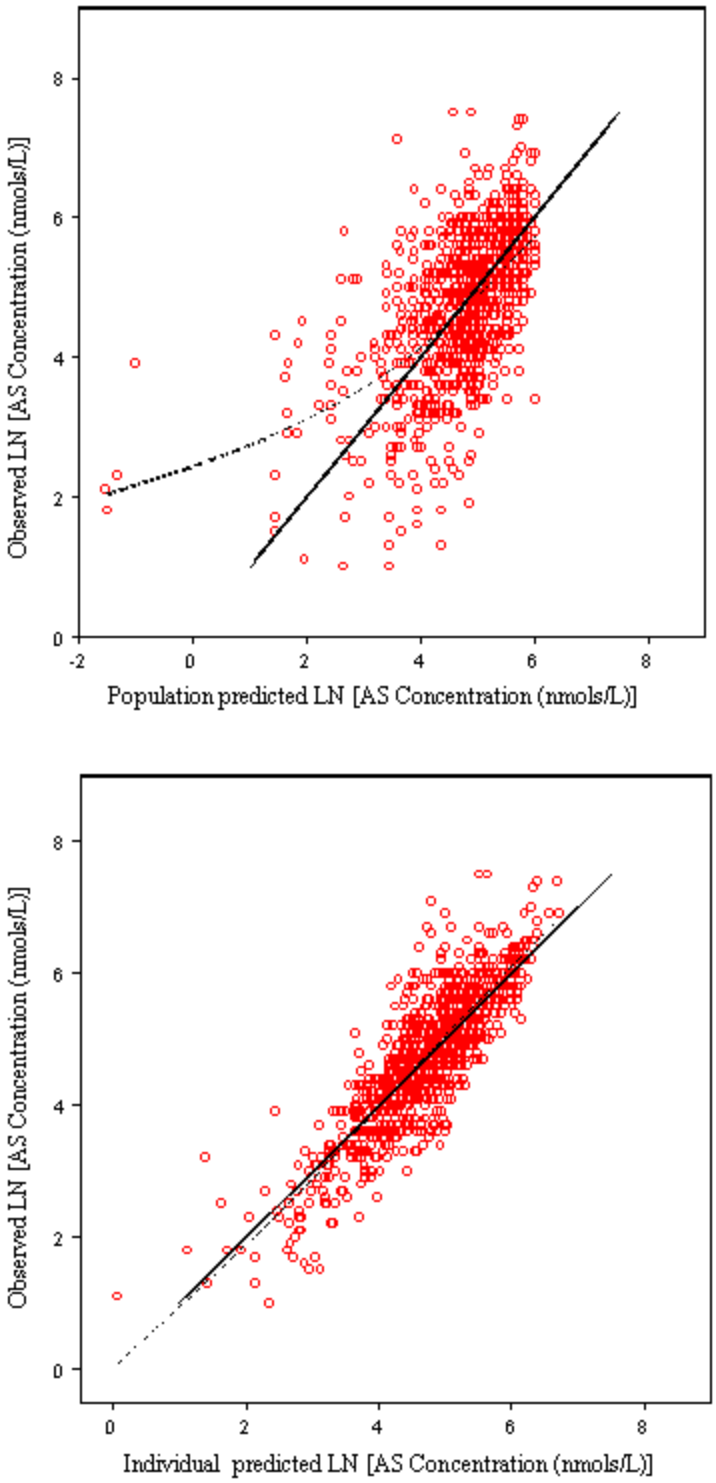

Figure 2.9 Conditional weighted residual plots of artesunate (AS) for the final model. The broken lines are smoothing lines.

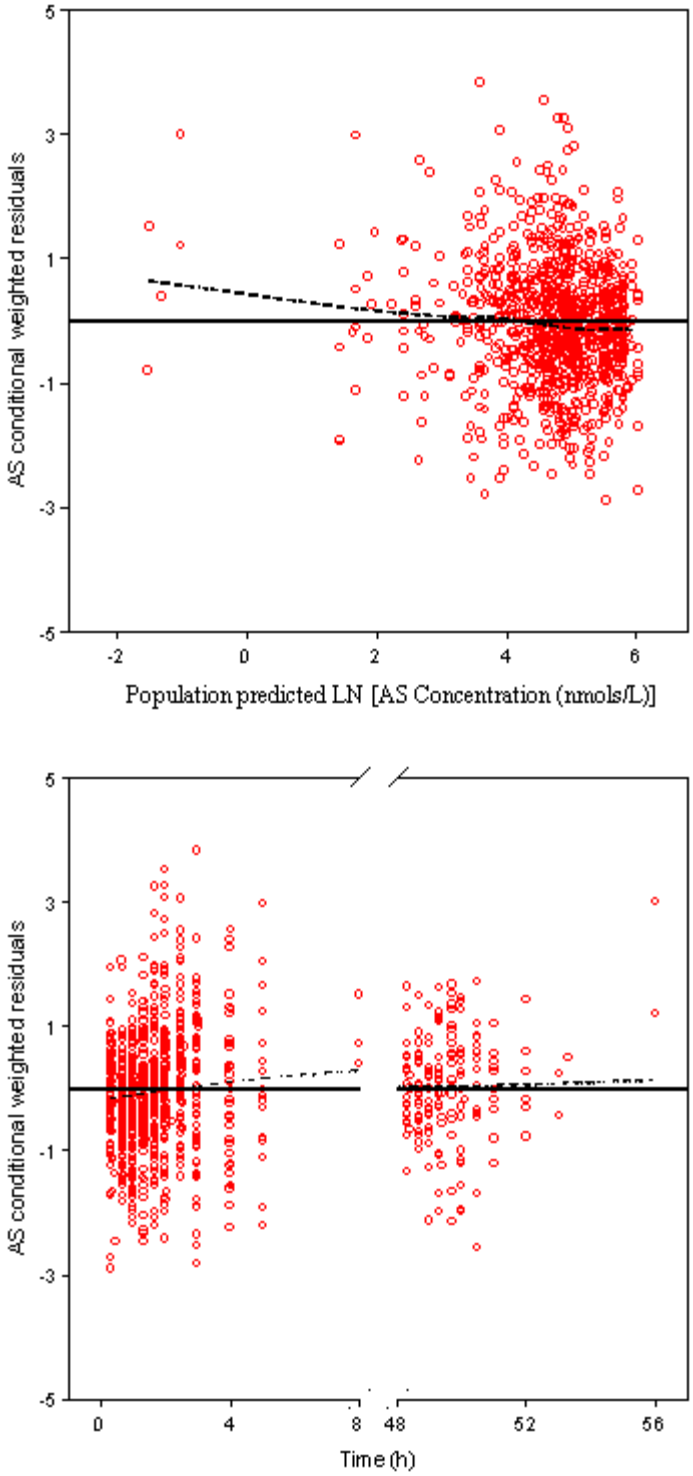

Figure 2.10 Population and individual predicted concentration versus observed concentration plots of dihydroartemisinin (DHA) for the final model. The solid lines are lines of identity. The broken lines are smoothing lines.

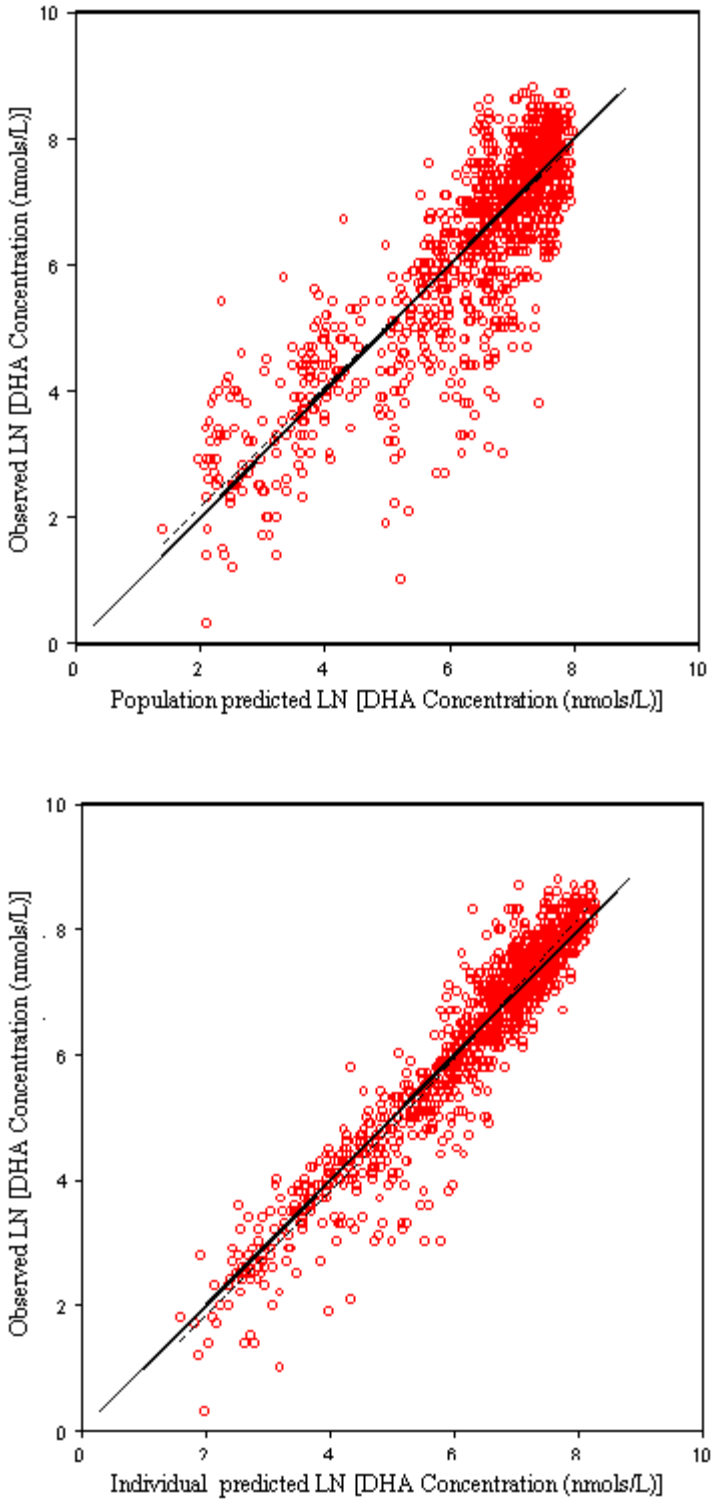

Figure 2.11 Conditional weighted residual plots of dihydroartemisinin (DHA) for the final model. The broken lines are smoothing lines.

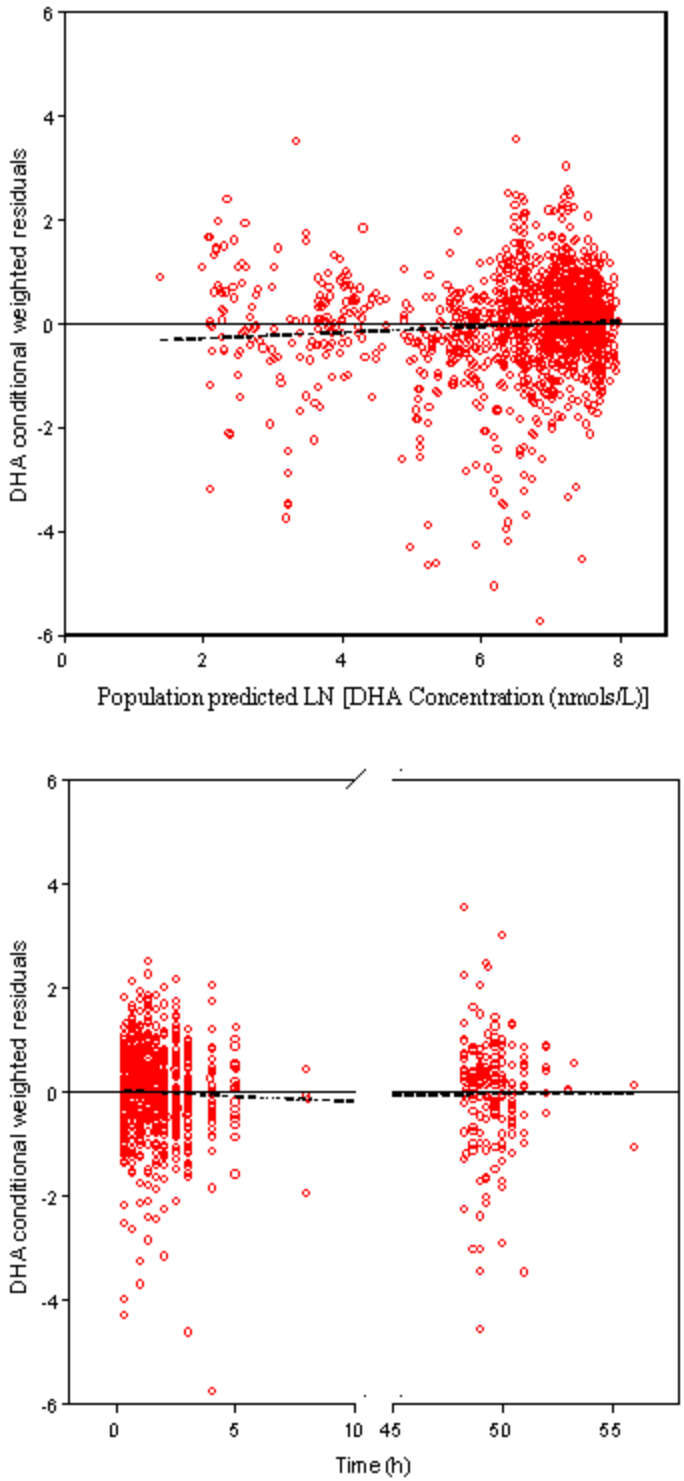

Figure 2.12 Plots of the artesunate (AS) observations (open circles), population predictions (broken lines), and individual predictions (solid lines) from the final model for selected subjects.

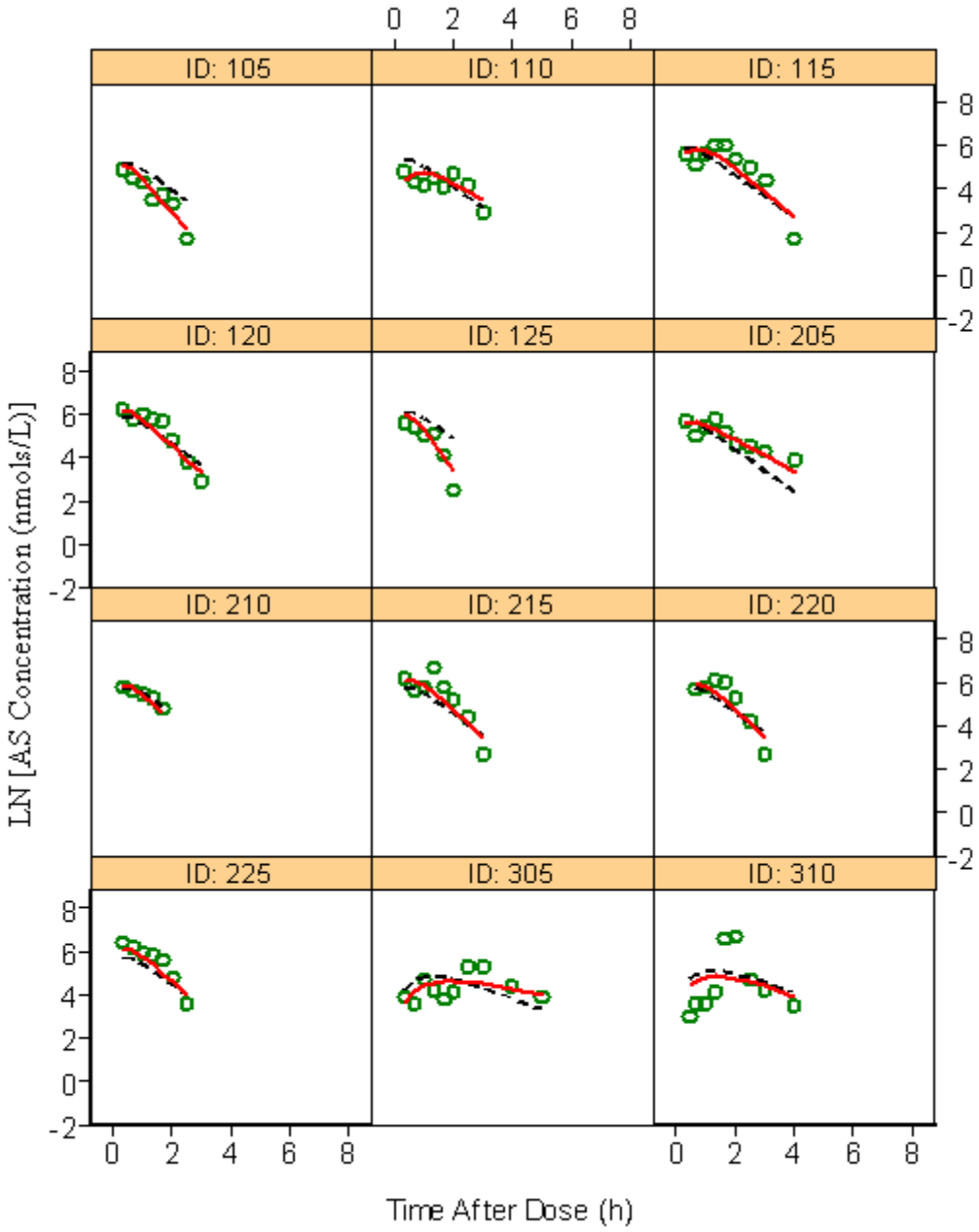

Figure 2.12 Continued

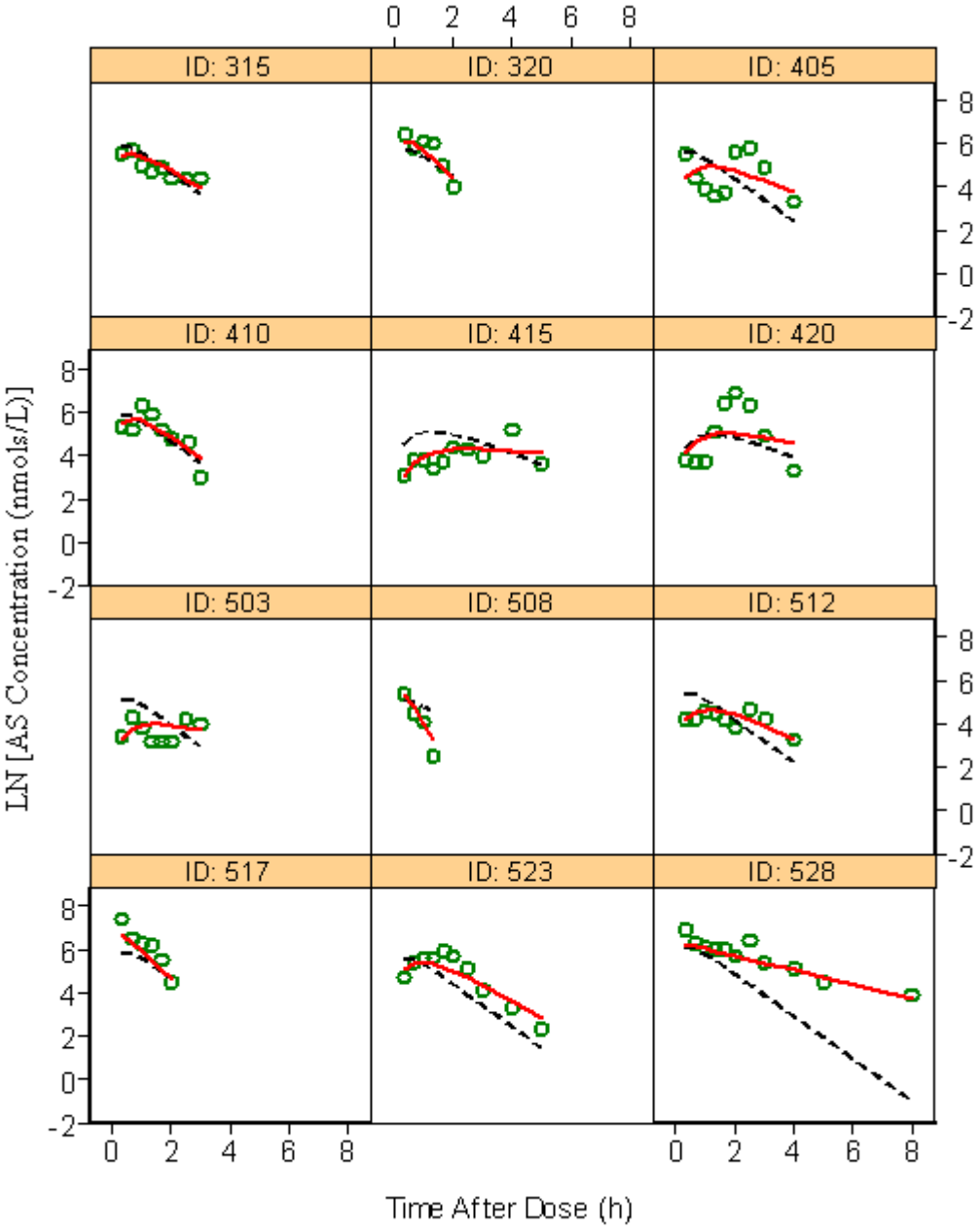

Figure 2.13 Plots of the dihydroartemisinin (DHA) observations (open circles), population predictions (broken lines), and individual predictions (solid lines) from the final model for selected subjects.

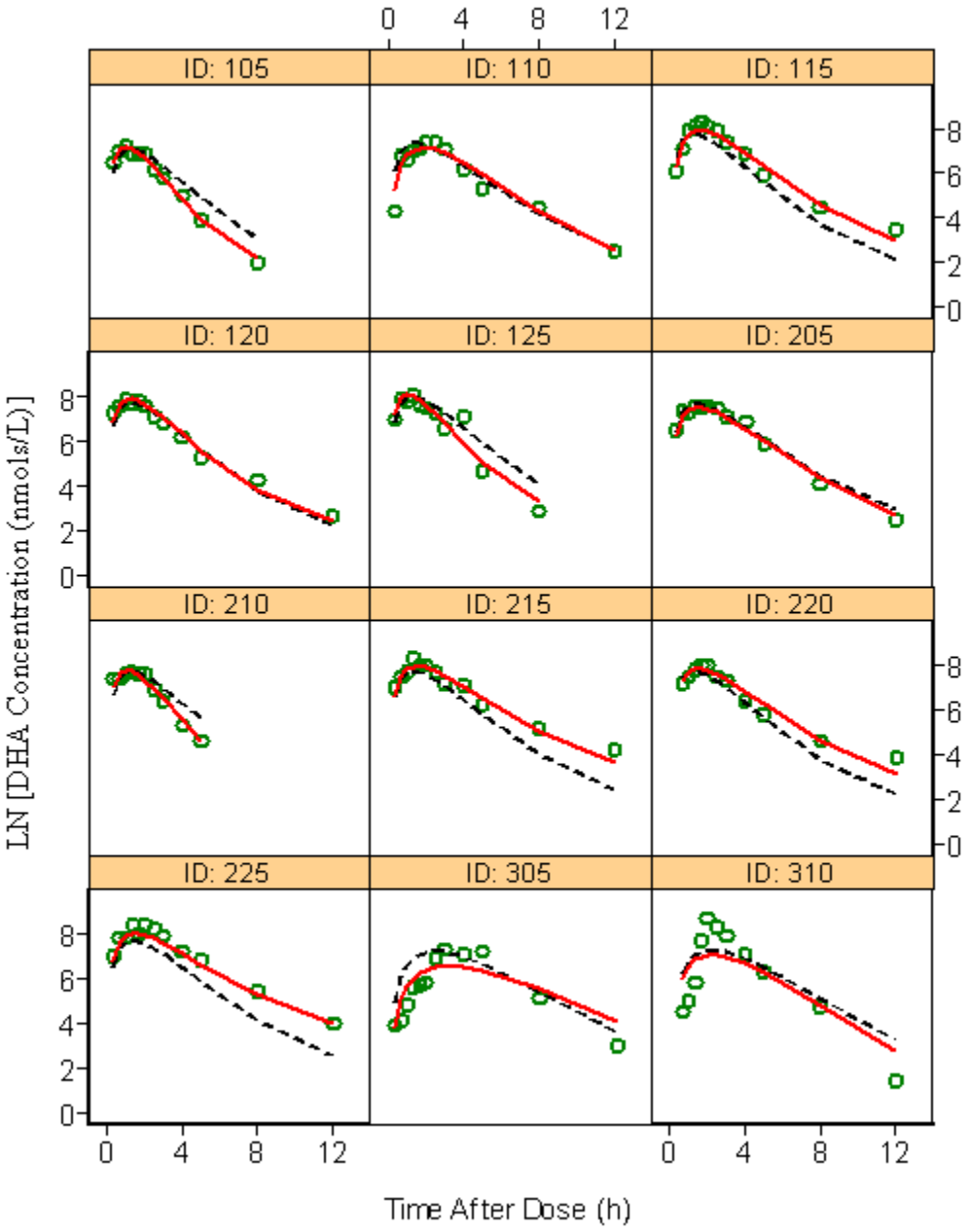

Figure 2.13 Continued

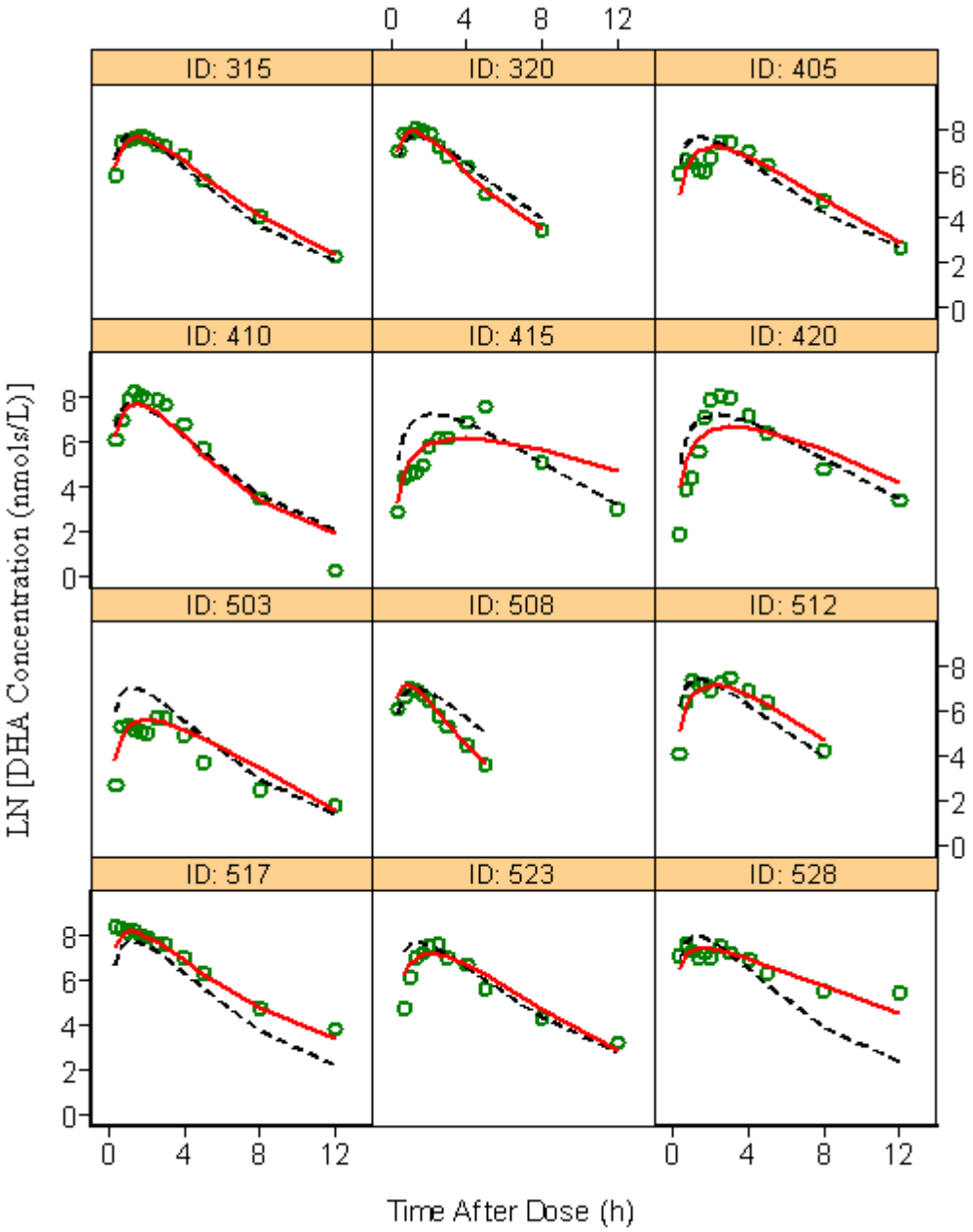

Figure 2.14 Visual predictive check of the final model for artesunate (AS) observations. The open circles represent the observed concentrations, solid lines represent the 90% confidence interval obtained from the simulations, and the dashed line represents the 50th percentile of the simulations.

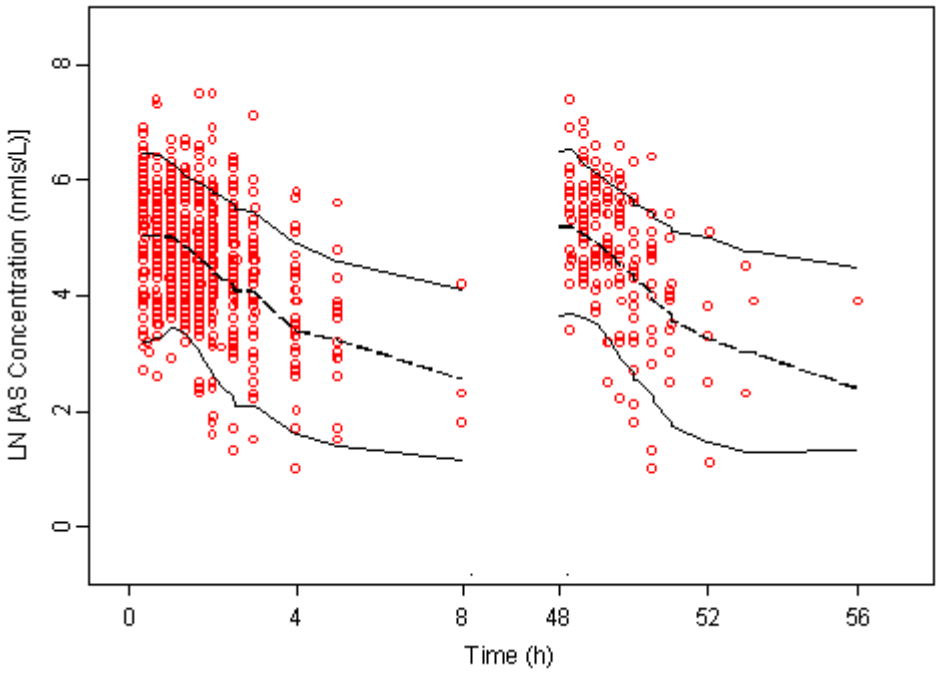

Figure 2.15 Visual predictive check of the final model for dihydroartemisinin (DHA) observations. The open circles represent the observed concentrations, solid lines represent the 90% confidence interval obtained from the simulations, and the dashed line represents the 50th percentile of the simulations.

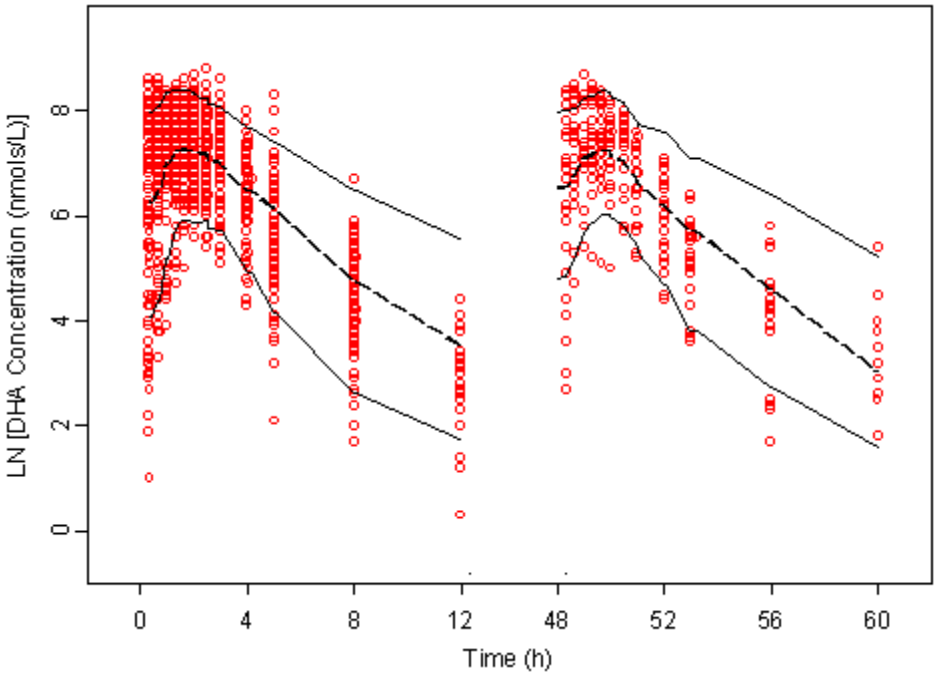

CHAPTER III

POPULATION PHARMACOKINETICS OF ARTESUNATE AND DIHYDROARTEMISININ FOLLOWING ORAL PYRONARIDINE/ARTESUNATE TREATMENT IN ADULTS AND CHILDREN WITH UNCOMPLICATED MALARIA

Introduction

Malaria is one of the deadliest infectious diseases in the world, causing nearly a million deaths among more than 3 billion people who were at risk in 2006 (1). Unfortunately, given the high burden of the disease, the number of available anti-malarial drugs is relatively small. On top of that, the emergence of resistance to the most affordable anti-malarial drugs has seriously undermined the global effort to control malaria. As the result of chloroquine and sulfadoxine-pyrimethamine resistance, millions of lives that could otherwise be saved were sacrificed over the past 30 years (135). Artemisinin-based combination therapies (ACTs) are now being widely used as the first-line treatments for *P. falciparum* malaria throughout the world.

Artemisinin derivatives are fast acting anti-malarial drugs producing the most rapid reduction in parasitemia (136). These agents also have gametocytocidal activity, which contributes to the reduction in the disease transmission (22, 137). Among the available derivatives, AS has the most appealing physicochemical and pharmacological properties and thus it is most widely used (138, 139). AS undergo rapid conversion *in vivo* to its active metabolite DHA which is responsible for most of the anti-malarial activity.

Pyronaridine (PYR) is a Mannich-base derivative anti-malarial that has been shown to be efficacious against erythrocytic stages of *P. falciparum* using *in vitro* models (140, 141). Clinical studies have also indicated that PYR is safe and efficacious against

P. falciparum even in area with chloroquine-resistant strains (143-145). Pyronaridine tetraphosphate plus artesunate (PA) is under development as a 3:1 fixed ratio combination for the treatment against *P. falciparum* and *P. vivax* malaria.

A recent literature search retrieved four studies on the population pharmacokinetics of AS. The population pharmacokinetics of AS and/or DHA following the administration of intra-rectal AS was characterized in 47 children by Karunajeewa et al. (146) and in 164 adult and pediatric patients by Simpson et al. (147). McGready et al. (148) studied the population pharmacokinetic of DHA in 24 pregnant women with acute uncomplicated falciparum malaria after the administration of oral AS, while Stepniewska et al. (157) evaluated the pharmacokinetics of AS in 66 African children who received oral AS and amodiaquine.

The aims of this analysis are to characterize the population pharmacokinetics of AS and DHA in large number of adult and pediatric patients with uncomplicated falciparum and vivax malaria following oral administration of PA combination and to identify covariates that might explain the variability seen in pharmacokinetic parameters of AS and DHA.

Materials and Methods

Subjects and Study Designs

PA fixed combination in the ratio of 3:1 has been evaluated extensively as a 3-day oral therapy for use in children and adults to treat acute, uncomplicated falciparum and blood stage vivax malaria. Plasma concentrations of AS and DHA from a Phase II study in pediatric patients and from four Phase III studies in adult and pediatric patients were included in this pharmacokinetic analysis.

The aim of the Phase II study SP-C-003-05 was to investigate the safety, tolerability and pharmacokinetics of the PA combination in tablets and granules formulations (Pyramax®; Shin Poong Pharm Co. Ltd., Seoul, Republic of Korea) for the

treatment of uncomplicated falciparum malaria in Gabonese patients aged 2-14 years. The study was designed as an open-label dose escalation study recruiting 15 patients sequentially in each treatment cohort. Study drugs were administered once daily for three days as co-formulated tablets at the following dose levels: 2:6 mg/kg, 3:9 mg/kg, and 4:12 mg/kg artesunate and pyronaridine, respectively. Additionally, a pediatric granule co-formulation was investigated at the medium dose strength (3:9 mg/kg) in a fourth cohort. Patients were hospitalized for the first 72 hours. They were further followed up until Day 42, with follow-up visits occurring on Days 7, 14, 21, 28, 35, and 42.The details of this clinical trial were described elsewhere (43).

Phase III study SP-C-004-06 was a multicenter, comparative, randomized, parallel group, non-inferiority study conducted to compare the efficacy and safety of the fixed combination of PA (Shin Poong Pharm Co. Ltd., Seoul, Republic of Korea) with that of mefloquine plus AS (Mepha Ltd, Aesch-Basel, Switzerland) in adult and pediatric patients with uncomplicated falciparum malaria. Patients were randomly assigned in 2:1 ratio to either receiving PA or mefloquine plus AS once a day for 3 consecutive days. The actual dose was based on body weight ranges for both PA combination and the comparator regimen. Patients were followed for 42 days, with the primary efficacy endpoint (PCR-corrected Adequate Clinical and Parasitological Response) occurring at 28 days after initiation of study drug administration (Day 28). Patients remained in the study facility for at least 4 days (Study Day 0, 1, 2 and 3) and returned to the study site for all scheduled follow up visits until completion of the study on Day 42. Incidence and severity of adverse events and of clinically significant laboratory results were monitored.

The study design of Phase III study SP-C-005-06 was similar to that of study SP-C-004-06. In this study, the efficacy and safety of the fixed combination of PA was compared with that of artemether/lumefantrine (Coartem®; Novartis SA., Basel, Switzerland). Adult and pediatric patients with uncomplicated falciparum malaria were randomly assigned in 2:1 ratio to either receiving PA once a day for 3 consecutive days

or artemether/lumefantrine twice a day for 3 consecutive days. The actual dose was based on body weight ranges for both PA combination and the comparator regimen. The safety and efficacy assessments were similar to study SP-C-004-06.

The aim of Phase III study SP-C-006-06 was to compare the safety and efficacy of PA with that of chloroquine (Shin Poong Pharm Co. Ltd., Seoul, Republic of Korea) in adult and pediatric patients with acute uncomplicated vivax malaria. It was a multicenter, comparative, randomized, parallel group, non-inferiority study. Patients were randomly assigned in 1:1 ratio to either receiving PA or chloroquine once a day for 3 consecutive days. The actual dose was based on body weight ranges for PA combination. The dosage of chloroquine used in the adults was 620mg on Days 0 and 1 and 310 mg on Day 2. The dosage used in children was 10 mg/kg of chloroquine on Days 0 and 1 and 5 mg/kg on Day 2. Patients who completed the study up to Day 28 and who have normal glucose-6-phosphate dehydrogenase (G6PD) activity were administered a 14-day course of 15 mg/day of primaquine (supplied by Shin Poong Pharm Co. Ltd., Seoul, Republic of Korea), starting on Day 28 to complete their radical cure. The primary efficacy endpoint of this study was the cure rate on Day 14 while the secondary efficacy endpoints included cure rates on Day 21 and 28 among others.

Phase III study SP-C-007-07 was a multi-center, randomized, open-labeled, parallel-group, non-inferiority study to compare the efficacy and safety of a three-day regimen of the fixed combination of PA granule formulation (pediatric Pyramax®; Shin Poong Pharm Co. Ltd., Seoul, Republic of Korea) versus artemether/lumefantrine crushed tablets in infants and children (between ≥ 5 kg and < 25 kg body weight) with acute uncomplicated falciparum malaria. The actual dose was based on body weight ranges for both PA combination and the comparator regimen. The safety and efficacy assessments were similar to study SP-C-004-06.

The efficacy endpoints and schedule of assessments selected generally followed the current WHO guidelines for monitoring drug efficacy (163). The trials were

conducted in accordance with the Guidelines of Good Clinical Practice and Declaration of Helsinki. Written informed consent, in accordance with local practice, was obtained and approval for the study was granted by local Ethics Committee.

Sample Collection and Storage

For the Phase II pediatric study, plasma samples were collected for pharmacokinetic analysis of AS and DHA at the following time points: prior to study drug administration, 0.25, 0.5, 1, 1.5, 2.5, 4, 8, 12 hours after first drug intake, prior to second drug administration and prior to third drug administration. For all Phase III studies at all participating clinical study sites, unless determined otherwise by the sponsors, the investigators were required to collect one or two blood samples from each patient at two different time points. One sample was drawn on Day 0 (0.15 to 12 hr post-dose) or Day 1 (0.15 to 12 hr post-dose), and a second on Day 2 (0.15 to 12 hr post-dose). Actual sampling time was recorded.

At each sampling time, 1 mL of venous blood was collected in into pre-chilled sampling tubes containing potassium oxalate/sodium fluoride (BD Vacutainer® No.: 367925 or equivalent) for the separation of plasma. The samples were placed on wet ice before centrifugation within 15 minutes of collection. Plasma was removed from cells and transferred into two approximately equal volume aliquots in screw cap cryovials (Nalgene No.: 50000012) immediately after the centrifugation. The plasma samples were immediately frozen at or below -80°C in a laboratory freezer. They were later shipped separately via air express frozen on dry ice to the Clinical Pharmacokinetics Laboratory at College of Pharmacy, the University of Iowa. All samples were stored at -80°C until drug analysis was performed. All samples were analyzed in the same laboratory.

Analytical Method

Plasma concentration of AS and DHA were determined using a validated liquid chromatography-mass spectrometric method described by Naik et al. (150) with slight

modifications. Briefly, AS, DHA and internal standard artemisinin were extracted from 0.25 mL of human plasma using solid phase extraction. The reconstituted extracts were chromatographed isocratically using a Phenomenex Synergi Max-RP, 4μ, 75 x 2.0 mm column with a mobile phase of 0.04% trifluoroacetic acid, methanol and acetonitrile (40:45:15, v/v/v) delivered at a flow rate of 0.18 mL/min.

Chromatographic analysis is carried out on a Shimadzu Model 2010 liquid chromatograph and mass spectrometer (Shimadzu, Columbia, MD, USA) using a LC-10AD Solvent Delivery system (Pump: A, B). The injection is made with a Shimadzu SIL-10AD automatic injector and analysis uses Shimadzu model 2010 data analysis software Lab Solutions Version 3. Methanol was added post-column to improve ionization and prevent probe needle clogging. The compounds were detected and quantified by mass spectroscopy. The lower limit of quantification (LOQ) for AS and DHA was 1 ng/mL (equivalent to 2.6 nmols/L for AS and 3.5 nmols/L for DHA). Both α and β tautomers of DHA were separated, however only the α tautomer of DHA was taken into account for quantitation. Under the chromatographic condition, the ratio of α and β was about 4:1. The coefficient of variation for intra-day and inter-day precision ranged from 2.2% to 9.2% and 5.8% to 8.6% for AS, and 1.7% to 6.2% and 6.5% to 8.2% for DHA, respectively. The intra-day and inter-day bias ranged from -13% to 10.5% and -7.2% to 6.2% for AS, and -9.6% to 13.8% and 0.4% to 5.5% for DHA, respectively.

Population Pharmacokinetics Analysis

Base Model Development

Population pharmacokinetic analyses were conducted using the first-order conditional estimation method with interaction (FOCEI) in NONMEM software version VI, level 2.0 (ICON Development Solutions, Ellicott City, MD) (119), as implemented on a Windows XP operating system (Microsoft Corporation, WA, Seattle) with G95 Fortran compiler (Free Software Foundation, Boston, MA). PDx-Pop 3.10 (ICON

Development Solutions, Ellicott City, MD) and Xpose version 4.0 (Uppsala University, Uppsala, Sweden) (151) were used to process the NONMEM output. Graphical plots were produced using S-PLUS version 8.0 (Insightful Inc, Seattle, WA) and R 2.8.1 (Free Software Foundation, Boston, MA).

Measurements below the lower LOQ of the assay were excluded from the dataset. Prior to modeling, AS and DHA concentrations were converted to the equivalent values in nmols/L and were transformed to the natural log scale. AS dose was also converted to the equivalent values in nmols.

Inter-individual variability (IIV) of the pharmacokinetic parameters was estimated by assuming a log-normal distribution, as shown below:

$$P_i = P_{pop} \bullet \exp(\eta_i)$$

where P_i denotes the estimated parameter value for individual i, P_{pop} represents the typical population estimate for the parameter and η_i is the difference between P_i and P_{pop}. The η random effects were assumed to be independent and symmetrically distributed with zero mean and variance ω^2. The magnitude of inter-individual variability was expressed as coefficient of variation (%CV).

The random residual variability (RV) was modeled using an additive model as shown below:

$$\ln C_{ij} = \ln C_{pred,ij} + \varepsilon_{ij}$$

where C_{ij} and $C_{pred,ij}$ represent the jth observed and model predicted AS or DHA concentrations, respectively, for individual i and ε_{ij} denotes the additive residual random error for individual i and observation j. The ε random effects were assumed to be independent and symmetrically distributed with zero mean and variance σ^2.

In the initial stage of model building, one- and two-compartmental pharmacokinetic models with first order absorption and first order elimination were fitted to the AS data to determine the best structural model for AS. The absorption of AS was also tested with zero-order model and Weibull-type absorption model (164-166).

Enterohepatic recirculation model was also examined since some patients exhibited double-peak kinetic profiles. Different models to account for enterohepatic recirculation phenomenon have been proposed (167-172). The model that we tested was based on the model proposed by Gabrielsson and Weiner (169) with slight modification. The model took into account only one bile release from the gall bladder and the release followed a zero-order process for an interval of 0.25 hour.

Once the best pharmacokinetic model for AS was determined, DHA data was modeled by assuming complete conversion of AS to DHA and that the conversion was irreversible (84). The conversion was also assumed to take place only in the central compartment. One- and two-compartmental models with first-order disposition were tested for DHA to develop the best metabolite structural model. For the two-compartmental model, it was assumed that DHA was eliminated only from the central compartment. A parent-metabolite model with two parallel first-order absorption processes, which conceptually corresponding to the absorption of AS from the gut and conversion of AS to DHA in the gut, was also tested. After the best structural model was determined, all parameters were estimated simultaneously using ADVAN 5 in NONMEM.

Criteria used for model selection included the plausibility of the estimates, minimum objective function value (MOFV), equal to minus twice the log-likelihood function, Akaike Information Criterion (AIC), equal to MOFV plus two times the number of parameters, condition number, defined as the ratio of the largest eigenvalue to the smallest eigenvalue, visual inspection of diagnostic plots and the precision of parameter estimates.

Covariate Model Development

Body weight was incorporated as a covariate in the base model *a priori* using the standard allometric function, as follow:

$$P_i = P_{pop} \bullet (WT/70)^{\theta}$$

where P_i is the estimated parameter value for individual i, P_{pop} represents the typical population estimate of the parameter for an individual with the standard weight of 70 kg, and θ is the allometric exponent. Θ was fixed to 0.75 for all clearance terms and 1 for all volume of distribution terms in the model (173).

Additional covariate analysis was also carried out to assess other variables as possible determinants of the variability seen in the pharmacokinetic estimates. Covariates examined include age, baseline hematocrit, baseline hemoglobin, baseline erythrocyte count, baseline AST, baseline ALT, baseline parasite count, gender, geographical region, and formulation of AS dose. Age, baseline hematocrit, baseline hemoglobin and baseline erythrocyte count were tested as continuous covariates while baseline AST, baseline ALT, baseline parasite count, gender, geographical region, and formulation of AS dose were tested as categorical covariates. The coding for the categorical variables is as follows:

1. Baseline AST was coded as 0 if the level was ≤ 1.5x upper limit of normal range or 1 if it was > 1.5x upper limit of normal range. Upper limit of normal range for AST were defined as 19 U/L and 41 U/L for Phase II and Phase III studies respectively.
2. Baseline ALT was coded as 0 if the level was ≤ 1.5x upper limit of normal range or 1 if it was > 1.5x upper limit of normal range. Upper limit of normal range for ALT were defined as 23 U/L and 45 U/L for Phase II and Phase III studies respectively.
3. Baseline parasite count was coded as 0 if baseline parasite count was ≤ 50,000 /μL or 1 if baseline parasite count was > 50,000 /μL.
4. Gender was coded as 0 for female or 1 for male.
5. Geographical region was coded as 0 for Asia or 1 for Africa.
6. Formulation of AS dose was coded as 0 for tablet form or 1 for granule form.

Potential covariates were initially identified using visual inspection of the inter-individual variability versus covariates plots and also using generalized additive modeling as implemented in the Xpose software. The potential covariates were then tested for statistical significance using stepwise forward addition followed by stepwise backward elimination procedure (152). The influences of the covariates were tested by adding a covariate to the model at a time in the forward addition step, and then by removing a covariate from the model at a time in the backward elimination step. The changes in MOFV between the 'full' and the 'reduced' models were then calculated. The difference in MOFV between two nested models was approximated by a χ^2 distribution. An MOFV change of 3.84 (corresponding to a significance level of 5% at one degree of freedom) was used as the cutoff to include a covariate in stepwise addition. When no more covariates could be included, the stepwise backward elimination was carried out. For a covariate to remain in the model, a change in MOFV of at least10.83 (corresponding to a significance level of 0.1% at one degree of freedom) was needed. An improvement in the precision of the parameter estimate (relative standard error), and reduction in inter-subject and residual variability were also used to determine the importance of the covariates as predictors. When finalizing the covariate model, in addition to using the stated statistical criteria, clinical consideration was also taken into consideration. For categorical variables, at least a 20% change in the affected parameter was needed for the covariate to be considered clinically meaningful.

Depending on the graphical exploration of the relationship between a covariate and a PK parameter, the effect of the covariate on the parameter was tested with a linear function and/or a power function and/or an exponential function, with the covariates centered or scaled at their median values:

$P = \theta_1+\theta_2 \bullet (COV-COV_{median})$, for linear function;

$P = \theta_1 \bullet (COV/COV_{median})^{\theta 2}$, for power function;

$P = \theta_1 \bullet Exp (\theta_2 \bullet (COV-COV_{median}))$, for exponential function;

where θ_1 represents the parameter estimate, P of an individual with median value of the covariate COV_{median}, and θ_2 is a factor describing the correlation between the covariate COV and the parameter. The influences of binary covariates on the parameter were modeled using a proportional and/or additive relationship, as follow:

$P = \theta_3 \bullet (1+\theta_4 \bullet COV)$, for proportional relationship;

$P = \theta_3+\theta_4 \bullet COV$, for additive relationship;

where θ_3 represents the parameter value in subjects with the categorical covariate coded as 0, and θ_4 is the fractional or additional change in the parameter in subjects with the categorical covariate coded as 1.

Model Evaluation

The final model was evaluated for its robustness, predictive power, and stability. Non-parametric bootstrap procedure was employed to evaluate the robustness of the final model. 250 bootstrap datasets were generated by repeated random sampling with replacement from the NONMEM input data file, and the final NONMEM model was fitted to the bootstrap datasets. The bootstrap estimates for the population parameters were calculated, and compared with the estimates from the final model. The bootstrap 95% confidence interval was calculated based on the percentile of the empirical distribution of the estimated parameters from the bootstrap runs.

The predictive power of the final model was assessed by performing visual predictive. 1000 virtual observations were simulated at each sampling time using the final model and its parameter estimates. The 5th, 50th and 95th percentiles of the simulated data above the LOQ were calculated and plotted alongside with the observed data. The percent of observed data outside the 90% prediction interval was also calculated.

Condition number, as defined as the ratio of the largest Eigen value to the smallest Eigen value, was used as a measure of the stability of the final model.

Simulations

Monte Carlo simulations of the population data were performed using NONMEM in order to reflect the expected range of variability of the response under the final model assumptions. A total of 500 concentration-time profiles for AS and DHA were simulated using the parameter estimates obtained from the final model, for a 70-kg patient who received an oral AS dose of 3.3 mg/kg, corresponding to the mean AS dose received by the subjects in this dataset, once daily for 3 days. The sampling times were set to 0.25, 0.5, 1, 1.5, 2.5, 4, 8, 12 hours after each dose, and immediately before the second and third dose. The expected AS and DHA observations and the 50th percentile of the simulated data were then plotted.

Subpopulation analysis

Due to the concerns of possible resistance to AS in Cambodia, an analysis was made to compare the demographic characteristics and pharmacokinetic parameters between Cambodian patients and Thai patients from study SP-C-004-06. All statistical analyses were conducted using SAS 9.2 (SAS Institute Inc., Cary, NC). Shapiro-Wilk test was first performed to check for normality of the data. The results revealed that not all variables to be tested were normally distributed. Therefore, two-sided Wilcoxon rank-sum test was used to compare the two subpopulations. A significance level of 0.05 was used.

Results

Data

Data arising from 632 adult and pediatric patients with uncomplicated falciparum and vivax malaria were pooled from one Phase II and four Phase III clinical studies. The subjects received oral PA once a day for three consecutive days. A total of 1572 concentration measurements were available for AS and DHA each. Out of these samples,

692 (44%) and 132 (8.4%) concentration measurements of AS and DHA respectively were below LOQ, and were therefore excluded from the dataset. The total number of concentration measurements above LOQ that were used in the modeling were 878 (55.9%) and 1438 (91.5%) for AS and DHA respectively. Two AS observations and two DHA observations were identified as suspicious observations and/or outliers and therefore were excluded from the dataset. Patient 248 had extremely high AS and DHA observations at 15.35 hours post-dose (1119.4 nmols/L and 6664.1 nmols/L respectively) and were identified and therefore removed from the dataset after the base model building step. Patient 845 had a sample taken at 79.87 hours after the first dose. The sampling time was questionable since the patients were given AS dose once daily for three days. Patient 526 had an observed AS concentration of 268.2 nmols/L at 10.55 hours post-dose but had a predicted concentration of 0.77 nmols/L. These two observations were removed from the dataset after the covariate building steps. The plots of observations versus time after dose for AS and DHA are shown in Figure 3.1 and Figure 3.2, respectively. Table 3.1 and Table 3.2 summarize the study and the data characteristics as well as demographics of the patients included in this analysis.

Model Development

A two-compartment model with first order absorption and first order elimination best described the AS data. The two-compartment model resulted in a significant reduction in MOFV and AIC of 84.1 unit and 76.1 unit, respectively, compared to a one-compartment model with first order absorption and first order elimination. Goodness-of-fit plots were also improved. Weibull-type absorption and zero-order absorption were also tested for the two-compartment model. Both models did not result in any improvements of the model selection criteria. When the AS data was fitted with a two-compartment model with first-order absorption and enterohepatic recirculation, a slight reduction of 3.4 unit in MOFV was seen. However, the AIC of the enterohepatic

recirculation model was 4.58 units higher than the two-compartment model without enterohepatic recirculation.

The DHA data were then sequentially modeled as a metabolite compartment connected to the central compartment of AS using a one-compartment model with linear elimination and also a two-compartment model. The two-compartment model did not improve any of the model selection criteria. A more complex model with two parallel first-order absorption processes conceptually corresponding to the conversion of AS to DHA in the gut compartment was also tested. However, this model was not superior to the parent-metabolite model with one first-order absorption. Thus, the best base structural model was a parent-metabolite model consisted of a dosing compartment, a central compartment and a peripheral compartment for AS, and a central compartment for DHA, as shown in Figure 3.3. The model was parameterized in terms of absorption rate constant for AS (Ka), apparent clearance for AS (CL/F, where F is the unknown oral bioavailability), apparent volume of distribution of the central compartment for AS (V2/F), apparent clearance for DHA from the central compartment (CLM/F), apparent central volume of distribution for DHA (V3/F), inter-compartmental clearance for AS (Q/F), and apparent peripheral volume of distribution for AS (V4/F). Both conventional model (Ka > Ke for AS) and flip-flop model (Ka < Ke for AS) were considered. The flip-flop model had lower MOFV (3059.216 vs. 3065.292) and AIC (3074.31 vs. 3097.29) compared to the conventional model.

A review of the correlation matrix of the base model revealed a high correlation between CL/F and CLM/F (r = 0.93), CL/F and V3/F (r = 0.92), CL/F and Q/F (r = 0.93), and CL/F and V4/F (r = 0.93). Hence, a reduced covariance matrix was developed and the model was modified to:

$CL/F = \theta_1 \bullet \exp(\eta_1)$

$V2/F = \theta_2 \bullet \exp(\eta_2)$

$KA = \theta_3 \bullet \exp(\eta_3)$

$CLM/F = \theta_4 \cdot \exp(\theta_8 \cdot \eta_1)$

$V3/F = \theta_5 \cdot \exp(\theta_9 \cdot \eta_1)$

$Q/F = \theta_6 \cdot \exp(\theta_{10} \cdot \eta_1)$

$V4/F = \theta_7 \cdot \exp(\theta_{11} \cdot \eta_1)$

where the variance of CLM/F, V3/F, Q/F and V4/F was a function of the variance of CL/F. The structure of the variance-covariance matrix for η_1, η_2, and η_3 was then tested with a full matrix containing all diagonal and off-diagonal elements, a diagonal matrix and other matrices with differing covariance patterns. A summary of the results is shown in Table 3.3. The model with a diagonal matrix is the only model with successful convergence and COVARIANCE ($COV) step in NONMEM, and was therefore used in the final base model. Unsuccessful $COV step is an indication of over-parameterization of the model.

A summary of the covariates evaluated is shown in Table 3.2. Body weight was incorporated in the model *a priori* using allometric scaling. None of the additional covariates examined were statistically significant.

The final model is a parent-metabolite model consisted a dosing compartment, a central compartment and a peripheral compartment for AS, and a central compartment for DHA. AS was rapidly absorbed with a population estimate of Ka of 1.05 h^{-1} with 41% inter-individual variability. The population estimates of CL/F and V2/F for AS were 1520L/h with 42.7% inter-individual variability and 477 L with 175% inter-individual variability, respectively. The population estimates of Q/F and V4/F for AS were 136 L/h and 1100 L, respectively. For DHA, the population estimates of CLM/F and V3/F were 110 L/h and 127 L, respectively. A summary of the results obtained from the final model is presented in Table 3.4. The goodness-of-fit plots of the final model are shown in Figure 3.4 and Figure 3.5 for AS, and Figure 3.6 and Figure 3.7 for DHA. Individual plots for every five subjects with intensive pharmacokinetic sampling are presented in Figure 3.8 and Figure 3.9 for AS and DHA, respectively.

Model Evaluation

The parameter estimates with standard error and 95% confidence interval generated from the bootstrap method are presented in 3.3. The parameter estimates obtained from the final model were reasonably close to the ones obtained from the bootstrap method. All the parameter estimates from the final model were also contained within the 95% bootstrap confidence intervals.

Figure 3.10 and Figure 3.11 show the results of the visual predictive check for AS and DHA. Overall, the final model adequately described the observed concentrations. About 9.2% and 8.2% of the AS and DHA observations respectively were not contained within the 90% prediction interval. Thus, the model is said to have adequate predictive power. The condition number of the final model was 492.6, indicating that the model was reasonably stable.

Subpopulation Analysis

The results of the comparisons in demographic and pharmacokinetic parameters between Cambodian patients and Thai patients from study SP-C-004-06 are shown in Table 3.5. Since body weight between the two subpopulations was statistically significant at α=0.05 level, pharmacokinetic parameters were normalized by weight wherever appropriate before comparison. Other variables that were statistically significant at α=0.05 level between the two groups included age, baseline AST, weight-normalized V3/F, weight-normalized V4/F, and $t_{1/2elim,DHA}$.

Discussion

The results of a population pharmacokinetic model of AS and DHA in adult and pediatric patients with uncomplicated falciparum and vivax malaria are reported in this paper.

Out of a total of 1572 concentration measurements available for AS and DHA each, 44% and 8.4% of AS and DHA concentration measurements respectively were

below LOQ, and were therefore excluded from the dataset. The percentage of AS samples below LOQ in this study was not unexpected since AS was very rapidly hydrolyzed to DHA. The percentage of undetectable samples (AS and DHA) reported in three other AS population pharmacokinetic reports were 10.4% and 7.8% (147), 62.7% and 39% (146), and 93.5% and 70.9% (148).

The final model in this analysis consisted of a dosing compartment, a central compartment and a peripheral compartment for AS, and a central compartment for DHA. Whenever model-dependent method was used, the pharmacokinetics of AS has almost always been modeled using one-compartment model (73, 74, 146, 174, 175). Occasionally, a two-compartment model was used to fit the AS data (75, 176). A two-compartment model fit the AS data in our analysis better than one-compartment model. AS is rapidly hydrolyzed to DHA and so its concentration is rarely detected after 6 hours post dose. However, we were able to detect the AS concentration up to 12 hours post dose (Figure 3.1). This can be explained by the fact that the patients in our study received a higher average AS dose (3.3 mg/kg) than the patients in the other compartmental pharmacokinetic analysis of oral AS (2mg/kg) (73, 74). In addition to the higher AS dose received, the assay method employed is this study was more sensitive (1 ng/mL) compared to the two studies (50 ng/mL).

Goodness-of-fit plots for AS and DHA indicated a reasonable fit of the model to the data (Figures 3.4-3.7). The parameters were well estimated in general, with percent relative standard error ranged from 3.75% to 43%. Parameter related to V2/F showed the most variability, with inter-individual variability for V2/F was estimated to be 175%. Flip-flop kinetics was observed in this dataset, where the absorption rate constant for AS is less than the conversion rate constant of AS to DHA. The flip-flop model had lower MOFV (3059.216 vs. 3065.292) and AIC (3074.31 vs. 3097.29) compared to the conventional model.

The elimination rate constant for AS obtained using the flip-flop model was 3.2

h^{-1}, which is consistent with the value reported in adult patients with severe falciparum malaria following intravenous AS (3.1 h^{-1}) (177). AS was rapidly absorbed into the systemic circulation, with an absorption half-life of 39.6 minutes as estimated in this analysis. The conversion of AS to DHA was also very rapid, with a half-life of about 13 minutes.

Population pharmacokinetics of AS and/or DHA in malaria patients have been described elsewhere in different populations using either rectal or oral AS (146-148, 157). Karunajeewa et al. (146) described the population pharmacokinetics of AS and DHA simultaneously in 47 pediatric patients with uncomplicated falciparum and vivax malaria who were treated with two doses of AS suppositories. In another report, Simpson et al. (147) presented the results of a population pharmacokinetic analysis of DHA in adult and pediatric patients with moderately severe falciparum malaria. All patients were treated with a single dose of 10 mg/kg of intra-rectal AS. However, the pharmacokinetics of AS data was not characterized in the study. Both the weight-normalized CL/F and V/F for AS obtained in our analysis are greater than the resulted reported by Karunajeewa et al. (146). The differences in the estimates seen might be due to the fact that the AS bioavailability is reduced when oral AS is given compared to rectal AS, as reported by Navaratnam et al. (76) in a study comparing pharmacokinetics of AS and DHA after administration of oral and rectal AS in 12 healthy male Malaysian volunteers. On the other hand, the weight-normalized CL/F and V/F for DHA reported in this analysis are smaller than those reported in the two reports (146, 147). One explanation is that the bioavailability of DHA was increased when oral AS was given compared to intra-rectal AS. This is consistent with the observations that the area under the concentration-time curve (AUC) for DHA following oral administration of AS was higher than that following rectal AS (76, 158).

The population pharmacokinetics of DHA in pregnant women with acute uncomplicated falciparum malaria was characterized in another study by McGready et al.

(148). The patients were treated with a three-day dosing of oral AS (4 mg/kg/day) and atovaquone plus proguanil. The pharmacokinetics of AS was not evaluated in the analysis because only 6.5% of the total available samples had detectable AS concentrations. They reported a weight-normalized oral clearance for DHA of 1.77 L/h/kg, which is similar in our analysis (1.57 L/h/kg). The population estimate for DHA apparent volume of distribution reported in their study was 4.63 L/kg, while we reported a population estimate of 1.81 L/kg, which is about 60 % lower. The larger volume of distribution seen in their study might be due to the physiological changes during pregnancy, resulting in a larger volume of distribution for DHA.

Stepniewska et al. described the population pharmacokinetics of DHA in African children with acute malaria from six months to five years old who received either the fixed dose combination of AS and amodiaquine or the separate tablets of both drugs. (157). The weight normalized CL/F and V/F of DHA reported in their study was 0.636 L/h/kg and 2.285 L/kg, repectively. The CL/F value was much lower than what we estimated, possibly related to the use of per-kg model in their study. In a review on developmental patterns of UGT system, de Wildt et al. suggested that the use of per-kg model for clearance is inadequate to address developmental changes in young children and may lead the underestimation of clearance by up to 200% in chilren under 3.4 kg of body weight (159). The capacity of UGT metabolizing enzymes responsible for DHA metabolism in young children could be much less than the full capacity in adults, and therefore resulted in lower CL/F of DHA. The reported weight-normalized V/F of DHA was quite similar to the value obtained in this analysis.

The pharmacokinetic parameters for DHA obtained in this analysis are similar to those reported elsewhere (75, 81). Newton et al. (75) studied the pharmacokinetics of oral AS in 19 adult patients with uncomplicated falciparum malaria following single AS dose of 2mg/kg. DHA pharmacokinetic parameters were calculated assuming the complete conversion of AS to DHA. They reported a DHA elimination half-life of 0.71 h (0.8 h in

this analysis), DHA apparent clearance of 1.38 L/h/kg (1.57 L/h/kg) and a DHA apparent volume of distribution of 1.33 L/kg (1.81 L/kg) during the acute phase treatment. Teja-Isavadharm and colleagues (81) studied the single-dose pharmacokinetics of AS following the administration of 100 mg of oral AS in 6 healthy subjects and 6 patients with uncomplicated falciparum malaria. Non-compartmental approach was used to derive the parameters in their analysis. They reported a DHA elimination half-life of 0.8 h (0.8 h in this analysis), DHA apparent clearance of 1.22 L/h/kg (1.57 L/h/kg) and a DHA apparent volume of distribution of 1.33 L/kg (1.81 L/kg).

In the present analysis, body weight was incorporated *a priori* as a covariate in the model using allometric function. This approach is physiologically and clinically relevant since the AS dosing administered was weight-based. The same approach was also used by Simpson et al. (147) in their population pharmacokinetic analysis of AS and DHA in adult and pediatric malaria patients following intra-rectal dosing of AS. No other covariates tested in this analysis were found significant.

The parameter estimates obtained from the final model were reasonably close to the ones generated from 250 bootstrap replicates, indicating that the final model was robust. The visual predictive check showed that the final parent-metabolite model proposed has adequate predictive power. However, all observed AS concentrations after 4 hours post-dose were above the 50th percentile of the simulations. This is not unexpected since more than 90% of the AS observations were recorded within the first 4 hours post-dose. In addition, most of the AS observations after 4 hours post-dose were below LOQ and were therefore excluded from the analysis. The model is also stable with a condition number of <1000. The simulations of AS and DHA for a 70-kg individual under the current model assumptions showed no accumulation in both AS and DHA concentrations after multiple dosing. Figure 3.12 and Figure 3.13 show the expected simulated concentration-time profile of AS and DHA for a 70-kg patient and its 90%

confidence interval. The simulations revealed that the possible concentration-time profiles for the simulated patient were highly variable.

A subpopulation analysis was performed to compare the demographic and pharmacokinetic characteristic between Cambodian patients and Thai patients in study SP-C-004-06. The main objective of this analysis was to investigate if there is any difference in pharmacokinetic profile between the two groups. Pharmacokinetic parameters that were statistically significant between the groups included weight-normalized V3/F (1.7 L/kg for Cambodian patients vs. 1.9 L/kg for Thai patients), weight-normalized V4/F (15 L/kg vs. 16.2 L/kg), and $t_{1/2elim,DHA}$ (0.69 h vs. 0.75 h). However, these differences were not deemed clinically significant. In their attempt to investigate drug-specific opportunities for the selection of resistance during elimination phase of anti-malarial drugs, Stepniewska and White (135) pointed out that rapidly eliminated drugs with elimination half-life of less than 1 day usually provide no window of selection for resistance at all. They further concluded that resistance to rapidly eliminated drugs such as artemisinins can only occur by inadequate treatment. In this subpopulation analysis, the AUC_{DHA} was used as a measure of systemic exposure to DHA and hence a measure of treatment adequacy. AUC_{DHA} of Cambodian patients was similar to that of Thai patients. Consequently, we conclude that Cambodian patients were exposed to DHA at a level similar to the Thai patients.

In conclusion, a descriptive, robust and predictive parent-metabolite model was successfully developed using population approach to characterize the pharmacokinetics of AS and DHA simultaneously in adult and pediatric patients with falciparum and vivax malaria following oral administration of AS. Body weight was the only covariate included in the final model.

Table 3.1 A summary of the study and data characteristics.

Characteristics	Phase II study SP-C-003-05	Phase III study SP-C-004-06	Phase III study SP-C-005-06	Phase III study SP-C-006-06	Phase III study SP-C-007-07	All studies combined
Number of subjects	57	268	197	23	87	632
Mean AS dose received (mg/kg) (± S.D.)	3.3 ± 0.9	3.3 ± 0.4	3.4 ± 0.7	3.4 ± 0.5	3.0 ± 0.5	3.3 ± 0.6
Total number of observations	456	536	380	42	158	1572
Number of observations used in the dataset [N (%)]						
AS	289	305	187	26	71	878
DHA	388	519	342	39	150	1438
Number of observations <LOQ [N (%)]						
AS	167 (36.6)	230 (42.9)	192 (50.5)	16 (38.1)	87 (55.1)	692 (44)
DHA	68 (14.9)	16 (3.0)	38 (10)	3 (7.1)	7 (4.4)	132 (8.4)

Table 3.2 A summary of the subject demographics and covariates included in the analysis.

Characteristics	Phase II study SP-C-003-05	Phase III study SP-C-004-06	Phase III study SP-C-005-06	Phase III study SP-C-006-06	Phase III study SP-C-007-07	All studies combined
Age (years)	5 (2-14)	24 (5-58)	11 (5-55)	19 (9-42)	5 (0.8-11)	14 (0.8-58)
Weight (kg)	16.2 (10-36.4)	50.2 (20-72.3)	30 (20-80)	46.7 (20-67)	17.1 (8-24.8)	38.3 (8-80)
Gender [N (%)]						
Female	28 (49.1)	62 (23.1)	105 (53.3)	9 (39.1)	45 (51.7)	249 (39.4)
Male	29 (50.9)	206 (76.9)	92 (46.7)	14 (60.9)	42 (48.3)	383 (60.6)
Geographical region [N (%)]						
Asia	0 (0)	244 (91)	0 (0)	23 (100)	0 (0)	267 (42.2)
Africa	57 (100)	24 (9)	197 (100)	0 (0)	87 (100)	365 (57.8)
Baseline parasite count (per μL)	6,304 (1,072-174,241)	12,838 (1,040-97,500)	12,476 (1,000-93,923)	10,275 (1,193-51,947)	10,074 (78-149,977)	11,430 (78-174,241)
Baseline hematocrit (%)	29.6 (24.3-38.2)	36 (23.9-50)	34.2 (24.1-57.2)	35.5 (28.6-40.6)	30.2 (24.3-37.1)	34 (23.9-57.2)
Baseline hemoglobin (g/L)	102 (74-129)	121 (80-171)	117 (84-208)	115 (93-136)	100 (80-130)	115 (74-208)
Baseline erythrocyte count ($x10^{12}$ /L)	4.1 (3.3-6)	4.6 (2.6-6.5)	4.6 (3.1-7.3)	4.3 (3.3-6.2)	4.1 (3.1-5.8)	4.4 (2.6-7.3)
Baseline Alanine Aminotransferase (U/L)	18 (5-70)	22 (2-95)	22 (11-87)	17 (10-122)	22 (5-56)	22 (2-122)
Baseline Aspartate Aminotransferase (U/L)	32 (18-71)	31 (5-114)	39 (18-94)	33 (28-138)	37 (15-75)	35 (5-138)

Continuous variables are given as median (range).

Table 3.3 Evaluation of different patterns of the model's Ω matrix.

Pattern of Ω matrix	Successful minimization	Successful $COV step	MOFV	AIC
Full Ω matrix	Yes	No	3012.277	3040.28
Diagonal Ω matrix	Yes	Yes	3059.216	3091.22
Reduced Ω matrix with covariance term between η_1 & η_2	Yes	No	3015.408	3045.41
Reduced Ω matrix with covariance term between η_1 & η_3	Yes	No	3073.147	3103.15
Reduced Ω matrix with covariance term between η_2 & η_3	Yes	No	3079.126	3109.13
Reduced Ω matrix with covariance term between η_1 & η_2, and η_2 & η_3	No	No	3008.638	3036.64

Table 3.4 A summary of the result obtained from the final model and the bootstrap analysis.

Parameter	Estimate	%RSE	Bootstrap estimate (95% CI)
CL/F (L/h)	1520	5.83	1490 (1310-1660)
V2/F (L)	477	12.5	480 (307-694)
Ka (h^{-1})	1.05	8.49	1.12 (0.893-1.63)
CLM/F (L/h)	110	3.75	110 (101-120)
V3/F (L)	127	6.50	127 (110-143)
Q/F (L/h)	136	16.3	162 (101-292)
V4/F (L)	1100	33.3	1126 (625-2220)
Theta (8)	0.914	24.6	0.976 (0.553-1.52)
Theta (9)	1.44	26.6	1.47 (0.735-2.44)
Theta (10)	0.921	39.0	1.12 (0.010-4.35)
Theta (11)	1.47	39.0	1.42 (0.010-4.72)
IIV (variances and %CV)			
IIV-CL/F	0.182 (42.7)	29.6	0.173 (0.049-0.325)
IIV-V2/F	3.07 (175)	13.8	3.07 (2.02-4.43)
IIV-Ka	0.168 (41.0)	43.0	0.254 (0.0001-0.694)
RV (%CV)			
AS (nmols/L)	84.8	9.60	82.5 (63.6-102)
DHA (nmols/L)	105	7.15	105 (86.1-123)

RSE, relative standard error; CL/F, apparent clearance for AS; F, unknown bioavailability; V2/F, apparent volume of distribution of the central compartment for AS; Ka, absorption rate constant for AS, CLM/F, apparent clearance for DHA from the central compartment; V3/F, apparent central volume of distribution for DHA; Q/F, inter-compartmental clearance for AS; V4/F, apparent peripheral volume of distribution for AS; CV, coefficient of variation; IIV, inter-individual variability; RV, residual variability; AS, artesunate; DHA, dihydroartemisinin.

Table 3.5 Comparisons of demographic and pharmacokinetic characteristics between Cambodian patients and Thai patients in study SP-C-004-06.

Characteristics[a]	Cambodian patients (N=110)	Thai patients (N=134)	P-value[d]
Demographics			
AS dose received (mg/kg)	3.2 (2.4-4.5)	3.4 (2.4-4.6)	0.14
Age (years)	21.5 (5-58)	25.5 (10-55)	0.008[e]
Weight (kg)	46.6 (20-70)	51.6 (21-72.3)	0.0001[e]
Baseline parasite count (per μL)	14690 (1160-97500)	11689 (1040-97500)	0.12
Baseline hematocrit (%)	35.6 (23.9-50)	36.7 (24-49)	0.16
Baseline hemoglobin (g/L)	119 (80-171)	124 (81-165)	0.11
Baseline erythrocyte count ($x10^{12}$ /L)	4.6 (2.8-6.3)	4.6 (2.6-6.5)	0.74
Baseline ALT (U/L)	20 (8-75)	22 (2-95)	0.33
Baseline AST (U/L)	35 (14.7-114)	27 (5-104)	<0.0001[e]
Pharmacokinetics			
CL/F/kg (L/h/kg)	23.2 (11.8-46.3)	24 (12.6-50)	0.27
V2/F/kg (L/kg)	6 (2.4-116.5)	6.1 (2.1-365.7)	0.92
Ka (h^{-1})	1.1 (0.74-1.7)	1.1 (0.71-1.8)	0.66
CLM/F/kg (L/h/kg)	1.7 (0.9-3.2)	1.73 (0.96-3.4)	0.33
V3/F/kg (L/kg)	1.7 (0.72-4.6)	1.9 (0.67-5.7)	0.018[e]
Q/F/kg (L/h/kg)	2.1 (1.1-4)	2.2 (1.2-4.21)	0.33
V4/F/kg (L/kg)	15 (6.1-40)	16.2 (5.7-50.2)	0.018[e]
$t_{1/2F}$ (h)[b]	0.18 (0.06-3.42)	0.19 (0.06-10.8)	0.85
$t_{1/2elim,DHA}$ (h)[c]	0.69 (0.43-1.1)	0.75 (0.55-1.17)	<0.0001[e]
AUC_{DHA} (nmols.h.L-1)	5063 (2292-8577)	5100 (2146-11279)	0.76

[a] All values are presented as median (range).

[b] $t_{1/2F}$ (h) = ln(2)*V2/CL

[c] $t_{1/2elim,DHA}$ (h) = ln(2)*V3/CLM

[d] P-value based on two-sided Wilcoxon rank-sum test.

[e] Statistically significant at α=0.05.

Figure 3.1 Semi-logarithmic plot of observed artesunate (AS) concentrations versus time after dose. The solid line is smoothing line.

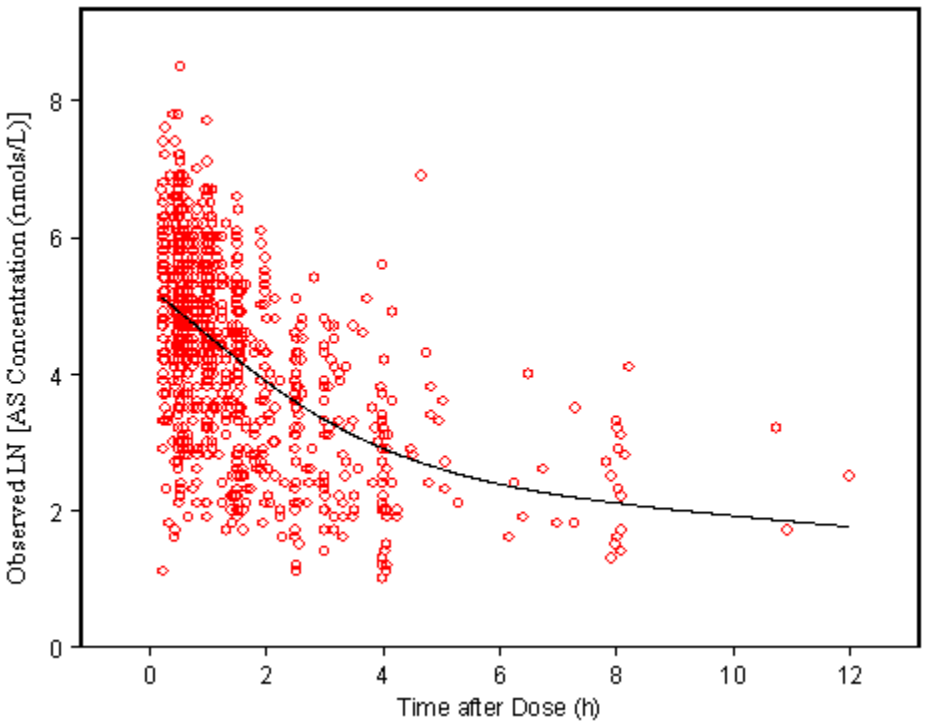

Figure 3.2 Semi-logarithmic plot of observed dihydroartemisinin (DHA) concentrations versus time after dose. The solid line is smoothing line.

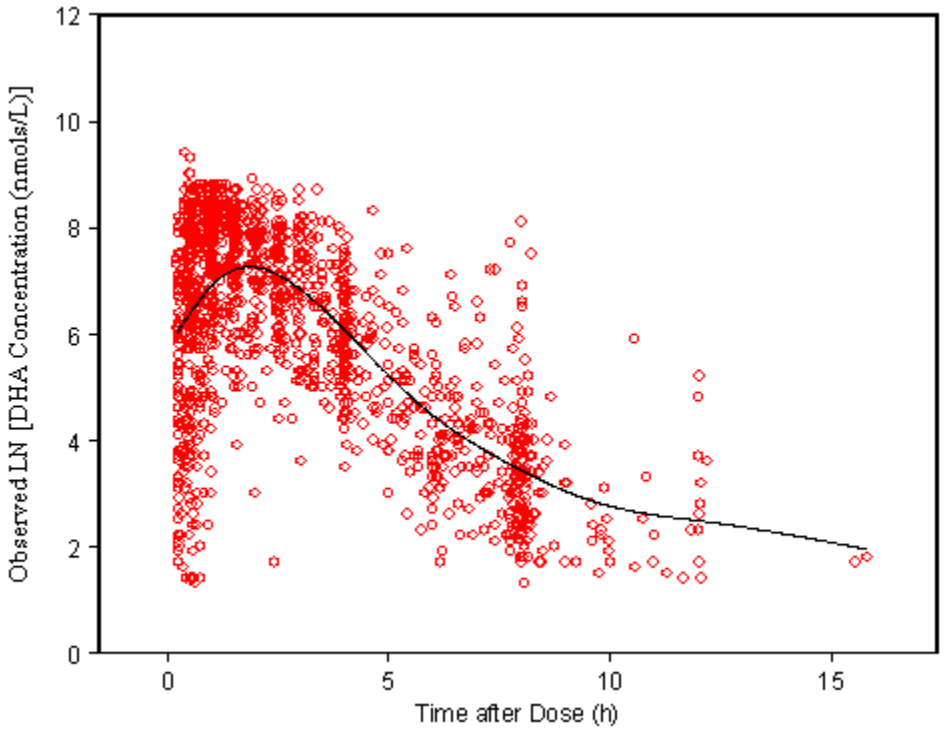

Figure 3.3 Schematic representation of the final structural model.

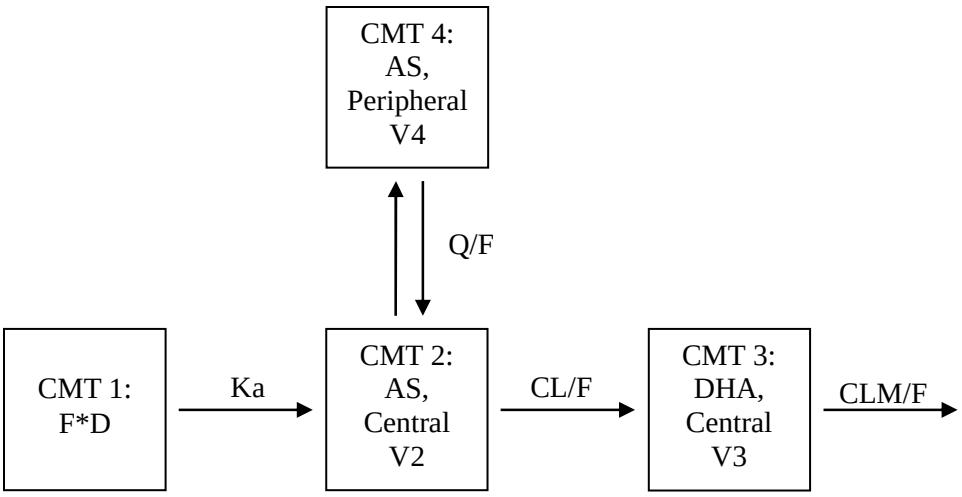

CMT, compartment; AS: artesunate; DHA, dihydroartemisinin; F, oral bioavailability; D, AS dose; Ka, absorption rate constant; CL, AS clearance; V2: central volume of distribution for AS; CLM, DHA clearance; V3; central volume of distribution for DHA; Q, inter-compartmental clearance; V4, peripheral volume of distribution for AS.

Figure 3.4 Population and individual predicted concentration versus observed concentration plot of artesunate (AS) for the final model. The solid lines are lines of identity. The broken lines are smoothing lines.

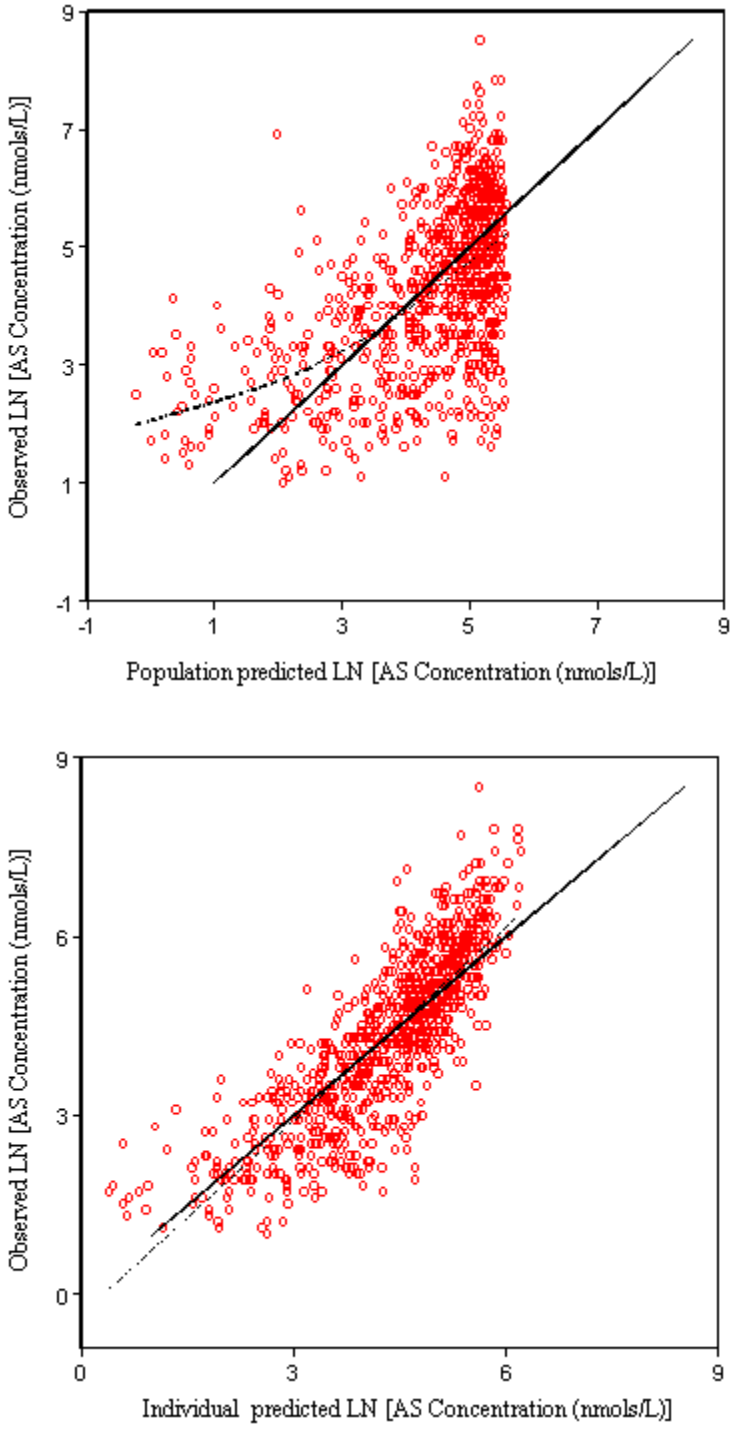

Figure 3.5 Conditional weighted residual plots of artesunate (AS) for the final model. The broken lines are smoothing lines.

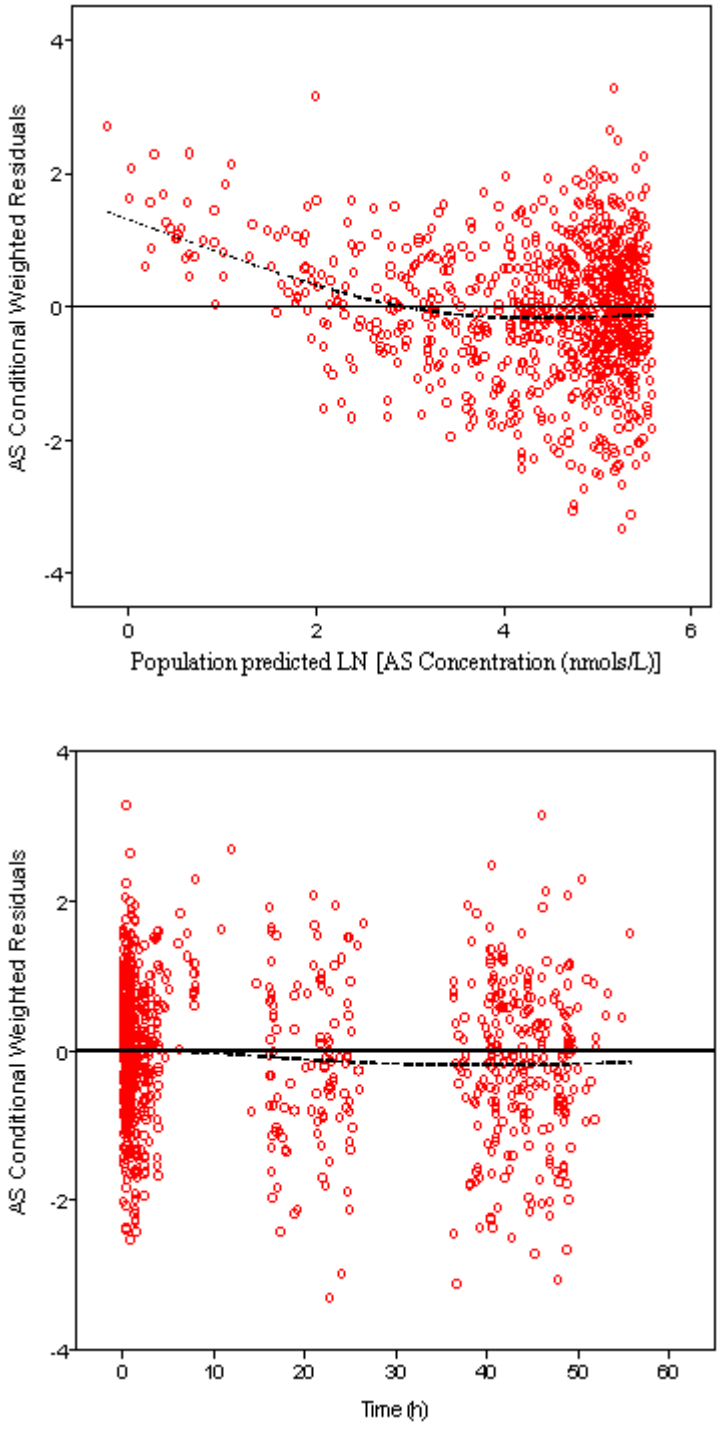

Figure 3.6 Population and individual predicted concentration versus observed concentration plots of dihydroartemisinin (DHA) for the final model. The solid lines are lines of identity. The broken lines are smoothing lines.

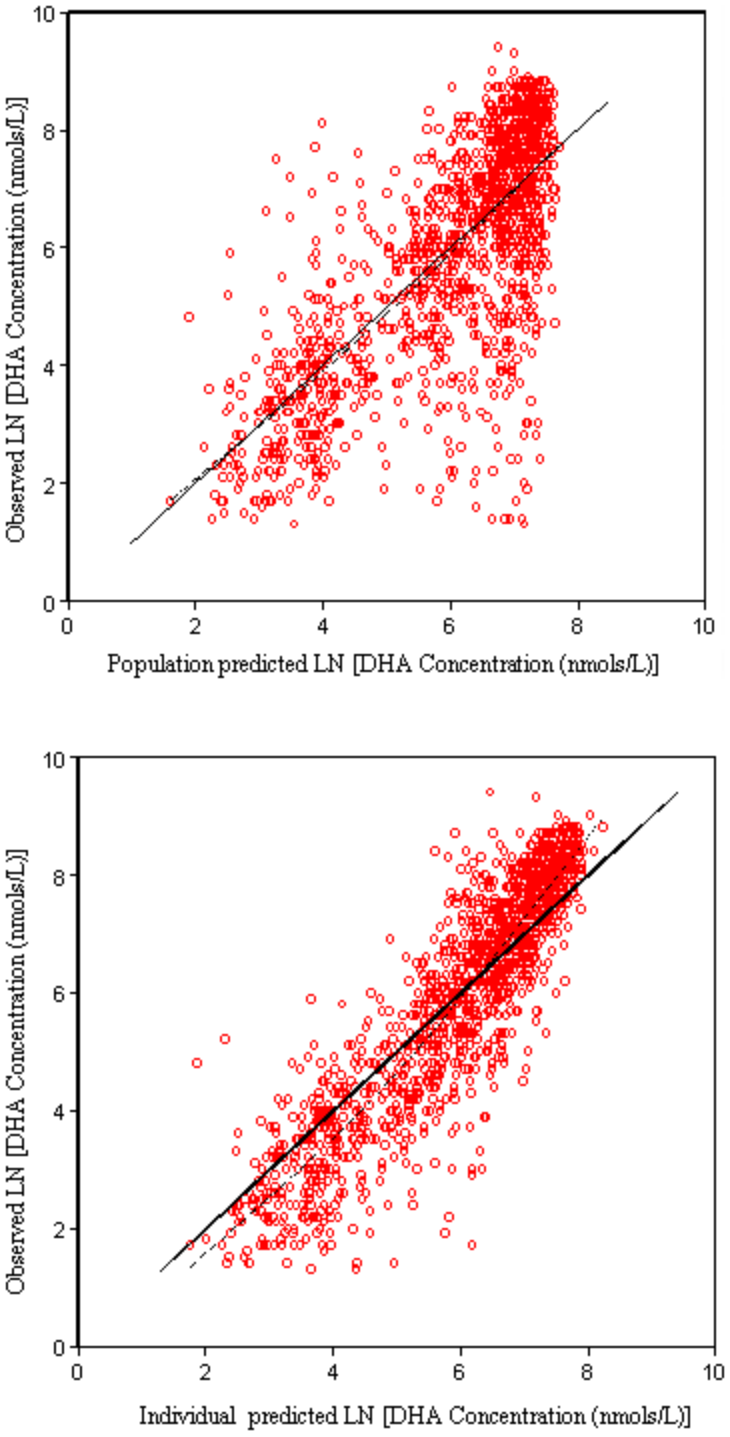

Figure 3.7 Conditional weighted residual plots of dihydroartemisinin (DHA) for the final model. The broken lines are smoothing lines.

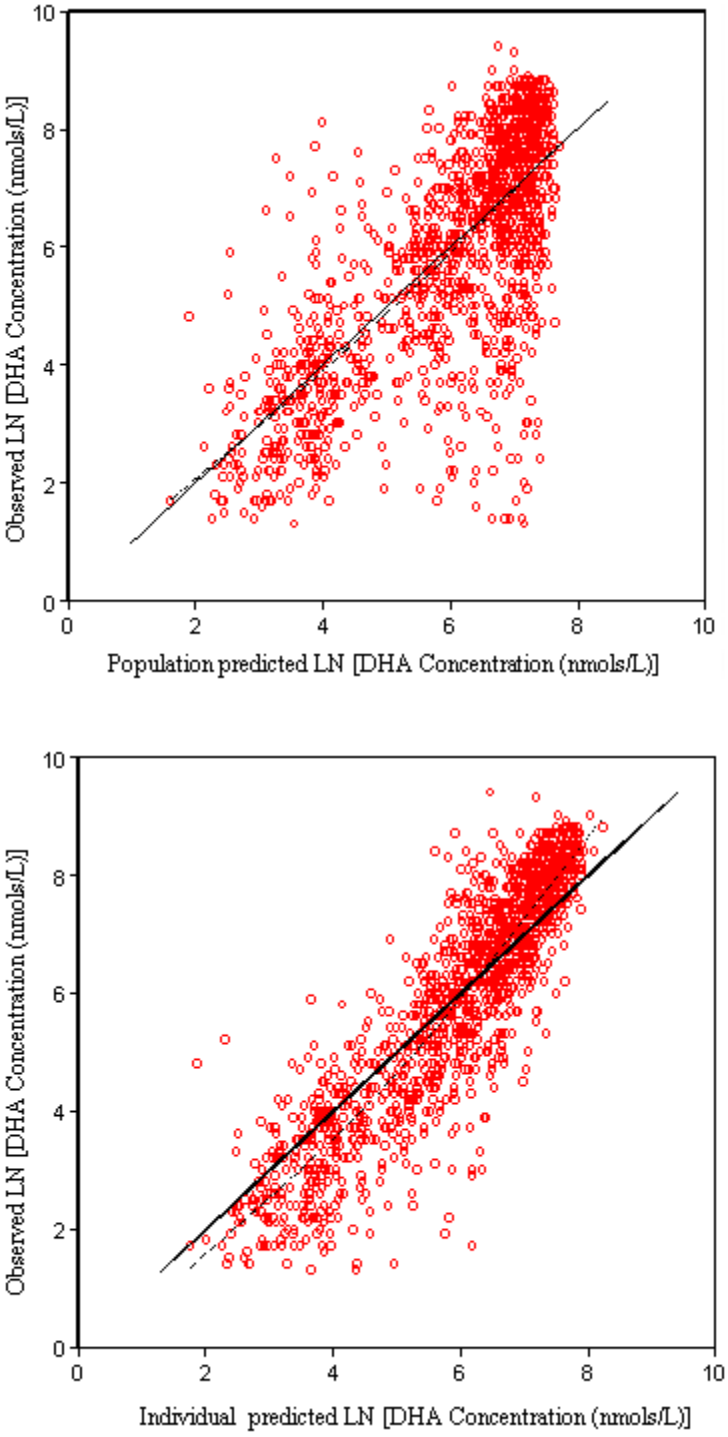

Figure 3.8 Plots of the artesunate (AS) observations (open circles), population predictions (broken lines), and individual predictions (solid lines) from the final model for selected subjects.

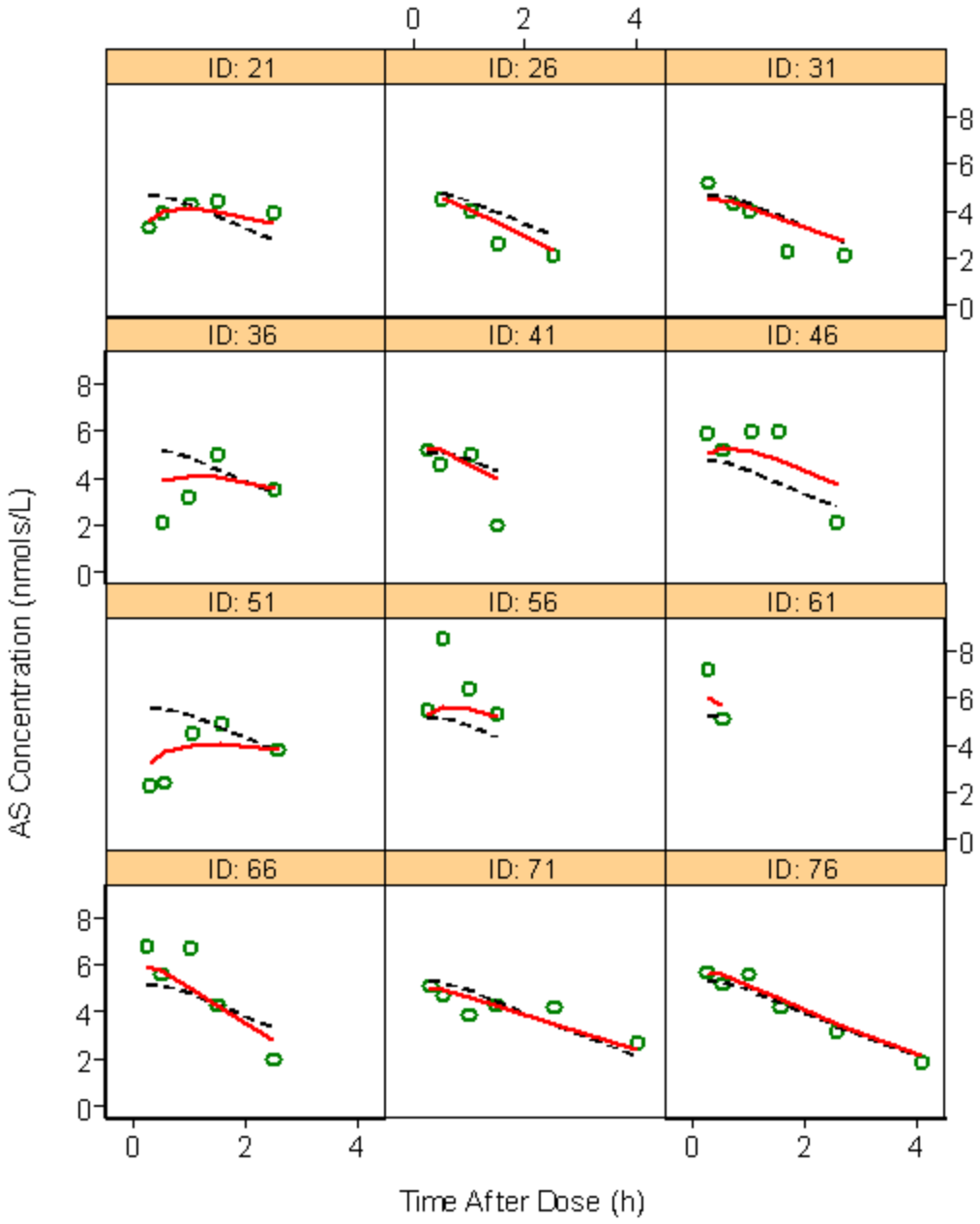

Figure 3.9 Plots of the dihydroartemisinin (DHA) observations (open circles), population predictions (broken lines), and individual predictions (solid lines) from the final model for selected subjects.

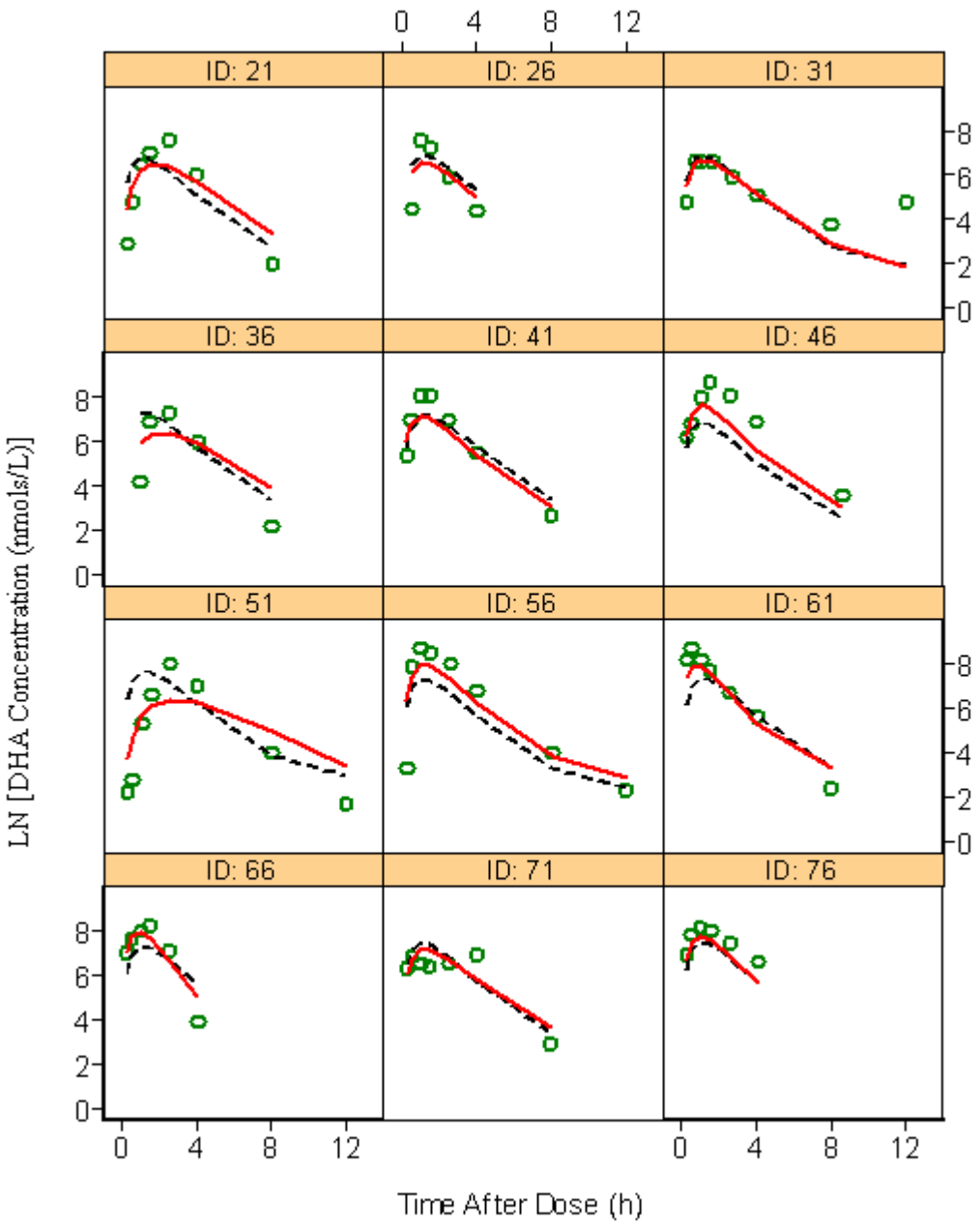

Figure 3.10 Visual predictive check of the final model for artesunate (AS) observations. The open circles represent the observed concentrations, solid lines represent the 90% confidence interval obtained from the simulations, and the dashed line represents the 50th percentile of the simulations.

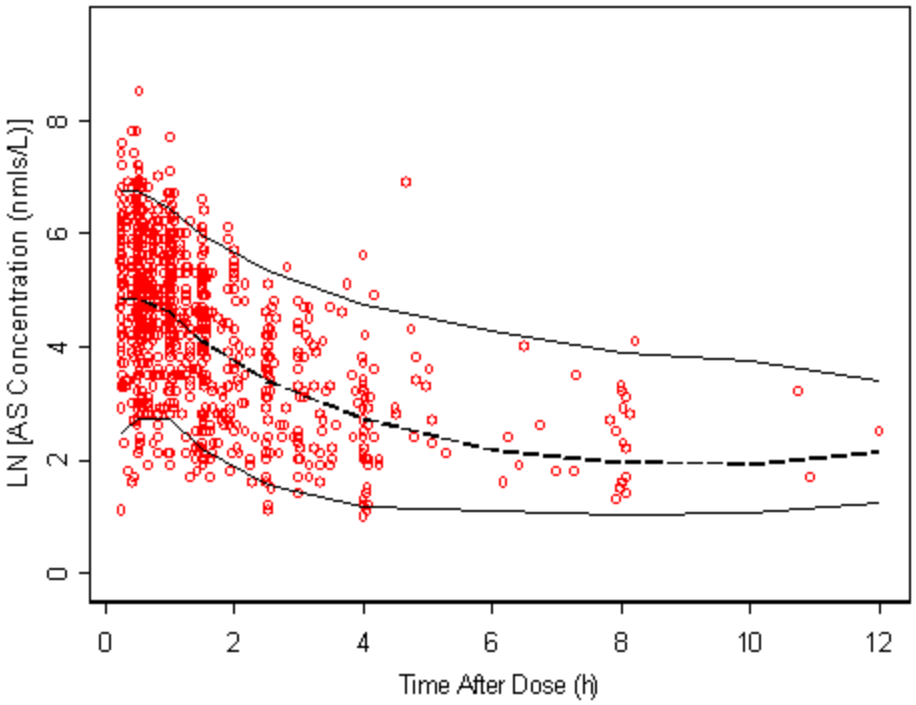

Figure 3.11 Visual predictive check of the final model for dihydroartemisinin (DHA) observations. The open circles represent the observed concentrations, solid lines represent the 90% confidence interval obtained from the simulations, and the dashed line represents the 50th percentile of the simulations.

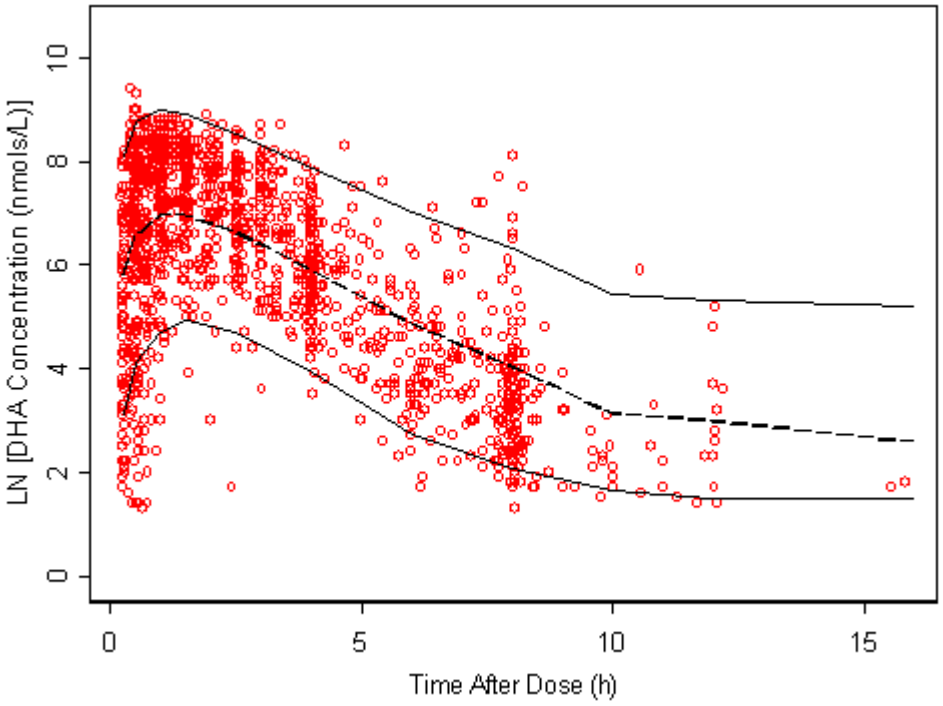

Figure 3.12 Plot of 500 simulated concentration-time profiles for artesunate (AS) using the estimates from the final model and standard weight of 70 kg. The open circles represent the simulated concentrations, solid lines represent the 90% confidence interval obtained from the simulations, and the dashed line represents the 50th percentile of the simulations.

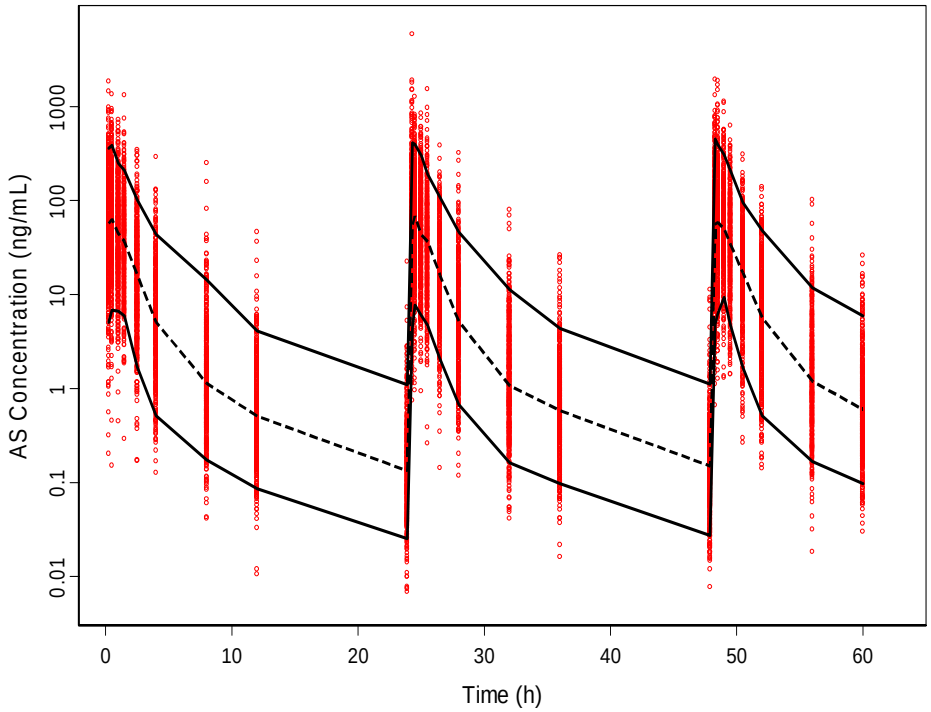

Figure 3.13 Plot of 500 simulated concentration-time profiles for dihydroartemisinin (DHA) using the estimates from the final model and standard weight of 70 kg. The open circles represent the simulated concentrations, solid lines represent the 90% confidence interval obtained from the simulations, and the dashed line represents the 50th percentile of the simulations.

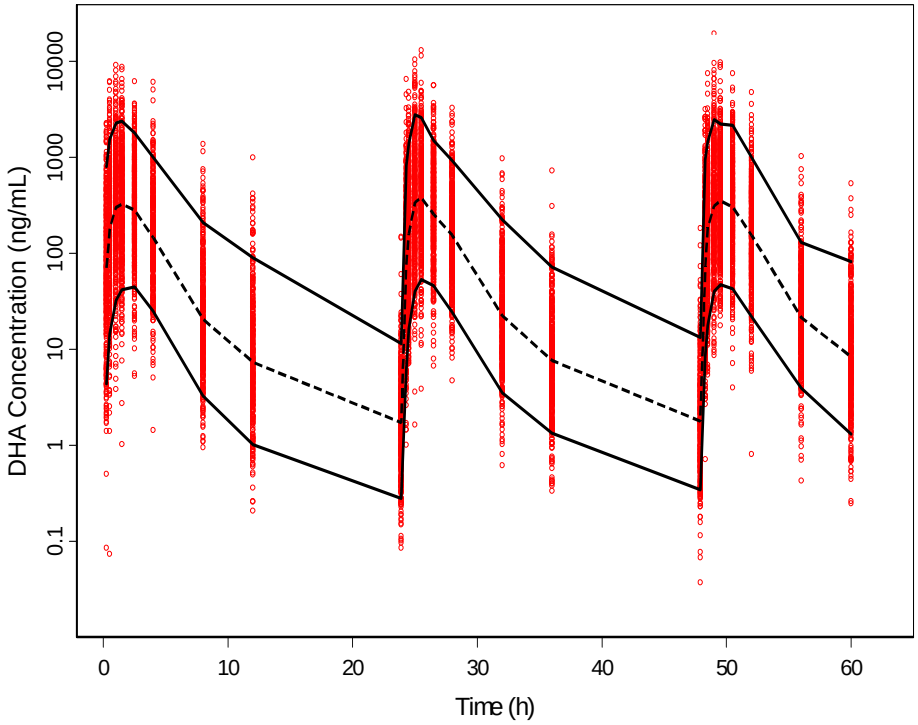

CHAPTER IV

SUMMARY AND RECOMMENDATION FOR FUTURE WORK

Summary

Artemisinin and its derivatives are the most potent anti-malarial drugs available in the market. AS, a water-soluble hemisuccinate derivative of artemisinin, is the most widely used derivative. Today, malaria treatment is largely relies on the artemisinin-based combination therapies. AS is rapidly absorbed and hydrolyzed to its active metabolite DHA.

The pharmacokinetics of AS and DHA has been studied in different populations (73, 74, 81, 154, 174, 175, 177-179). However, these earlier pharmacokinetic studies of AS were conducted in small sample of subjects with intensive blood sampling schedule. The data collected were often analyzed using non-compartmental analysis and the results were presented as mean ± standard deviation or median and range. Due to the small sample size and the use of non-compartmental approach, the results were hardly representative of the population of interest. The results of these analyses were therefore limited to describing the data at hand and can not be extrapolated to the population at-large.

The introduction of the population modeling approach and the advance in computing performance in recent years have changed the way pharmacokinetic studies are conducted. Using the statistical-based population modeling which is more computer-intensive, it is now possible to conduct pharmacokinetic studies with sparse sampling schedule. This approach has opened the door to ethically conducting pharmacokinetic studies in special populations, such as children and pregnant women, who have limited immunity and therefore most susceptible to the clinical sequelae of malaria. Population pharmacokinetics of AS and/or DHA following administration of AS has been described in pediatric patients with uncomplicated falciparum and vivax malaria who were treated

with two doses of intra-rectal AS (146), in adult and pediatric patients with moderately severe falciparum malaria who were treated with a single dose of intra-rectal AS (147), in pregnant women with acute uncomplicated falciparum malaria after a three-day dosing of oral AS in combination with atovaquone plus proguanil (156), and in African children with uncomplicated falciparum malaria who received fixed dose combination of AS and amodiaquine orally (157). However, the number of AS observations available for modeling was limited in all of these studies due to several reasons, such as insufficiency in sampling processing or assay method, relatively small sample size, and limited sampling scheme. Consequently, the analyses have been able to model only the DHA data (147, 156, 157) and/or fit only a one-compartmental model to AS and/or DHA data (146, 147, 156, 157). Sometimes, fixing of certain pharmacokinetic parameter to an arbitrary value was also required (147). On top of these limitations, none of the models was evaluated for its predictive performance.

In this thesis, the population pharmacokinetics of AS and DHA following different dosing and treatment regimens of oral AS were characterized in different populations. In Chapter II, we developed a population pharmacokinetic model of AS and DHA in 91 healthy subjects. The data was pooled from four Phase I studies. These subjects received either single- or multiple-dosing of oral AS, as a monotherapy regimen or in combination with pyronaridine, with or without food. In Chapter III, we developed a population pharmacokinetic model of AS and DHA in adult and pediatric patients with uncomplicated falciparum and vivax malaria who were administered oral pyronaridine/artesunate combination once daily for 3 days. We pooled the data of 632 patients from a Phase II and four Phase III clinical trials.

In both analyses, we were able to model the AS and DHA data simultaneously using a parent-metabolite model that assumed complete conversion of AS to DHA. Inter-individual variability for almost all pharmacokinetic parameters and residual variability for both compounds were defined. AS was rapidly absorbed and hydrolyzed to form

DHA. The elimination half-lives of AS and DHA were very short. Substantial variability was seen in the pharmacokinetic parameters between the subjects.

Intake of food with the dose was found to significantly delay the absorption of AS in healthy subjects. Weight was also included in this model as a determinant of DHA clearance. When modeling the data from pediatric and adult patients, we included weight as part of the model *a priori* using an established and commonly used allometric function. No other covariates examined in the analysis were statistically significant.

Finally, the models developed were evaluated for model adequacy, robustness, stability and predictive performance using a combination of different approaches. This is important to ensure that the models are not only descriptive but also predictive, such that the results can be used for simulation and extrapolation purposes. Both models were found to adequately described the data at hand, and robust with sufficient predictive power.

The final structural model in healthy subjects consisted of a central compartment for AS and central and peripheral compartments for DHA. In malarial patients, the data was best described with two-compartmental model for AS and one-compartmental model for DHA. The difference in structural models used in the two analyses can be attributed to the empirical approach used in the modeling. The distribution of pharmacokinetic data was greatly influenced by the choice of sampling times and type of sampling (intensive sampling and sparse sampling). It is therefore not surprising that the final structural models were different in the analyses since the choice was largely driven by the data at hand.

Direct comparison of the pharmacokinetic parameters in the two analyses was made complicated because different structural models were used to describe the data arise from the two populations. The typical apparent clearance values for both AS and DHA were lower in the healthy population compared to the patient population. Therefore, using the formula: AUC = Dose/clearance, the AUC of AS and DHA would be higher for a

typical healthy subject than for a typical malarial patient given the same dose. Figure 4.1 and Figure 4.2 shows the typical concentration-time profiles of AS and DHA for a healthy subject and a malaria patient who received an AS dose of 200 mg, using the population parameter estimates for each of the models. The typical concentration-time curves for both AS and DHA looked very similar for the healthy subject and malarial patient. However, the C_{max} and AUC values of both AS and DHA were lower for the patient population compared to the healthy population. This is contrary to the results reported by Teja-Isavadharm et al. (81). They studied the single-dose pharmacokinetics of AS in 6 malaria patients and 6 healthy subjects and compared the pharmacokinetic parameters of DHA between patients and healthy subjects. The mean C_{max} and AUC values of DHA were significantly higher in the patient group than in the healthy subjects.

In summary, descriptive, robust and predictive population pharmacokinetic models of AS and DHA were developed for healthy and patient populations. The model developed in the patient population can be used as the base to develop a population pharmacokinetic-pharmacodynamic model which will be discussed further in the following section. It can also be used as prior information in guiding the selection of optimal sampling schedule for future pharmacokinetic studies of AS.

Recommendation for Future Work

Application of Pharmacogenomics

In our work and other published works on population pharmacokinetics of AS (146, 147, 156, 157), high inter-individual and residual variability in AS and DHA pharmacokinetics were observed. Different covariates that partly explained the variability seen in various populations were identified, including weight on the volume of distribution of DHA (146, 147), gender on the clearance of DHA (147), and age on the volume of distribution of DHA. As presented in Chapter II, food intake and weight were influential on the absorption rate constant of AS and volume of distribution of DHA,

respectively. The results of covariate analysis from all these reports show that size (age and gender are highly and positively correlated with weight) is the primary covariate for the clearance and volume of distribution of AS and DHA. Since weight is an easily measured marker of size, an allometric-based model for weight with a coefficient of 0.75 for clearance terms and 1 for volume terms for use in pharmacokinetics was proposed (173, 180). We therefore adopted this strategy when modeling the population pharmacokinetics of AS and DHA in malarial patients, as detailed in Chapter III. However, even after taking into account the effect of weight on all clearance and volume terms, the inter-individual and residual variability observed was still pretty substantial. The simulation exercise in Chapter III again showed the large variability in the simulated concentrations.

Genetic variation has been found to influence the disposition of many drugs. Gene polymorphisms were incorporated in some population pharmacokinetic studies as covariates to explain the variability in drug pharmacokinetics, particularly for anti-viral drugs (181-184), anti-cancer drugs (185-187) and some other drugs (188, 189). We suggest that polymorphisms in drug metabolizing enzyme can be utilized to explain part of the variability in the pharmacokinetics of DHA. In human, the glucuronidation of DHA was catalyzed by UDP-glucuronosyltransferases (UGTs), in particular UGT1A9 and UGT2B7 (84).

The UGT2B7 single nucleotide polymorphisms (SNPs) are highly prevalent in many populations. The reported frequencies of UGT2B7 polymorphisms are: 211G>T (17.5% in Japanese, 9% in Asian-Americans, 2% in Hispanic-Americans), 802C>T (25.4% in Japanese, 48.9-53.7% in Caucasians, 21% in West Africans, 28% in Papua New Guineans), and 1192G>A (<1% in Japanese) (190-193). The UGT1A9 variant alleles are less common. The reported frequencies of UGT1A9 polymorphisms are: 8G>A (2.5% in African-Americans, 1% in Asian-Americans), 98T>C (2.2-3.6% in

Caucasians, 1% in Asian-Americans), 766G>A (<1% in Japanese, 1% in Asian-Americans), and 726T>G (0.5% in Japanese) (193-196).

Given the high prevalence of UGT2B7 polymorphisms in West African and Papua New Guinean populations, it is important to characterize the metabolic and phenotypic consequences of this genetic variation on the pharmacokinetic and pharmacodynamic of DHA. Due to the substantial inter-individual variability in the pharmacokinetic properties of DHA, it is possible that some of the patients who received AS treatment were exposed to subtherapeutic DHA concentrations. This has important implication on the dosing of AS, since resistance to AS can only occur due to inadequate treatment (135).

Population Pharmacokinetic/Pharmacodynamic Modeling

Despite the fact that AS is the most commonly used artemisinin derivative, information regarding its pharmacokinetic/pharmacodynamic relationship is scanty. In most studies that described the relationship between pharmacokinetic and pharmacodynamic variables of AS, the approaches used were generally limited to either multiple regression or logistic analysis (73, 74, 147, 174). Nonlinear relationship was not explored in any of these studies.

AS dose-response relationship using modeling approach has been characterized in only one occasion (197). In this study, 47 adult patients with acute uncomplicated falciparum malaria were randomized to receive a single oral dose of either 0, 25, 50, 75, 100, 150, 200, or 250 mg of AS, followed by a single oral dose of mefloquine. Pharmacodynamic measures of outcome used were the time to 50% reduction in parasitemia (PC_{50}), the time to 90% reduction in parasitemia (PC_{90}) and the parasite clearance time (PCT). A sigmoid inhibitory effect model was chosen *a priori* to fit the relationship between AS dose and the pharmacodynamic parameters. The estimated AS

doses that result in 50% of the maximum effect (ED_{50}s) for the study population were 0.7, 1.2, and 1.4 mg/kg for PC_{50}, PC_{90} and PCT, respectively. The estimated lowest dose to produce maximum effect (E_{max}) was 2 mg/kg. They suggest that 2 mg/kg would be the lowest AS dose to be given to an "average" patient in order to produce maximum parasite clearance effect. However, considering the substantial variability between the patients, they recommended higher AS dose to be given. Although the dose-response relationship of AS was characterized in this study, pharmacokinetic modeling was not done. It is therefore not known which pharmacokinetic parameter is the most important determinant of the parasite killing effect of AS. Also, since the inter-individual variability was not characterized statistically, the minimum AS dose to be given to produce desirable effect in most of the patients is not known.

We recommend that a population pharmacokinetic/pharmacodynamic model be developed to examine the relationship between different pharmacokinetic parameters and the anti-malarial efficacy of AS. Specific pharmacokinetic parameters of interest include area under the plasma concentration-time curve (AUC) and time above minimum inhibitory concentration (MIC) of AS and DHA. AUC is the measure of systemic exposure and has been identified to correlate with the anti-malarial activities of artemisinin compounds. In 24 patients with severe falciparum malaria who received intravenous AS, the AUC for DHA was found to inversely correlate with PCT_{50} (174). In patients treated with artemether/lumefantrine combination, the AUCs of both DHA and artemether contributed equally to the parasite clearance time (198). Time above MIC should be examined because concentrations below the MIC are associated with net parasite growth. In order to cure the blood-stage infections in non-immune patients, the anti-malarial blood concentrations need to exceed MIC until all asexual parasites are cleared from the blood (199). Relevant outcome measures may include PCT_{50}, PCT_{90}, parasite clearance time, fever clearance time and treatment failure.

Considering the large variability in the pharmacokinetic and pharmacodynamic measures of AS and the importance to ensure adequate treatment in the patients, a population pharmacokinetic/pharmacodynamic model would be very useful in guiding the search for the optimal AS dose. Using such model, which takes into account the variability component, a particular target clinical effect can be translated into a target dose through simulation.

Figure 4.14 Typical concentration-time profiles for artesunate (AS) in healthy subject (solid line) and malarial patient (dashed line).

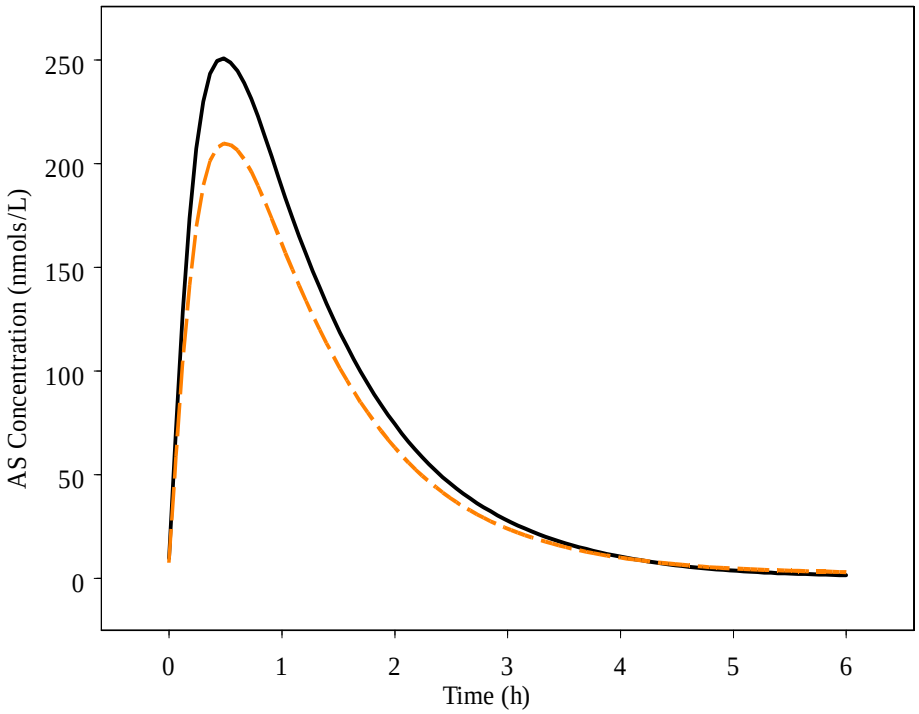

Figure 4.2 Typical concentration-time profiles for dihydroartemisinin (DHA) in healthy subject (solid line) and malarial patient (dashed line).

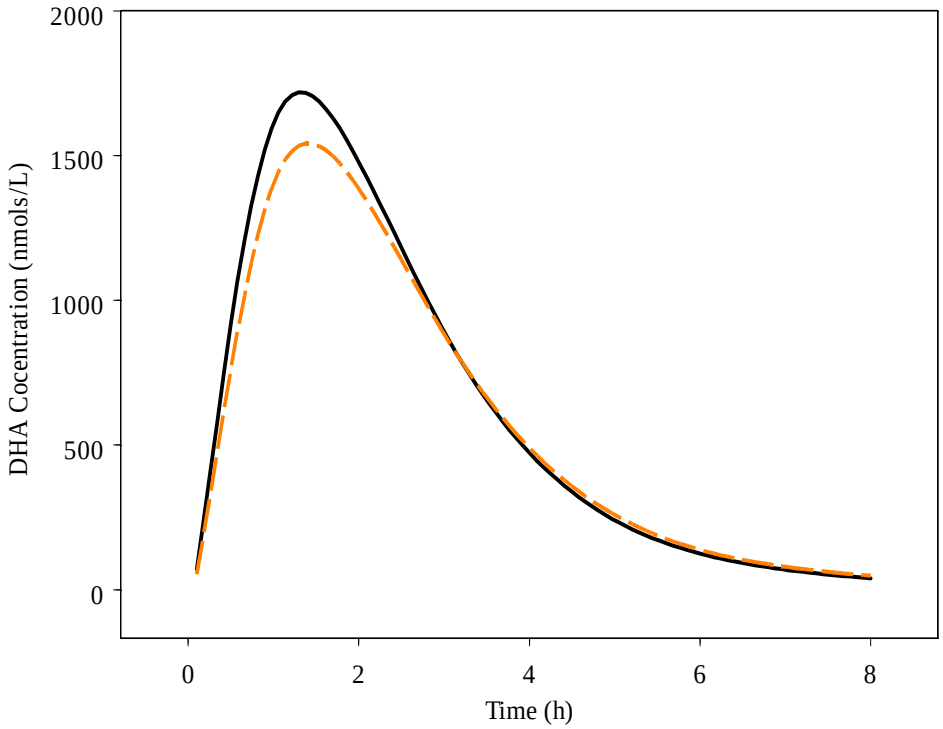

APPENDIX A

NONMEM CONTROL FILE FOR THE FINAL MODEL IN

CHAPTER II

```
;Model Desc: final model, 1cmt AS, 2 cmt DHA
;Project Name: phase1
;Project ID: PHASE 1

$PROB RUN# 033
$INPUT C ID TIME TAD AMT ODV DV MDV EVID CMT ADDL II AGE SEX WT DOS
FOOD
$DATA PHASE1ASDHA.CSV IGNORE=C
$ABB COMRES=9
$SUBROUTINE ADVAN6 TRANS=1 TOL=4

$MODEL
 NCOMPS=4
 COMP= (DEPOT,DEFDOSE)
 COMP= (CENTRAL,DEFOBS)
 COMP= (METABOL,NODOSE)
 COMP= (PERI,NODOSE)

$PK
"FIRST
"COMMON/PRCOMG/IDUM1,IDUM2,IMAX,IDUM4,IDUM5
"INTEGER IDUM1,IDUM2,IMAX,IDUM4,IDUM5
"IMAX=200000

;AS PARAMETERS
TVCL=THETA(1)
CL=TVCL*EXP(ETA(1))

TVV2=THETA(2)
V2=TVV2*EXP(ETA(2))

TVKA=THETA(3)*(1+THETA(8)*FOOD)
KA=TVKA*EXP(ETA(3))

;DHA PARAMETERS
TVCLM=THETA(4)+THETA(9)*(WT-61.5)
CLM=TVCLM*EXP(ETA(4))

TVV3=THETA(5)
V3=TVV3*EXP(ETA(5))

TVQ=THETA(6)
Q=TVQ*EXP(ETA(6))

TVV4=THETA(7)
V4=TVV4*EXP(ETA(7))

;SCALING AND REPARAMTERISATION
K23=CL/V2
K30=CLM/V3
K34=Q/V3
K43=Q/V4
S2=V2
S3=V3
SID=ID
```

```
OBS=DV

$INFN
IF (ICALL.EQ.3) THEN
 OPEN(50,FILE='CWTAB033.est')
 WRITE (50,*) 'ETAS'

DO WHILE(DATA)
IF (NEWIND.LE.1) WRITE(50,*) ETA
ENDDO
 WRITE (50,*) 'THETAS'
 WRITE (50,*) THETA
 WRITE (50,*) 'OMEGAS'
 WRITE (50,*) OMEGA(BLOCK)
 WRITE (50,*) 'SIGMAS'
 WRITE (50,*) SIGMA(BLOCK)
ENDIF

$DES
DADT(1)=-KA*A(1)
DADT(2)=KA*A(1)-K23*A(2)
DADT(3)=K23*A(2)+K43*A(4)-K30*A(3)-K34*A(3)
DADT(4)=K34*A(3)-K43*A(4)

$ERROR
PROP=0
IF(CMT.EQ.2)PROP=EPS(1)
IF(CMT.EQ.3)PROP=EPS(2)
IPRED=-3
IF(F.GT.0) IPRED=LOG(F)
W=1
IRES=DV-IPRED
IWRES=IRES/W
Y=IPRED+W*PROP

"LAST
"  COM(1)=G(1,1)
"  COM(2)=G(2,1)
"  COM(3)=G(3,1)
"  COM(4)=G(4,1)
"  COM(5)=G(5,1)
"  COM(6)=G(6,1)
"  COM(7)=G(7,1)
"  COM(8)=HH(1,1)
"  COM(9)=HH(2,1)

$EST METHOD=1 POSTHOC PRINT=5 MAX=9999 SIG=3 MSFO=033.msf

$THETA
  (0.1,2000) ;[CL]
  (0.1,2000) ;[V2]
  (0.1,5)    ;[KA]
  (0.1,200)  ;[CLM]
  (0.1,300)  ;[V3]
  (0.1,50)   ;[Q]
  (0.1,50)   ;[V4]
  (-1, -.3)  ;[FOOD_KA]
  (0, 5)     ;[WT_CLM]

$OMEGA
  1 ;[P] omega(1,1)
  1 ;[P] omega(2,2)
  1 ;[P] omega(3,3)
  1 ;[P] omega(4,4)
```

```
  1 ;[P] omega(5,5)
  0 FIXED ;[P] omega(6,6)
  0 FIXED ;[P] omega(7,7)

$SIGMA
  1 ;[A] sigma(1,1)
  1 ;[A] sigma(2,2)

$COV PRINT=E

$TABLE ID SID TIME TAD IPRED CMT CL CLM V2 V3 KA Q V4
AGE WT SEX FOOD DOS ONEHEADER NOPRINT FILE=033.tab

$TABLE ID CL CLM Q V2 V3 V4 KA K23 K30 K34 K43
ONEHEADER NOPRINT FILE=033.par

$TABLE ID ETA1 ETA2 ETA3 ETA4 ETA5
ONEHEADER NOPRINT FILE=033.eta

$TABLE ID TIME TAD IPRED IWRES EVID MDV
ONEHEADER NOPRINT FILE=SDTAB033

$TABLE ID CL KA V2 V3 CLM Q V4
ONEHEADER NOPRINT FILE=PATAB033

$TABLE ID AGE WT
ONEHEADER NOPRINT FILE=COTAB033

$TABLE ID SEX DOS FOOD CMT
ONEHEADER NOPRINT FILE=CATAB033

$TABLE ID COM(1)=G11 COM(2)=G21 COM(3)=G31 COM(4)=G41
COM(5)=G51 COM(6)=G61 COM(7)=G71 COM(8)=H11 COM(9)=H21
IPRED MDV NOPRINT ONEHEADER FILE=033.deriv
```

APPENDIX B

THE OUTPUT SUMMARY FOR THE FINAL MODEL IN

CHAPTER II

```
PDx-Pop 3.0 Run Summary File Run No: 033

[18MAY2008 Revision]
Date: ==== START TIME ====
Output Extracted from file: c:\pdxpop3\phase1\033.res
DataFile:  PHASE1ASDHA.CSV

MINIMIZATION STATUS
  MINIMIZATION SUCCESSFUL
  NO. OF FUNCTION EVALUATIONS USED:      653
  NO. OF SIG. DIGITS IN FINAL EST.:  3.2

  ETABAR IS THE ARITHMETIC MEAN OF THE ETA-ESTIMATES,
  AND THE P-VALUE IS GIVEN FOR THE NULL HYPOTHESIS THAT THE TRUE MEAN IS 0.

  ETABAR:   0.30E-02 -0.37E-01 -0.86E-01  0.12E-02  0.92E-02  0.00E+00  0.00E+00
  SE:       0.28E-01  0.39E-01  0.73E-01  0.23E-01  0.17E-01  0.00E+00  0.00E+00

  P VAL.:   0.91E+00  0.34E+00  0.24E+00  0.96E+00  0.58E+00  0.10E+01  0.10E+01
  MINIMUM VALUE OF OBJECTIVE FUNCTION :    487.204

ETABAR P VAL. FOR NO ETA < 0.05

MODEL DEFINITION
"FIRST
"COMMON/PRCOMG/IDUM1,IDUM2,IMAX,IDUM4,IDUM5
"INTEGER IDUM1,IDUM2,IMAX,IDUM4,IDUM5
"IMAX=200000

;ARTS PARAMETERS
TVCL=THETA(1)
CL=TVCL*EXP(ETA(1))

TVV2=THETA(2)
V2=TVV2*EXP(ETA(2))

TVKA=THETA(3)*(1+THETA(8)*FOOD)
KA=TVKA*EXP(ETA(3))

;DHA PARAMETERS
TVCLM=THETA(4)+THETA(9)*(WT-61.5)
CLM=TVCLM*EXP(ETA(4))

TVV3=THETA(5)
V3=TVV3*EXP(ETA(5))

TVQ=THETA(6)
Q=TVQ*EXP(ETA(6))

TVV4=THETA(7)
V4=TVV4*EXP(ETA(7))

;SCALING AND REPARAMTERISATION
K23=CL/V2
K30=CLM/V3
K34=Q/V3
K43=Q/V4
S2=V2
S3=V3
SID=ID
OBS=DV


PROP=0
IF(CMT.EQ.2)PROP=EPS(1)
IF(CMT.EQ.3)PROP=EPS(2)
IPRED=-3
IF(F.GT.0) IPRED=LOG(F)
```

```
W=1
IRES=DV-IPRED
IWRES=IRES/W
Y=IPRED+W*PROP

"LAST
"  COM(1)=G(1,1)
"  COM(2)=G(2,1)
"  COM(3)=G(3,1)
"  COM(4)=G(4,1)
"  COM(5)=G(5,1)
"  COM(6)=G(6,1)
"  COM(7)=G(7,1)
"  COM(8)=HH(1,1)
"  COM(9)=HH(2,1)
```

	FINAL ESTIMATE	%RSE	95% CONFIDENCE INTERVAL LBOUND	UBOUND	DESCRIPTOR/ VARIABILITY	
THETA						
1	1.19e+003	4.20%	1.09e+003	1.29e+003		CL
2	1.21e+003	5.77%	1.07e+003	1.35e+003		V2
3	3.85	3.61%	3.58	4.12		KA
4	93.7	3.30%	87.6	99.8		CLM
5	97.1	4.85%	87.9	106		V3
6	5.74	12.8%	4.30	7.18		Q
7	18.5	10.6%	14.7	22.3		V4
8	-0.840	2.32%	-0.878	-0.802		FOOD_KA
9	1.90	16.3%	1.29	2.51		WT_CLM
OMEGA					INTERINDIVIDUAL VARIABILITY	
1,1	0.131	17.8%	0.0853	0.177	CV =	36.2%
2,2	0.330	20.9%	0.195	0.465	CV =	57.4%
3,3	1.26	15.4%	0.880	1.64	CV =	112%
4,4	0.0786	22.5%	0.0439	0.113	CV =	28.0%
5,5	0.0901	36.0%	0.0266	0.154	CV =	30.0%
6,6	0.00	...	...	...	CV =	...
7,7	0.00	...	...	...	CV =	...
SIGMA					RESIDUAL VARIABILITY	
1,1	0.375	9.73%	0.303	0.447	SD =	0.612
2,2	0.282	11.2%	0.220	0.344	SD =	0.531

*Indicates 95% confidence interval that includes zero
%RSE is percent relative standard error (100% x SE/EST)

```
        Akaike Information Criterion: 523.204
        Schwarz Bayesian Criterion:   626.284
CONDITION NUMBER = 24.0 (DOES NOT EXCEED 1000)
```

APPENDIX C

NONMEM CONTROL FILE FOR THE FINAL MODEL IN

CHAPTER III

```
;Model Desc: final model
;Project Name: phase2&3_cov
;Project ID: AS_DHA

$PROB RUN# 183
$INPUT C ID TIME TAD AMT DV MDV EVID CMT AGE WT HT=DROP BMI=DROP
LBW=DROP SEX GEO COUN=DROP XPAR=DROP PARA HCT HGB RBC XALT=DROP ALT
XAST=DROP AST IFXN=DROP OCC=DROP FORM TOUT=DROP

$DATA phase2_3_final.csv IGNORE=C
$ABB COMRES=5
$SUBROUTINE ADVAN5
$MODEL
 NCOMPS=4
 COMP= (DEPOT,DEFDOSE)
 COMP= (CENTRAL,DEFOBS)
 COMP= (METAB)
 COMP= (AS_PERI)

$PK
   TVCL=THETA(1)*(WT/70)**.75
   CL=TVCL*EXP(ETA(1))

   TVV2=THETA(2)*(WT/70)
   V2=TVV2*EXP(ETA(2))

   TVKA=THETA(3)
   KA=TVKA*EXP(ETA(3))

   TVCLM=THETA(4)*(WT/70)**.75
   CLM=TVCLM*EXP(THETA(8)*ETA(1))

   TVV3=THETA(5)*(WT/70)
   V3=TVV3*EXP(THETA(9)*ETA(1))

   TVQ=THETA(6)*(WT/70)**.75
   Q=TVQ*EXP(THETA(10)*ETA(1))

   TVV4=THETA(7)*(WT/70)
   V4=TVV4 *EXP(THETA(11)*ETA(1))

   K12=KA
   K23=CL/V2
   K24=Q/V2
   K42=Q/V4
   K30=CLM/V3
   S2=V2
   S3=V3
   SID=ID
   OBS=DV

$INFN
IF (ICALL.EQ.3) THEN
 OPEN(50,FILE='CWTAB183.est')
 WRITE (50,*) 'ETAS'
```

```
DO WHILE(DATA)
IF (NEWIND.LE.1) WRITE(50,*) ETA
ENDDO
 WRITE (50,*) 'THETAS'
 WRITE (50,*) THETA
 WRITE (50,*) 'OMEGAS'
 WRITE (50,*) OMEGA(BLOCK)
 WRITE (50,*) 'SIGMAS'
 WRITE (50,*) SIGMA(BLOCK)
ENDIF

$ERROR
PROP=0
IF(CMT.EQ.2)PROP=EPS(1)
IF(CMT.EQ.3)PROP=EPS(2)
IPRED=LOG(1)
IF(F.GT.0)IPRED=LOG(F)
W=1
IRES=DV-IPRED
IWRES=IRES/W
Y=IPRED+W*PROP

"LAST
"  COM(1)=G(1,1)
"  COM(2)=G(2,1)
"  COM(3)=G(3,1)
"  COM(4)=HH(1,1)
"  COM(5)=HH(2,1)

$EST METHOD=1 INTERACTION NOABORT POSTHOC PRINT=5 MAX=9999 SIG=3
MSFO=183.msf

$THETA
  (0, 1500);[CL]
  (0, 500, 5000);[V2]
  (0, 1)   ;[KA]
  (0, 100)  ;[CLM]
  (0, 130) ;[V3]
  (0, 150) ;[Q]
  (0, 1000);[V4]
  (0, 1)   ;[THETA8]
  (0, 1)   ;[THETA9]
  (0, 1)   ;[THETA10]
  (0, 1)   ;[THETA11]

$OMEGA
  1 ;[P] omega(1,1)
  1 ;[P] omega(2,2)
  1 ;[P] omega(3,3)

$SIGMA
  1 ;[A] AS
  1 ;[A] DHA

$COV PRINT=E

$TABLE ID SID TIME TAD IPRED CMT CL V2 KA CLM V3 Q V4
WT PARA HCT ALT AST AGE RBC SEX GEO HGB FORM
ONEHEADER NOPRINT FILE=183.tab

$TABLE ID ETA1 ETA2 ETA3
ONEHEADER NOPRINT FILE=183.eta
```

```
$TABLE ID CL V2 KA CLM V3 Q V4
ONEHEADER NOPRINT FILE=183.par

$TABLE ID TIME IPRED IWRES EVID MDV CMT TAD
ONEHEADER NOPRINT FILE=SDTAB183

$TABLE ID CL V2 KA CLM V3 Q V4 ETA1 ETA2 ETA3
ONEHEADER NOPRINT FILE=PATAB183

$TABLE ID WT PARA HCT ALT AST AGE RBC HGB
ONEHEADER NOPRINT FILE=COTAB183

$TABLE ID SEX GEO FORM
ONEHEADER NOPRINT FILE=CATAB183

$TABLE ID COM(1)=G11 COM(2)=G21 COM(3)=G31 COM(4)=H11
COM(5)=H21 IPRED MDV NOPRINT ONEHEADER FILE=CWTAB183.deriv
```

APPENDIX D

THE OUTPUT SUMMARY FOR THE FINAL MODEL IN

CHAPTER III

```
PDx-Pop 3.0 Run Summary File Run No: 183

[18MAY2008 Revision]
Date: ==== START TIME ====
Output Extracted from file: c:\pdxpop3\phase2&3_cov\183.res
DataFile:  phase2_3_final.csv

MINIMIZATION STATUS
  MINIMIZATION SUCCESSFUL
  NO. OF FUNCTION EVALUATIONS USED:      611
  NO. OF SIG. DIGITS IN FINAL EST.:  3.4

  ETABAR IS THE ARITHMETIC MEAN OF THE ETA-ESTIMATES,
  AND THE P-VALUE IS GIVEN FOR THE NULL HYPOTHESIS THAT THE TRUE MEAN IS 0.

  ETABAR:  -0.17E-01  0.26E+00  0.35E-01
  SE:       0.89E-02  0.40E-01  0.62E-02

  P VAL.:   0.50E-01  0.13E-09  0.28E-07
  MINIMUM VALUE OF OBJECTIVE FUNCTION :    3042.310

ETABAR P VAL. FOR ETA2 , ETA3  < 0.05


MODEL DEFINITION
   TVCL=THETA(1)*(WT/70)**.75
   CL=TVCL*EXP(ETA(1))

   TVV2=THETA(2)*(WT/70)
   V2=TVV2*EXP(ETA(2))

   TVKA=THETA(3)
   KA=TVKA*EXP(ETA(3))

   TVCLM=THETA(4)*(WT/70)**.75
   CLM=TVCLM*EXP(THETA(8)*ETA(1))

   TVV3=THETA(5)*(WT/70)
   V3=TVV3*EXP(THETA(9)*ETA(1))

   TVQ=THETA(6)*(WT/70)**.75
   Q=TVQ*EXP(THETA(10)*ETA(1))

   TVV4=THETA(7)*(WT/70)
   V4=TVV4 *EXP(THETA(11)*ETA(1))

   K12=KA
   K23=CL/V2
   K24=Q/V2
   K42=Q/V4
   K30=CLM/V3
   S2=V2
   S3=V3
   SID=ID
   OBS=DV


PROP=0
IF(CMT.EQ.2)PROP=EPS(1)
IF(CMT.EQ.3)PROP=EPS(2)
IPRED=LOG(1)
IF(F.GT.0)IPRED=LOG(F)
W=1
IRES=DV-IPRED
IWRES=IRES/W
Y=IPRED+W*PROP
```

```
"LAST
"   COM(1)=G(1,1)
"   COM(2)=G(2,1)
"   COM(3)=G(3,1)
"   COM(4)=HH(1,1)
"   COM(5)=HH(2,1)
```

	FINAL ESTIMATE	%RSE	95% CONFIDENCE INTERVAL LBOUND	UBOUND	DESCRIPTOR/ VARIABILITY	
THETA						
1	1.52e+003	5.83%	1.35e+003	1.69e+003		CL
2	477	12.5%	360	594		V2
3	1.05	8.49%	0.875	1.22		KA
4	110	3.75%	102	118		CLM
5	127	6.50%	111	143		V3
6	136	16.3%	92.7	179		Q
7	1.10e+003	33.3%	383	1.82e+003		V4
8	0.914	24.6%	0.473	1.36		THETA8
9	1.44	26.6%	0.689	2.19		THETA9
10	0.921	39.0%	0.217	1.62		THETA10
11	1.47	39.0%	0.347	2.59		THETA11
OMEGA					INTERINDIVIDUAL VARIABILITY	
1,1	0.182	29.6%	0.0764	0.288	CV =	42.7%
2,2	3.07	13.8%	2.24	3.90	CV =	175%
3,3	0.168	43.0%	0.0265	0.310	CV =	41.0%
SIGMA					RESIDUAL VARIABILITY	
1,1	0.848	9.60%	0.688	1.01	SD =	0.921
2,2	1.05	7.15%	0.903	1.20	SD =	1.02

*Indicates 95% confidence interval that includes zero
%RSE is percent relative standard error (100% x SE/EST)

Akaike Information Criterion: 3074.31
Schwarz Bayesian Criterion: 3166.27
CONDITION NUMBER = 492.6 (DOES NOT EXCEED 1000)

REFERENCES

1. World Health Organization. World malaria report 2008. Geneva, Switzerland: WHO; 2008. Report No.: WHO/HTM/GMP/2008.1.

2. Sachs J, Malaney P. The economic and social burden of malaria. Nature. 2002 Feb 7;415(6872):680-5.

3. Singh B, Kim Sung L, Matusop A, Radhakrishnan A, Shamsul SS, Cox-Singh J, et al. A large focus of naturally acquired *Plasmodium knowlesi* infections in human beings. Lancet. 2004 Mar 27;363(9414):1017-24.

4. Vythilingam I, Tan CH, Asmad M, Chan ST, Lee KS, Singh B. Natural transmission of *Plasmodium knowles* to humans by Anopheles latens in Sarawak, Malaysia. Trans R Soc Trop Med Hyg. 2006 Nov;100(11):1087-8.

5. Ng OT, Ooi EE, Lee CC, Lee PJ, Ng LC, Pei SW, et al. Naturally acquired human *Plasmodium knowlesi* infection, Singapore. Emerg Infect Dis. 2008 May;14(5):814-6.

6. Cox-Singh J, Davis TM, Lee KS, Shamsul SS, Matusop A, Ratnam S, et al. *Plasmodium knowlesi* malaria in humans is widely distributed and potentially life threatening. Clin Infect Dis. 2008 Jan 15;46(2):165-71.

7. Schema of the life cycle of malaria [homepage on the Internet]. Centers for Disease Control and Prevention. 2006 February 17 [cited September 11, 2009]. Available from: http://www.cdc.gov/Malaria/biology/life_cycle.htm.

8. Breman JG, Alilio MS, Mills A. Conquering the intolerable burden of malaria: What's new, what's needed: A summary. Am J Trop Med Hyg. 2004 Aug;71(2 Suppl):1-15.

9. White NJ. Antimalarial drug resistance. J Clin Invest. 2004 Apr;113(8):1084-92.

10. Greenwood BM. Control to elimination: Implications for malaria research. Trends Parasitol. 2008 Oct;24(10):449-54.

11. Haynes RK, Vonwiller SC. Extraction of artemisinin and artemisinic acid: Preparation of artemether and new analogues. Trans R Soc Trop Med Hyg. 1994 Jun;88 Suppl 1:S23-6.

12. Webster HK, Lehnert EK. Chemistry of artemisinin: An overview. Trans R Soc Trop Med Hyg. 1994 Jun;88 Suppl 1:S27-9.

13. Bray PG, Ward SA, O'Neill PM. Quinolines and artemisinin: Chemistry, biology and history. Curr Top Microbiol Immunol. 2005;295:3-38.

14. Haynes RK, Krishna S. Artemisinins: Activities and actions. Microbes Infect. 2004 Nov;6(14):1339-46.

15. Krishna S, Uhlemann AC, Haynes RK. Artemisinins: Mechanisms of action and potential for resistance. Drug Resist Updat. 2004 Aug-Oct;7(4-5):233-44.

16. Golenser J, Waknine JH, Krugliak M, Hunt NH, Grau GE. Current perspectives on the mechanism of action of artemisinins. Int J Parasitol. 2006 Dec;36(14):1427-41.

17. ter Kuile F, White NJ, Holloway P, Pasvol G, Krishna S. *Plasmodium falciparum*: In vitro studies of the pharmacodynamic properties of drugs used for the treatment of severe malaria. Exp Parasitol. 1993 Feb;76(1):85-95.

18. Hassan Alin M, Bjorkman A, Landberg-Lindgren A, Ashton M. The effect of artemisinin, its derivatives and mefloquine against chloroquine-resistant strains of *Plasmodium falciparum* in vitro. Trans R Soc Trop Med Hyg. 1992 Jul-Aug;86(4):365-7.

19. Price R, van Vugt M, Nosten F, Luxemburger C, Brockman A, Phaipun L, et al. Artesunate versus artemether for the treatment of recrudescent multidrug-resistant falciparum malaria. Am J Trop Med Hyg. 1998 Dec;59(6):883-8.

20. Price R, Luxemburger C, van Vugt M, Nosten F, Kham A, Simpson J, et al. Artesunate and mefloquine in the treatment of uncomplicated multidrug-resistant hyperparasitaemic falciparum malaria. Trans R Soc Trop Med Hyg. 1998 Mar-Apr;92(2):207-11.

21. Fivelman QL, Walden JC, Smith PJ, Folb PI, Barnes KI. The effect of artesunate combined with standard antimalarials against chloroquine-sensitive and chloroquine-resistant strains of *Plasmodium falciparum* in vitro. Trans R Soc Trop Med Hyg. 1999 Jul-Aug;93(4):429-32.

22. Okell LC, Drakeley CJ, Ghani AC, Bousema T, Sutherland CJ. Reduction of transmission from malaria patients by artemisinin combination therapies: A pooled analysis of six randomized trials. Malar J. 2008 Jul 9;7:125.

23. Brockman A, Price RN, van Vugt M, Heppner DG, Walsh D, Sookto P, et al. *Plasmodium falciparum* antimalarial drug susceptibility on the north-western border of Thailand during five years of extensive use of artesunate-mefloquine. Trans R Soc Trop Med Hyg. 2000 Sep-Oct;94(5):537-44.

24. White NJ. Assessment of the pharmacodynamic properties of antimalarial drugs in vivo. Antimicrob Agents Chemother. 1997 Jul;41(7):1413-22.

25. Nyunt MM, Plowe CV. Pharmacologic advances in the global control and treatment of malaria: Combination therapy and resistance. Clin Pharmacol Ther. 2007 Nov;82(5):601-5.

26. McIntosh HM, Olliaro P. Artemisinin derivatives for treating uncomplicated malaria. Cochrane Database Syst Rev. 2000;(2)(2):CD000256.

27. McIntosh HM, Olliaro P. Artemisinin derivatives for treating severe malaria. Cochrane Database Syst Rev. 2000;(2)(2):CD000527.

28. Price RN. Artemisinin drugs: Novel antimalarial agents. Expert Opin Investig Drugs. 2000 Aug;9(8):1815-27.

29. Gautam A, Ahmed T, Batra V, Paliwal J. Pharmacokinetics and pharmacodynamics of endoperoxide antimalarials. Curr Drug Metab. 2009 Mar;10(3):289-306.

30. Brewer TG, Peggins JO, Grate SJ, Petras JM, Levine BS, Weina PJ, et al. Neurotoxicity in animals due to arteether and artemether. Trans R Soc Trop Med Hyg. 1994 Jun;88 Suppl 1:S33-6.

31. Genovese RF, Newman DB, Li Q, Peggins JO, Brewer TG. Dose-dependent brainstem neuropathology following repeated arteether administration in rats. Brain Res Bull. 1998;45(2):199-202.

32. Genovese RF, Newman DB, Brewer TG. Behavioral and neural toxicity of the artemisinin antimalarial, arteether, but not artesunate and artelinate, in rats. Pharmacol Biochem Behav. 2000 Sep;67(1):37-44.

33. Petras JM, Young GD, Bauman RA, Kyle DE, Gettayacamin M, Webster HK, et al. Arteether-induced brain injury in *Macaca mulatta*. I. The precerebellar nuclei: The lateral reticular nuclei, paramedian reticular nuclei, and perihypoglossal nuclei. Anat Embryol (Berl). 2000 May;201(5):383-97.

34. Nontprasert A, Pukrittayakamee S, Dondorp AM, Clemens R, Looareesuwan S, White NJ. Neuropathologic toxicity of artemisinin derivatives in a mouse model. Am J Trop Med Hyg. 2002 Oct;67(4):423-9.

35. Taylor WR, White NJ. Antimalarial drug toxicity: A review. Drug Saf. 2004;27(1):25-61.

36. Makanga M, Premji Z, Falade C, Karbwang J, Mueller EA, Andriano K, et al. Efficacy and safety of the six-dose regimen of artemether-lumefantrine in pediatrics with uncomplicated *Plasmodium falciparum* malaria: A pooled analysis of individual patient data. Am J Trop Med Hyg. 2006 Jun;74(6):991-8.

37. Doherty JF, Sadiq AD, Bayo L, Alloueche A, Olliaro P, Milligan P, et al. A randomized safety and tolerability trial of artesunate plus sulfadoxine--pyrimethamine versus sulfadoxine-pyrimethamine alone for the treatment of uncomplicated malaria in Gambian children. Trans R Soc Trop Med Hyg. 1999 Sep-Oct;93(5):543-6.

38. Kongpatanakul S, Chatsiricharoenkul S, Sathirakul K, Suputtamongkol Y, Atipas S, Watnasirichaikul S, et al. Evaluation of the safety and relative bioavailability of a new dihydroartemisinin tablet formulation in healthy Thai volunteers. Trans R Soc Trop Med Hyg. 2007 Oct;101(10):972-9.

39. Krudsood S, Chalermrut K, Pengruksa C, Srivilairit S, Silachamroon U, Treeprasertsuk S, et al. Comparative clinical trial of two-fixed combinations dihydroartemisinin-napthoquine-trimethoprim (DNP) and artemether-lumefantrine (Coartem/Riamet) in the treatment of acute uncomplicated falciparum malaria in Thailand. Southeast Asian J Trop Med Public Health. 2003 Jun;34(2):316-21.

40. Ndiaye JL, Randrianarivelojosia M, Sagara I, Brasseur P, Ndiaye I, Faye B, et al. Randomized, multicentre assessment of the efficacy and safety of ASAQ--a fixed-dose artesunate-amodiaquine combination therapy in the treatment of uncomplicated *Plasmodium falciparum* malaria. Malar J. 2009 Jun 8;8:125.

41. Sagara I, Rulisa S, Mbacham W, Adam I, Sissoko K, Maiga H, et al. Efficacy and safety of a fixed dose artesunate-sulphamethoxypyrazine-pyrimethamine compared to artemether-lumefantrine for the treatment of uncomplicated falciparum malaria across Africa: A randomized multi-centre trial. Malar J. 2009 Apr 14;8:63.

42. Tangpukdee N, Krudsood S, Thanachartwet V, Pengruksa C, Phophak N, Kano S, et al. Efficacy of artequick versus artesunate-mefloquine in the treatment of acute uncomplicated falciparum malaria in Thailand. Southeast Asian J Trop Med Public Health. 2008 Jan;39(1):1-8.

43. Ramharter M, Kurth F, Schreier AC, Nemeth J, Glasenapp I, Bélard S, et al. Fixed-dose pyronaridine-artesunate combination for treatment of uncomplicated falciparum malaria in pediatric patients in Gabon. J Infect Dis. 2008;198(6):911-9.

44. Ribeiro IR, Olliaro P. Safety of artemisinin and its derivatives. A review of published and unpublished clinical trials. Med Trop (Mars). 1998;58(3 Suppl):50-3.

45. Price R, van Vugt M, Phaipun L, Luxemburger C, Simpson J, McGready R, et al. Adverse effects in patients with acute falciparum malaria treated with artemisinin derivatives. Am J Trop Med Hyg. 1999 Apr;60(4):547-55.

46. Gordi T, Lepist EI. Artemisinin derivatives: Toxic for laboratory animals, safe for humans? Toxicol Lett. 2004 Mar 1;147(2):99-107.

47. Clark RL, Arima A, Makori N, Nakata Y, Bernard F, Gristwood W, et al. Artesunate: Developmental toxicity and toxicokinetics in monkeys. Birth Defects Res B Dev Reprod Toxicol. 2008 Aug;83(4):418-34.

48. Clark RL, Lerman SA, Cox EM, Gristwood WE, White TE. Developmental toxicity of artesunate in the rat: Comparison to other artemisinins, comparison of embryotoxicity and kinetics by oral and intravenous routes, and relationship to maternal reticulocyte count. Birth Defects Res B Dev Reprod Toxicol. 2008 Aug;83(4):397-406.

49. Clark RL, White TE, A Clode S, Gaunt I, Winstanley P, Ward SA. Developmental toxicity of artesunate and an artesunate combination in the rat and rabbit. Birth Defects Res B Dev Reprod Toxicol. 2004 Dec;71(6):380-94.

50. Li Q, Si Y, Smith KS, Zeng Q, Weina PJ. Embryotoxicity of artesunate in animal species related to drug tissue distribution and toxicokinetic profiles. Birth Defects Res B Dev Reprod Toxicol. 2008 Aug;83(4):435-45.

51. Deen JL, von Seidlein L, Pinder M, Walraven GE, Greenwood BM. The safety of the combination artesunate and pyrimethamine-sulfadoxine given during pregnancy. Trans R Soc Trop Med Hyg. 2001 Jul-Aug;95(4):424-8.

52. McGready R, Brockman A, Cho T, Cho D, van Vugt M, Luxemburger C, et al. Randomized comparison of mefloquine-artesunate versus quinine in the treatment of multidrug-resistant falciparum malaria in pregnancy. Trans R Soc Trop Med Hyg. 2000 Nov-Dec;94(6):689-93.

53. McGready R, Tan SO, Ashley EA, Pimanpanarak M, Viladpai-Nguen J, Phaiphun L, et al. A randomized controlled trial of artemether-lumefantrine versus artesunate for uncomplicated *Plasmodium falciparum* treatment in pregnancy. PLoS Med. 2008 Dec 23;5(12):e253.

54. McGready R, Cho T, Keo NK, Thwai KL, Villegas L, Looareesuwan S, et al. Artemisinin antimalarials in pregnancy: A prospective treatment study of 539 episodes of multidrug-resistant *Plasmodium falciparum*. Clin Infect Dis. 2001 Dec 15;33(12):2009-16.

55. Ashton M, Gordi T, Trinh NH, Nguyen VH, Nguyen DS, Nguyen TN, et al. Artemisinin pharmacokinetics in healthy adults after 250, 500 and 1000 mg single oral doses. Biopharm Drug Dispos. 1998 May;19(4):245-50.

56. Ashton M, Hai TN, Sy ND, Huong DX, Van Huong N, Nieu NT, et al. Artemisinin pharmacokinetics is time-dependent during repeated oral administration in healthy male adults. Drug Metab Dispos. 1998 Jan;26(1):25-7.

57. Zhang SQ, Hai TN, Ilett KF, Huong DX, Davis TM, Ashton M. Multiple dose study of interactions between artesunate and artemisinin in healthy volunteers. Br J Clin Pharmacol. 2001 Oct;52(4):377-85.

58. Ashton M, Nguyen DS, Nguyen VH, Gordi T, Trinh NH, Dinh XH, et al. Artemisinin kinetics and dynamics during oral and rectal treatment of uncomplicated malaria. Clin Pharmacol Ther. 1998 Apr;63(4):482-93.

59. Gordi T, Huong DX, Hai TN, Nieu NT, Ashton M. Artemisinin pharmacokinetics and efficacy in uncomplicated-malaria patients treated with two different dosage regimens. Antimicrob Agents Chemother. 2002 Apr;46(4):1026-31.

60. Svensson US, Ashton M, Trinh NH, Bertilsson L, Dinh XH, Nguyen VH, et al. Artemisinin induces omeprazole metabolism in human beings. Clin Pharmacol Ther. 1998 Aug;64(2):160-7.

61. Mihara K, Svensson US, Tybring G, Hai TN, Bertilsson L, Ashton M. Stereospecific analysis of omeprazole supports artemisinin as a potent inducer of CYP2C19. Fundam Clin Pharmacol. 1999;13(6):671-5.

62. Simonsson USH, Jansson B, Hai TN, Huong DX, Tybring G, Ashton M. Artemisinin autoinduction is caused by involvement of cytochrome P450 2B6 but not 2C9. Clin Pharmacol Ther. 2003;74(1):32-43.

63. Burk O, Arnold KA, Nussler AK, Schaeffeler E, Efimova E, Avery BA, et al. Antimalarial artemisinin drugs induce cytochrome P450 and MDR1 expression by activation of xenosensors pregnane X receptor and constitutive androstane receptor. Mol Pharmacol. 2005 Jun;67(6):1954-65.

64. Gordi T, Xie R, Huong NV, Huong DX, Karlsson MO, Ashton M. A semiphysiological pharmacokinetic model for artemisinin in healthy subjects incorporating autoinduction of metabolism and saturable first-pass hepatic extraction. Br J Clin Pharmacol. 2005;59(2):189-98.

65. Gordi T, Xie R, Jusko WJ. Semi-mechanistic pharmacokinetic/pharmacodynamic modelling of the antimalarial effect of artemisinin. Br J Clin Pharmacol. 2005;60(6):594-604.

66. van Agtmael MA, Cheng-Qi S, Qing JX, Mull R, van Boxtel CJ. Multiple dose pharmacokinetics of artemether in Chinese patients with uncomplicated falciparum malaria. Int J Antimicrob Agents. 1999 Jul;12(2):151-8.

67. Lefevre G, Bindschedler M, Ezzet F, Schaeffer N, Meyer I, Thomsen MS. Pharmacokinetic interaction trial between co-artemether and mefloquine. Eur J Pharm Sci. 2000 Apr;10(2):141-51.

68. Khanh NX, de Vries PJ, Ha LD, van Boxtel CJ, Koopmans R, Kager PA. Declining concentrations of dihydroartemisinin in plasma during 5-day oral treatment with artesunate for falciparum malaria. Antimicrob Agents Chemother. 1999 Mar;43(3):690-2.

69. Diem Thuy LT, Ngoc Hung L, Danh PT, Na-Bangchang K. Absence of time-dependent artesunate pharmacokinetics in healthy subjects during 5-day oral administration. Eur J Clin Pharmacol. 2008;64(10):993-8.

70. Le Thi DT, Le NH, Nguyen CH, Phan Thi D, Na-Bangchang K. Pharmacokinetics of a five-day oral dihydroartemisinin monotherapy regimen in patients with uncomplicated falciparum malaria. Drug Metab Pharmacokinet. 2008;23(3):158-64.

71. World Health Organization. Guidelines for the treatment of malaria. Geneva, Switzerland: WHO; 2006. Report No.: WHO/HTM/MAL/2006.1108.

72. Nosten F, Brasseur P. Combination therapy for malaria: The way forward? Drugs. 2002;62(9):1315-29.

73. Batty KT, Thu LT, Davis TM, Ilett KF, Mai TX, Hung NC, et al. A pharmacokinetic and pharmacodynamic study of intravenous vs. oral artesunate in uncomplicated falciparum malaria. Br J Clin Pharmacol. 1998 Feb;45(2):123-9.

74. Batty KT, Le AT, Ilett KF, Nguyen PT, Powell SM, Nguyen CH, et al. A pharmacokinetic and pharmacodynamic study of artesunate for vivax malaria. Am J Trop Med Hyg. 1998 Nov;59(5):823-7.

75. Newton P, Suputtamongkol Y, Teja-Isavadharm P, Pukrittayakamee S, Navaratnam V, Bates I, et al. Antimalarial bioavailability and disposition of artesunate in acute falciparum malaria. Antimicrob Agents Chemother. 2000 Apr;44(4):972-7.

76. Navaratnam V, Mansor SM, Mordi MN, Akbar A, Abdullah MN. Comparative pharmacokinetic study of oral and rectal formulations of artesunic acid in healthy volunteers. Eur J Clin Pharmacol. 1998 Jul;54(5):411-4.

77. Krishna S, Planche T, Agbenyega T, Woodrow C, Agranoff D, Bedu-Addo G, et al. Bioavailability and preliminary clinical efficacy of intrarectal artesunate in Ghanaian children with moderate malaria. Antimicrob Agents Chemother. 2001 Feb;45(2):509-16.

78. Li Q, Xie L, Zhang J, Weina PJ. The distribution pattern of intravenous [(14)C] artesunate in rat tissues by quantitative whole-body autoradiography and tissue dissection techniques. J Pharm Biomed Anal. 2008 Nov 4;48(3):876-84.

79. Xie LH, Li Q, Zhang J, Weina PJ. Pharmacokinetics, tissue distribution and mass balance of radiolabeled dihydroartemisinin in male rats. Malar J. 2009 May 26;8:112.

80. Li Q, Xie LH, Haeberle A, Zhang J, Weina P. The evaluation of radiolabeled artesunate on tissue distribution in rats and protein binding in humans. Am J Trop Med Hyg. 2006 Nov;75(5):817-26.

81. Teja-Isavadharm P, Watt G, Eamsila C, Jongsakul K, Li Q, Keeratithakul G, et al. Comparative pharmacokinetics and effect kinetics of orally administered artesunate in healthy volunteers and patients with uncomplicated falciparum malaria. Am J Trop Med Hyg. 2001 Dec;65(6):717-21.

82. Maggs JL, Madden S, Bishop LP, O'Neill PM, Park BK. The rat biliary metabolites of dihydroartemisinin, an antimalarial endoperoxide. Drug Metab Dispos. 1997 Oct;25(10):1200-4.

83. Maggs JL, Bishop LP, Edwards G, O'Neill PM, Ward SA, Winstanley PA, et al. Biliary metabolites of beta-artemether in rats: Biotransformations of an antimalarial endoperoxide. Drug Metab Dispos. 2000 Feb;28(2):209-17.

84. Ilett KF, Ethell BT, Maggs JL, Davis TM, Batty KT, Burchell B, et al. Glucuronidation of dihydroartemisinin in vivo and by human liver microsomes and expressed UDP-glucuronosyltransferases. Drug Metab Dispos. 2002 Sep;30(9):1005-12.

85. Batty KT, Ilett KF, Edwards G, Powell SM, Maggs JL, Park BK, et al. Assessment of the effect of malaria infection on hepatic clearance of dihydroartemisinin using rat liver perfusions and microsomes. Br J Pharmacol. 1998 Sep;125(1):159-67.

86. Batty KT, Iletr KE, Powell SM, Martin J, Davis TM. Relative bioavailability of artesunate and dihydroartemisinin: Investigations in the isolated perfused rat liver and in healthy Caucasian volunteers. Am J Trop Med Hyg. 2002 Feb;66(2):130-6.

87. Williams PJ, Ette EI. Pharmacometrics: Impacting drug development and pharmacotherapy. In: Williams PJ, Ette EI, editors. Pharmacometrics: The Science of Quantitative Pharmacology. Hoboken, New Jersey: John Wiley & Sons, Inc.; 2007. p. 1-21.

88. U.S. Department of Health and Human Services, Food and Drug Administration. Challenges and opportunity on the critical path to new medical products. Rockville, MD: FDA; 2004.

89. Kola I, Landis J. Can the pharmaceutical industry reduce attrition rates? Nat Rev Drug Discov. 2004 Aug;3(8):711-5.

90. Gobburu JV, Marroum PJ. Utilization of pharmacokinetic-pharmacodynamic modelling and simulation in regulatory decision-making. Clin Pharmacokinet. 2001;40(12):883-92.

91. Powell JR, Gobburu JV. Pharmacometrics at FDA: Evolution and impact on decisions. Clin Pharmacol Ther. 2007 Jul;82(1):97-102.

92. Bhattaram VA, Booth BP, Ramchandani RP, Beasley BN, Wang Y, Tandon V, et al. Impact of pharmacometrics on drug approval and labeling decisions: A survey of 42 new drug applications. AAPS J. 2005 Oct 7;7(3):E503-12.

93. Bhattaram VA, Bonapace C, Chilukuri DM, Duan JZ, Garnett C, Gobburu JV, et al. Impact of pharmacometric reviews on new drug approval and labeling decisions--a survey of 31 new drug applications submitted between 2005 and 2006. Clin Pharmacol Ther. 2007 Feb;81(2):213-21.

94. U.S. Department of Health and Human Services, Food and Drug Administration, Center for Drug Evaluation and Research, Center for Biologics Evaluation and Research. Guidance for industry: Population pharmacokinetics. Rockville, MD: FDA; 1999. Report No.: CP1.

95. European Medicines Agency, Committee for Medicinal Products for Human Use. Guideline on reporting the results of population pharmacokinetic analyses. London, UK: EMEA; 2008. Report No.: CHMP/EWP/185990/06.

96. Aarons L. Population pharmacokinetics: Theory and practice. Br J Clin Pharmacol. 1991 Dec;32(6):669-70.

97. Ette EI, Williams PJ. Population pharmacokinetics I: Background, concepts, and models. Ann Pharmacother. 2004 Oct;38(10):1702-6.

98. Williams PJ, Ette EI. The role of population pharmacokinetics in drug development in light of the food and drug administration's 'Guidance for industry: Population pharmacokinetics'. Clin Pharmacokinet. 2000 Dec;39(6):385-95.

99. Sheiner LB. Learning versus confirming in clinical drug development. Clin Pharmacol Ther. 1997 Mar;61(3):275-91.

100. Ette EI, Williams PJ, Lane JR. Population pharmacokinetics III: Design, analysis, and application of population pharmacokinetic studies. Ann Pharmacother. 2004 Dec;38(12):2136-44.

101. Aarons L, Karlsson MO, Mentre F, Rombout F, Steimer JL, van Peer A, et al. Role of modelling and simulation in phase I drug development. Eur J Pharm Sci. 2001 May;13(2):115-22.

102. Zuppa AF, Mondick JT, Davis L, Cohen D. Population pharmacokinetics of ketorolac in neonates and young infants. Am J Ther. 2009 Mar-Apr;16(2):143-6.

103. Sherwin CM, Svahn S, Van der Linden A, Broadbent RS, Medlicott NJ, Reith DM. Individualised dosing of amikacin in neonates: A pharmacokinetic/pharmacodynamic analysis. Eur J Clin Pharmacol. 2009 Jul;65(7):705-13.

104. Mukherjee A, Dombi T, Wittke B, Lalonde R. Population pharmacokinetics of sildenafil in term neonates: Evidence of rapid maturation of metabolic clearance in the early postnatal period. Clin Pharmacol Ther. 2009 Jan;85(1):56-63.

105. Nielsen EI, Sandstrom M, Honore PH, Ewald U, Friberg LE. Developmental pharmacokinetics of gentamicin in preterm and term neonates: Population modelling of a prospective study. Clin Pharmacokinet. 2009;48(4):253-63.

106. Garrido MJ, Habre W, Rombout F, Troconiz IF. Population pharmacokinetic/pharmacodynamic modelling of the analgesic effects of tramadol in pediatrics. Pharm Res. 2006 Sep;23(9):2014-23.

107. Bressolle F, Rochette A, Khier S, Dadure C, Ouaki J, Capdevila X. Population pharmacokinetics of the two enantiomers of tramadol and O-demethyl tramadol after surgery in children. Br J Anaesth. 2009 Mar;102(3):390-9.

108. Herd DW, Anderson BJ, Holford NH. Modeling the norketamine metabolite in children and the implications for analgesia. Paediatr Anaesth. 2007 Sep;17(9):831-40.

109. Tarning J, McGready R, Lindegardh N, Ashley EA, Pimanpanarak M, Kamanikom B, et al. Population pharmacokinetics of lumefantrine in pregnant women treated with artemether-lumefantrine for uncomplicated *Plasmodium falciparum* malaria. Antimicrob Agents Chemother. 2009 Sep;53(9):3837-46.

110. Bouillon-Pichault M, Jullien V, Azria E, Pannier E, Firtion G, Krivine A, et al. Population analysis of the pregnancy-related modifications in lopinavir pharmacokinetics and their possible consequences for dose adjustment. J Antimicrob Chemother. 2009 Jun;63(6):1223-32.

111. Muller AE, Dorr PJ, Mouton JW, De Jongh J, Oostvogel PM, Steegers EA, et al. The influence of labour on the pharmacokinetics of intravenously administered amoxicillin in pregnant women. Br J Clin Pharmacol. 2008 Dec;66(6):866-74.

112. Roberts JA, Kirkpatrick CM, Roberts MS, Robertson TA, Dalley AJ, Lipman J. Meropenem dosing in critically ill patients with sepsis and without renal dysfunction: Intermittent bolus versus continuous administration? Monte Carlo dosing simulations and subcutaneous tissue distribution. J Antimicrob Chemother. 2009 Jul;64(1):142-50.

113. Nicasio AM, Ariano RE, Zelenitsky SA, Kim A, Crandon JL, Kuti JL, et al. Population pharmacokinetics of high-dose, prolonged-infusion cefepime in adult critically ill patients with ventilator-associated pneumonia. Antimicrob Agents Chemother. 2009 Apr;53(4):1476-81.

114. Isla A, Rodriguez-Gascon A, Troconiz IF, Bueno L, Solinis MA, Maynar J, et al. Population pharmacokinetics of meropenem in critically ill patients undergoing continuous renal replacement therapy. Clin Pharmacokinet. 2008;47(3):173-80.

115. Sakka SG, Glauner AK, Bulitta JB, Kinzig-Schippers M, Pfister W, Drusano GL, et al. Population pharmacokinetics and pharmacodynamics of continuous versus short-term infusion of imipenem-cilastatin in critically ill patients in a randomized, controlled trial. Antimicrob Agents Chemother. 2007 Sep;51(9):3304-10.

116. Feng Y, Pollock BG, Coley K, Marder S, Miller D, Kirshner M, et al. Population pharmacokinetic analysis for risperidone using highly sparse sampling measurements from the CATIE study. Br J Clin Pharmacol. 2008 Nov;66(5):629-39.

117. Lehr T, Staab A, Tillmann C, Trommeshauser D, Raschig A, Schaefer HG, et al. Population pharmacokinetic modelling of NS2330 (tesofensine) and its major metabolite in patients with Alzheimer's disease. Br J Clin Pharmacol. 2007 Jul;64(1):36-48.

118. Ette EI, Williams PJ. Population pharmacokinetics II: Estimation methods. Ann Pharmacother. 2004 Nov;38(11):1907-15.

119. Beal SL, Sheiner LB. NONMEM users' guides. NONMEM Project Group, University of San Francisco, CA; 1998.

120. Sheiner LB, Ludden TM. Population pharmacokinetics/dynamics. Annu Rev Pharmacol Toxicol. 1992;32:185-209.

121. Sheiner L, Grasela T. An introduction to mixed effect modeling: Concepts, definitions, and justification. J Pharmacokinet Biopharm. 1991 06/01;19(0):11S-24S.

122. Yano Y, Beal SL, Sheiner LB. Evaluating pharmacokinetic/pharmacodynamic models using the posterior predictive check. J Pharmacokinet Pharmacodyn. 2001 Apr;28(2):171-92.

123. Ette EI, Williams PJ, Kim YH, Lane JR, Liu MJ, Capparelli EV. Model appropriateness and population pharmacokinetic modeling. J Clin Pharmacol. 2003 Jun;43(6):610-23.

124. Brendel K, Dartois C, Comets E, Lemenuel-Diot A, Laveille C, Tranchand B, et al. Are population pharmacokinetic and/or pharmacodynamic models adequately evaluated? A survey of the literature from 2002 to 2004. Clin Pharmacokinet. 2007;46(3):221-34.

125. Ette EI, Ludden TM. Population pharmacokinetic modeling: The importance of informative graphics. Pharm Res. 1995 Dec;12(12):1845-55.

126. Karlsson MO, Savic RM. Diagnosing model diagnostics. Clin Pharmacol Ther. 2007;82(1):17-20.

127. Efron B. Bootstrap methods: Another look at the jackknife. Ann Statist. 1979;7(1):1-26.

128. Efron B, Gong G. A leisurely look at the bootstrap, the jackknife, and cross-validation. JSTOR. 1983 Feb.;37(1):36-48.

129. Holford NHG. In: The visual predictive check – superiority to standard diagnostic (Rorschach) plots. PAGE meeting 2005; 16-17 June; Pamplona, Spain. ; 2005. p. 14.

130. Karlsson MO, Holford NHG. In: A tutorial on visual predictive checks. PAGE meeting 2008; 18-20 June; Marseille, France. ; 2008. p. 17.

131. Post TM, Freijer JI, Ploeger BA, Danhof M. Extensions to the visual predictive check to facilitate model performance evaluation. J Pharmacokinet Pharmacodyn. 2008 Apr;35(2):185-202.

132. Bachman WJ, editor. PDx-pop version 3.10 release notes. Ellicott City, MD: ICON Development Solutions; 2008.

133. Bonate PL. Pharmacokinetic-pharmacodynamic modeling and simulation. New York: Springer; 2006.

134. Bachman WJ. Model diagnostics. NMusers. 2003.

135. Stepniewska K, White NJ. Pharmacokinetic determinants of the window of selection for antimalarial drug resistance. Antimicrob Agents Chemother. 2008 May;52(5):1589-96.

136. International Artemisinin Study Group. Artesunate combinations for treatment of malaria: Meta-analysis. Lancet. 2004 Jan 3;363(9402):9-17.

137. Price RN, Nosten F, Luxemburger C, ter Kuile FO, Paiphun L, Chongsuphajaisiddhi T, et al. Effects of artemisinin derivatives on malaria transmissibility. Lancet. 1996 Jun 15;347(9016):1654-8.

138. Davis TM, Karunajeewa HA, Ilett KF. Artemisinin-based combination therapies for uncomplicated malaria. Med J Aust. 2005 Feb 21;182(4):181-5.

139. Haynes RK, Chan HW, Lung CM, Ng NC, Wong HN, Shek LY, et al. Artesunate and dihydroartemisinin (DHA): Unusual decomposition products formed under mild conditions and comments on the fitness of DHA as an antimalarial drug. ChemMedChem. 2007;2(10):1448-63.

140. Alin MH, Bjorkman A, Ashton M. In vitro activity of artemisinin, its derivatives, and pyronaridine against different strains of *Plasmodium falciparum* . Trans R Soc Trop Med Hyg. 1990 Sep-Oct;84(5):635-7.

141. Ringwald P, Eboumbou EC, Bickii J, Basco LK. In vitro activities of pyronaridine, alone and in combination with other antimalarial drugs, against *Plasmodium falciparum*. Antimicrob Agents Chemother. 1999 Jun;43(6):1525-7.

142. Kurth F, Pongratz P, Belard S, Mordmuller B, Kremsner PG, Ramharter M. In vitro activity of pyronaridine against *Plasmodium falciparum* and comparative evaluation of anti-malarial drug susceptibility assays. Malar J. 2009 Apr 23;8:79.

143. Ringwald P, Bickii J, Basco L. Randomized trial of pyronaridine versus chloroquine for acute uncomplicated falciparum malaria in Africa. Lancet. 1996 Jan 6;347(8993):24-8.

144. Looareesuwan S, Kyle DE, Viravan C, Vanijanonta S, Wilairatana P, Wernsdorfer WH. Clinical study of pyronaridine for the treatment of acute uncomplicated falciparum malaria in Thailand. Am J Trop Med Hyg. 1996 Feb;54(2):205-9.

145. Ringwald P, Bickii J, Basco LK. Efficacy of oral pyronaridine for the treatment of acute uncomplicated falciparum malaria in African children. Clin Infect Dis. 1998 Apr;26(4):946-53.

146. Karunajeewa HA, Ilett KF, Dufall K, Kemiki A, Bockarie M, Alpers MP, et al. Disposition of artesunate and dihydroartemisinin after administration of artesunate suppositories in children from Papua New Guinea with uncomplicated malaria. Antimicrob Agents Chemother. 2004;48(8):2966-72.

147. Simpson JA, Agbenyega T, Barnes KI, Di Perri G, Folb P, Gomes M, et al. Population pharmacokinetics of artesunate and dihydroartemisinin following intra-rectal dosing of artesunate in malaria patients. PLoS medicine. 2006;3(11):e444.

148. McGready R, Stepniewska K, Ward SA, Cho T, Gilveray G, Looareesuwan S, et al. Pharmacokinetics of dihydroartemisinin following oral artesunate treatment of pregnant women with acute uncomplicated falciparum malaria. Eur J Clin Pharmacol. 2006 May;62(5):367-71.

149. U.S. Department of Health and Human Services, Food and Drug Administration, Center for Drug Evaluation and Research. Guidance for industry: Food-effect bioavailability and fed bioequivalence studies. Rockville, MD: FDA; 2002. Report No.: BP.

150. Naik H, Murry DJ, Kirsch LE, Fleckenstein L. Development and validation of a high-performance liquid chromatography-mass spectroscopy assay for determination of artesunate and dihydroartemisinin in human plasma. J Chromatogr B Analyt Technol Biomed Life Sci. 2005;816(1-2):233-42.

151. Jonsson EN, Karlsson MO. Xpose--an S-PLUS based population pharmacokinetic/pharmacodynamic model building aid for NONMEM. Comput Methods Programs Biomed. 1999 Jan;58(1):51-64.

152. Mandema JW, Verotta D, Sheiner LB. Building population pharmacokinetic--pharmacodynamic models. I. models for covariate effects. J Pharmacokinet Biopharm. 1992 Oct;20(5):511-28.

153. Yu KS, Jang IJ, Craft JC, Shin CS, Jung D, Fleckenstein L. Single and multiple, oral ascending dose pharmacokinetics and safety of pyronaridine-artesunate combination given in a 3:1 ratio in healthy subjects. Br J Clin Pharmacol. In press 2009.

154. Benakis A, Paris M, Loutan L, Plessas CT, Plessas ST. Pharmacokinetics of artemisinin and artesunate after oral administration in healthy volunteers. Am J Trop Med Hyg. 1997 Jan;56(1):17-23.

155. Teja-Isavadharm P, Watt G, Eamsila C, Jongsakul K, Li Q, Keeratithakul G, et al. Comparative pharmacokinetics and effect kinetics of orally administered artesunate in healthy volunteers and patients with uncomplicated falciparum malaria. Am J Trop Med Hyg. 2001 Dec;65(6):717-21.

156. Na-Bangchang K, Krudsood S, Silachamroon U, Molunto P, Tasanor O, Chalermrut K, et al. The pharmacokinetics of oral dihydroartemisinin and artesunate in healthy Thai volunteers. Southeast Asian J Trop Med Public Health. 2004 Sep;35(3):575-82.

157. McGready R, Stepniewska K, Ward SA, Cho T, Gilveray G, Looareesuwan S, et al. Pharmacokinetics of dihydroartemisinin following oral artesunate treatment of pregnant women with acute uncomplicated falciparum malaria. Eur J Clin Pharmacol. 2006;62(5):367-71.

158. Awad MI, Eltayeb IB, Baraka OZ, Behrens RH, Alkadru AM. Pharmacokinetics of artesunate following oral and rectal administration in healthy Sudanese volunteers. Trop Doct. 2004 Jul;34(3):132-5.

159. Alin MH, Ashton M, Kihamia CM, Mtey GJ, Bjorkman A. Clinical efficacy and pharmacokinetics of artemisinin monotherapy and in combination with mefloquine in patients with falciparum malaria. Br J Clin Pharmacol. 1996 Jun;41(6):587-92.

160. Asimus S, Elsherbiny D, Hai TN, Jansson B, Huong NV, Petzold MG, et al. Artemisinin antimalarials moderately affect cytochrome P450 enzyme activity in healthy subjects. Fundam Clin Pharmacol. 2007 Jun;21(3):307-16.

161. Elsherbiny DA, Asimus SA, Karlsson MO, Ashton M, Simonsson USH. A model based assessment of the CYP2B6 and CYP2C19 inductive properties by artemisinin antimalarials: Implications for combination regimens. J Pharmacokinet Pharmacodyn. 2008;35(2):203-17.

162. Stepniewska K, Taylor W, Sirima SB, Ouedraogo EB, Ouedraogo A, Gansane A, et al. Population pharmacokinetics of artesunate and amodiaquine in African children. Malar J. 2009 Aug 20;8(1):200.

163. World Health Organization. Assessment and monitoring of antimalarial drug efficacy for the treatment of uncomplicated falciparum malaria. Geneva, Switzerland: WHO; 2003. Report No.: WHO/HTM/RBM/2003.50.

164. Piotrovskii VK. The use of weibull distribution to describe the in vivo absorption kinetics. J Pharmacokinet Biopharm. 1987 Dec;15(6):681-6.

165. Bressolle F, Gomeni R, Alric R, Royer-Morrot MJ, Necciari J. A double weibull input function describes the complex absorption of sustained-release oral sodium valproate. J Pharm Sci. 1994 Oct;83(10):1461-4.

166. Rietbrock S, Merz PG, Fuhr U, Harder S, Marschner JP, Loew D, et al. Absorption behavior of sulpiride described using weibull functions. Int J Clin Pharmacol Ther. 1995 May;33(5):299-303.

167. Funaki T. Enterohepatic circulation model for population pharmacokinetic analysis. J Pharm Pharmacol. 1999 Oct;51(10):1143-8.

168. Ezzet F, Krishna G, Wexler DB, Statkevich P, Kosoglou T, Batra VK. A population pharmacokinetic model that describes multiple peaks due to enterohepatic recirculation of ezetimibe. Clin Ther. 2001 Jun;23(6):871-85.

169. Gabrielsson J, Weiner D. Pharmacokinetic and pharmacodynamic data analysis: Concepts and applications, 4th edition. Stockholm, Sweden: Swedish Phamarceutical Press; 2006.

170. Moon YJ, Wang L, DiCenzo R, Morris ME. Quercetin pharmacokinetics in humans. Biopharm Drug Dispos. 2008 May;29(4):205-17.

171. Sam WJ, Akhlaghi F, Rosenbaum SE. Population pharmacokinetics of mycophenolic acid and its 2 glucuronidated metabolites in kidney transplant recipients. J Clin Pharmacol. 2009 Feb;49(2):185-95.

172. Younis IR, Malone S, Friedman HS, Schaaf LJ, Petros WP. Enterohepatic recirculation model of irinotecan (CPT-11) and metabolite pharmacokinetics in patients with glioma. Cancer Chemother Pharmacol. 2009 Feb;63(3):517-24.

173. Holford NH. A size standard for pharmacokinetics. Clin Pharmacokinet. 1996 May;30(5):329-32.

174. Davis TM, Phuong HL, Ilett KF, Hung NC, Batty KT, Phuong VD, et al. Pharmacokinetics and pharmacodynamics of intravenous artesunate in severe falciparum malaria. Antimicrob Agents Chemother. 2001 Jan;45(1):181-6.

175. Ilett KF, Batty KT, Powell SM, Binh TQ, Thu le TA, Phuong HL, et al. The pharmacokinetic properties of intramuscular artesunate and rectal dihydroartemisinin in uncomplicated falciparum malaria. Br J Clin Pharmacol. 2002 Jan;53(1):23-30.

176. Li Q, Weina PJ. In: Compartmental model-dependent analysis of pharmacokinetic data of artesunate following short-term infusion in health volunteers. New Orleans, LA. ; 2008. p. 54.

177. Newton PN, Barnes KI, Smith PJ, Evans AC, Chierakul W, Ruangveerayuth R, et al. The pharmacokinetics of intravenous artesunate in adults with severe falciparum malaria. Eur J Clin Pharmacol. 2006 Dec;62(12):1003-9.

178. Batty KT, Ashton M, Ilett KF, Edwards G, Davis TM. The pharmacokinetics of artemisinin (ART) and artesunate (ARTS) in healthy volunteers. Am J Trop Med Hyg. 1998 Feb;58(2):125-6.

179. Karbwang J, Na-Bangchang K, Congpoung K, Thanavibul A, Harinasuta T. Pharmacokinetics of oral artesunate in Thai patients with uncomplicated falciparum malaria. Clin Drug Investig. 1998;15(1):37-43.

180. Anderson BJ, Holford NHG. Mechanism-based concepts of size and maturity in pharmacokinetics. Annu Rev Pharmacol Toxicol. 2008;48:303-32.

181. Gupta SK, Rosenkranz SL, Cramer YS, Koletar SL, Szczech LA, Amorosa V, et al. The pharmacokinetics and pharmacogenomics of efavirenz and lopinavir/ritonavir in HIV-infected persons requiring hemodialysis. AIDS. 2008 Oct 1;22(15):1919-27.

182. ter Heine R, Scherpbier HJ, Crommentuyn KM, Bekker V, Beijnen JH, Kuijpers TW, et al. A pharmacokinetic and pharmacogenetic study of efavirenz in children: Dosing guidelines can result in subtherapeutic concentrations. Antivir Ther. 2008;13(6):779-87.

183. Arab-Alameddine M, Di Iulio J, Buclin T, Rotger M, Lubomirov R, Cavassini M, et al. Pharmacogenetics-based population pharmacokinetic analysis of efavirenz in HIV-1-infected individuals. Clin Pharmacol Ther. 2009 May;85(5):485-94.

184. Bertrand J, Treluyer JM, Panhard X, Tran A, Auleley S, Rey E, et al. Influence of pharmacogenetics on indinavir disposition and short-term response in HIV patients initiating HAART. Eur J Clin Pharmacol. 2009 Jul;65(7):667-78.

185. Henningsson A, Marsh S, Loos WJ, Karlsson MO, Garsa A, Mross K, et al. Association of CYP2C8, CYP3A4, CYP3A5, and ABCB1 polymorphisms with the pharmacokinetics of paclitaxel. Clin Cancer Res. 2005 Nov 15;11(22):8097-104.

186. Hawwa AF, Collier PS, Millership JS, McCarthy A, Dempsey S, Cairns C, et al. Population pharmacokinetic and pharmacogenetic analysis of 6-mercaptopurine in paediatric patients with acute lymphoblastic leukaemia. Br J Clin Pharmacol. 2008 Dec;66(6):826-37.

187. Petain A, Kattygnarath D, Azard J, Chatelut E, Delbaldo C, Geoerger B, et al. Population pharmacokinetics and pharmacogenetics of imatinib in children and adults. Clin Cancer Res. 2008 Nov 1;14(21):7102-9.

188. Mamiya K, Ieiri I, Shimamoto J, Yukawa E, Imai J, Ninomiya H, et al. The effects of genetic polymorphisms of CYP2C9 and CYP2C19 on phenytoin metabolism in Japanese adult patients with epilepsy: Studies in stereoselective hydroxylation and population pharmacokinetics. Epilepsia. 1998 Dec;39(12):1317-23.

189. Yamasaki Y, Ieiri I, Kusuhara H, Sasaki T, Kimura M, Tabuchi H, et al. Pharmacogenetic characterization of sulfasalazine disposition based on NAT2 and ABCG2 (BCRP) gene polymorphisms in humans. Clin Pharmacol Ther. 2008 Jul;84(1):95-103.

190. Saeki M, Saito Y, Jinno H, Tanaka-Kagawa T, Ohno A, Ozawa S, et al. Single nucleotide polymorphisms and haplotype frequencies of UGT2B4 and UGT2B7 in a Japanese population. Drug Metab Dispos. 2004 Sep;32(9):1048-54.

191. Bhasker CR, McKinnon W, Stone A, Lo AC, Kubota T, Ishizaki T, et al. Genetic polymorphism of UDP-glucuronosyltransferase 2B7 (UGT2B7) at amino acid 268: Ethnic diversity of alleles and potential clinical significance. Pharmacogenetics. 2000 Nov;10(8):679-85.

192. Lampe JW, Bigler J, Bush AC, Potter JD. Prevalence of polymorphisms in the human UDP-glucuronosyltransferase 2B family: UGT2B4(D458E), UGT2B7(H268Y), and UGT2B15(D85Y). Cancer Epidemiol Biomarkers Prev. 2000 Mar;9(3):329-33.

193. Mehlotra RK, Bockarie MJ, Zimmerman PA. Prevalence of UGT1A9 and UGT2B7 nonsynonymous single nucleotide polymorphisms in west African, Papua New Guinean, and north American populations. Eur J Clin Pharmacol. 2007 Jan;63(1):1-8.

194. Saeki M, Saito Y, Jinno H, Sai K, Komamura K, Ueno K, et al. Three novel single nucleotide polymorphisms in UGT1A9. Drug Metab Pharmacokinet. 2003;18(2):146-9.

195. Villeneuve L, Girard H, Fortier LC, Gagne JF, Guillemette C. Novel functional polymorphisms in the UGT1A7 and UGT1A9 glucuronidating enzymes in Caucasian and African-American subjects and their impact on the metabolism of 7-ethyl-10-hydroxycamptothecin and flavopiridol anticancer drugs. J Pharmacol Exp Ther. 2003 Oct;307(1):117-28.

196. Jinno H, Saeki M, Saito Y, Tanaka-Kagawa T, Hanioka N, Sai K, et al. Functional characterization of human UDP-glucuronosyltransferase 1A9 variant, D256N, found in Japanese cancer patients. J Pharmacol Exp Ther. 2003 Aug;306(2):688-93.

197. Angus BJ, Thaiaporn I, Chanthapadith K, Suputtamongkol Y, White NJ. Oral artesunate dose-response relationship in acute falciparum malaria. Antimicrob Agents Chemother. 2002 Mar;46(3):778-82.

198. White NJ, van Vugt M, Ezzet F. Clinical pharmacokinetics and pharmacodynamics of artemether-lumefantrine. Clin Pharmacokinet. 1999 Aug;37(2):105-25.

199. White NJ. The assessment of antimalarial drug efficacy. Trends Parasitol. 2002 Oct;18(10):458-64.